Geological Survey of Finland

Bulletin 389

Geochemistry of Palaeoproterozoic supracrustal and plutonic rocks in the Tampere–Hämeenlinna area, southern Finland

by Raimo Lahtinen

GEOCHEMISTRY OF PALAEOPROTEROZOIC SUPRACRUSTAL AND PLUTONIC ROCKS IN THE TAMPERE–HÄMEENLINNA AREA, SOUTHERN FINLAND

by

RAIMO LAHTINEN

with 36 figures and 5 tables

Lahtinen, Raimo 1996. Geochemistry of Palaeoproterozoic supracrustal and plutonic rocks in the Tampere–Hämeenlinna area, southern Finland. *Geological Survey of Finland, Bulletin 389*. 113 pages, 36 figures, 5 tables.

This is a regional-scale rock geochemical study in which bedrock types are classified into different tectono-magmatic and genetic groups. Areal differences and similarities, geochemical aspects of crustal evolution and plate tectonic implications are also considered. Over 40 major and trace elements were investigated in 403 bedrock samples.

Sedimentary rocks were divided into basement- and arc-related types where the latter show rapid erosion of arc material and subsequent deposition in arc-related basins. Basement-related sedimentary rocks are characterized by their more weathered source, recycled nature, quartz depletion, higher Th/U, increase in Cr and Ni and depletion in Ba, showing a variable but homogenized Archaean to Palaeoproterozoic source. Tonalitic migmatization is seen in the increase of Cl and in the variable depletion of B. Higher grade granitic migmatites show gain in Cl, F and possibly also Rb and loss of C, S, and B.

A mature ACM origin is suggested for the calc-alkaline volcanics in the Tampere Schist Belt (TSB) and a more 'primitive' origin for the calc-alkaline volcanics in the Hämeenlinna Schist Belt (HSB). Evolved tholeiitic basalts with DM–EM origin characterize the rift-related younger volcanism in the HSB. MORB-affinity volcanics and spatially associated DM-affinity mafic plutonics mark the occurrence of an inferred suture between the TSB and HSB.

Syn-tectonic granitoids (1.89–1.88 Ga) are dominated by high-K calc-alkaline granodiorites, being commonly hybrid rocks. Late- to post-tectonic granites (1.88–1.86 Ga) in the North of the TSB (NTSB) are divided into high-K and very high-K groups, interpreted to originate in vapour-phase-absent melting of an intermediate-felsic igneous source and WPB-underplate±crustal source, respectively. The sediment-assimilated granitoids of tholeiitic affinity (1.88–1.86 Ga) follow trends from WPB-affinity mafic rocks to strongly peraluminous granodiorites. S-type microcline granites (1.84–1.81 Ga) in the south have lost a fluid phase before the onset of vapour-phase-absent melting in the mainly sedimentary source.

Key words (GeoRef Thesaurus, AGI): geochemical surveys, schist belts, metasedimentary rocks, metavolcanic rocks, plutonic rocks, granites, geochemistry, genesis, plate tectonics, Proterozoic, Paleoproterozoic, Tampere, Hämeenlinna, Finland

Raimo Lahtinen, Geological Survey of Finland,
P. O. Box 96, FIN-02151 ESPOO, FINLAND

E-mail: raimo.lahtinen@gsf.fi

CONTENTS

ABBREVIATIONS

Areal

MC	Microcline granite Complex
HSB	Hämeenlinna Schist Belt
MB	Mica gneiss–migmatite Belt
TSB	Tampere Schist Belt
NTSB	North of TSB
HiSB	Hirsilä Schist Belt
CFGC	Central Finland Granitoid Complex

Group

SG1–SG8	sedimentary
VG1–VG8	volcanic
GG1–GG8	plutonic

Others

ACM	Active Continental Margin
AFC	Assimilation and Fractional Crystallization
BSE	Bulk Silicate Earth
CFB	Continental Flood Basalt
CIA	Chemical Index of Alteration; weathering
DCP	Direct-Current Plasma
DM	Depleted Mantle
EM (I and II)	Enriched Mantle
FAAS	Flame Atomic Absorption Spectrometry
Ga	Billion (10^9) years
GAAS	Graphite furnace Atomic Absorption Spectrometry
HAB	High-Alumina Basalt
IAT	Island-Arc Tholeiite
ICP-AES	Inductively Coupled Plasma-Atomic Emission Spectrometry
ICP-MS	Inductively Coupled Plasma-Mass Spectrometry
INAA	Instrumental Neutron Activation Analysis
HSFE	High Field Strength trace Elements
HIMU	High μ ($^{238}U/^{204}Pb$) mantle source region
kbar	pressure expressed in kilobars
LILE	Large Ion Lithophile Element
Ma	Million (10^6) years
MASH	Mixing-Assimilation-Storage-Homogenization
(N/T/E-)MORB	Mid-Ocean Ridge Basalt; N (Normal), T (Transitional), E (Enriched)
OIB	Ocean-Island Basalt
PIA	Primitive Island Arc
ppb	Parts per billion
ppm	Parts per million
PREMA	PREvalent MAantle reservoir
(L/H-)REE	Rare Earth Element; L (Light) and H (Heavy)
WPB	Within-Plate Basalt
XRF	X-Ray Fluorescence spectrometry

PREFACE

The bedrock of Finland, which is mainly Precambrian in age, is on average covered by some 7 metres of Quaternary sediments, such that only 3 % of the surface area is exposed. Because till, the most abundant material in the overburden, was derived from bedrock it generally corresponds compositionally to bedrock, though because of mixing and transport, till analysis only provides an overall view. On the other hand, the degree of exposure makes representative sampling of bedrock a real challenge.

A rock geochemistry research program was established in 1991 by the geochemistry department of Geological Survey of Finland. The final decision to start the research program was preceded by intensive discussions on the need, on the content, and on the methods of the program throughout most of the whole 1980's. Essential support to the program was given by Prof. G. Govett in his reports in 1986 and 1988, when he was evaluating the scientific achievements and role of the geochemistry department. The rock geochemistry program started and took shape rapidly following his second evaluation report. Raimo Lahtinen made the first preliminary project proposal in 1988, and a working group consisting of Pekka Lestinen (chairman), R. Lahtinen and Esko Korkiakoski was established in the department in order to prepare a plan for the whole research program. Their proposal was finalized already by the end of 1988. The essential content of this proposal was a pilot study project for the years 1989–1990. Because this kind of research program was quite unique even from an international viewpoint, it was natural to commence with a pilot study more thorough than usual. These publications were collected from the results of the pilot study, processing the data, and their practical applications. The research program began very soon after the results of pilot study were available, and the field work phase of the research program has already been completed.

The main emphasis of the pilot phase was to study the representativeness of sampling, selecting the correct sampling grid, determining the amount of samples needed, and selecting the analytical methods. All these more or less technical aspects were reported in an internal report in 1991.

One of the main principles of the rock geochemistry research program has been the use of the most modern analytical techniques, which make possible, in addition to ordinary major element analysis the obtaining of high quality data for minor and trace elements. In addition to geochemical data, petrophysical parameters of the samples are determined. The public domain data bank covering the whole country, which will be available on completion of the program, thus offers an exceptionally broad and high quality source of data for application and interpretation in bedrock geochemistry studies.

The aim of the rock research program was determined 'to collect geochemical data concentrated in trace elements from the area of the whole country, to produce background data for interpretations of regional till geochemistry data, to classify the rock types, and to clarify the metallogeny of the bedrock.

Geochemical changes pertaining to the crustal evolution will be studied, too'.

These issues of the GSF Bulletin are concerned with application of the data and provide examples of potential ways of using the data. Recently it has also been realized that the data are valuable in other quite unforeseen applications, such as in evaluation of water quality in drilled wells. The final results of the research program are planned to be published as soon as possible for the benefit not only of researchers in Finland but also in other countries interested in problems of Archaean and Proterozoic bedrock as well as for those studing regional health and environmental problems.

Espoo 19.11.1996   *Reijo Salminen*

Publications:

Lahtinen, R. 1996. Geochemistry of Palaeoproterozoic supracrustal and plutonic rocks in the Tampere–Hämeenlinna area, southern Finland. Geological Survey of Finland, Bulletin 389. 113 p.

Lahtinen, R. & Lestinen, P. 1996. Background variation of ore-related elements and regional-scale mineralization indications in Palaeoproterozoic bedrock in the Tampere–Hämeenlinna area, southern Finland. Geological Survey of Finland, Bulletin 390. 38 p.

Lestinen, P., Savolainen, H. & Lahtinen, R. 1996. New methods applying bedrock lithological and geochemical data to the interpretation of regional till geochemical data: a study in the Tampere–Hämeenlinna area, southern Finland. Geological Survey of Finland, Bulletin 391. 37 p.

Lahtinen, R. & Korhonen, J.V. 1996. Comparison of petrophysical and rock geochemical data in the Tampere–Hämeenlinna area, southern Finland. Geological Survey of Finland, Bulletin 392. 45 p.

Sandström, H. 1996. The analytical methods and the precision of the element determinations used in the regional bedrock geochemistry in the Tampere–Hämeenlinna area, southern Finland. Geological Survey of Finland, Bulletin 393. 25 p.

INTRODUCTION

The Precambrian bedrock of Finland has been mapped in 1:400 000 scale, and large areas also in 1:100 000 scale, and Finland is thus one of the best mapped Precambrian areas in the world. Although numerous studies describe the structural evolution, metamorphism and geochemistry of the Svecofennian rocks of southern Finland, most of these are concentrated in specific key areas. Examples are the Raahe–Ladoga zone (Korsman et al. 1984, 1988) and the well-preserved Tampere schist belt (Sederholm 1897, Kähkönen 1989). The geochemical studies have been directed mainly to volcanics and granitoids, and only a few to sedimentary rocks (Kähkönen & Leveinen 1994). Regional geochemical studies are entirely lacking, though the studies of Nurmi et al. (1984), Front & Nurmi (1987), Nironen (1989a) and Lahtinen (1994a) concentrating on the geochemistry of synkinematic granitoids in central and southern Finland have regional implications. There are many detailed studies, on the other hand, and while the results can be correlated within each study, there are major problems of different sampling techniques and strategies and different analytical methods if comparisons are to be made between studies. The Rock Geochemistry Research Project (RGRP) was launched by the Geological Survey of Finland in 1991 to obtain regional geochemical information about rock types throughout the country. The main objectives of the project are to obtain high quality and comparable analytical data for purposes of classifying the rocks into their tectono-magmatic and genetic groups, study-

ing the origin and evolution of these rocks, and clarifying the metallogenic features and crustal evolution. At the same time, the bedrock geochemical data is to be integrated with regional till geochemical data.

Before the RGRP was set up, a pilot study was conducted in the Tampere–Hämeenlinna area to develop sampling strategies and methods, analytical methods and interpretation procedures. This paper presents the results of the pilot study conserning the geochemistry of the various rock types. A description of the sampling strategy and sampling is followed by brief notes on the analytical methods (see Sandström 1996). The study area was divided into main five main units on the basis of lithological differences, and the general geology of these units is described, with brief notes on structure and metamorphism. After study on a sample by sample basis, the samples were grouped into three main lithological types: sedimentary rocks, volcanic rocks and plutonic rocks. The plutonic rocks were also subdivided into mafic plutonics and granitoids. Within these rock types, different groups were distinguished, mainly on the basis of geochemical criteria, but with areal and lithological features taken into consideration. The main characteristics of these groups, including the similarities and differences between them, are considered. Plate tectonic implications are suggested and the varying crustal evolution of the different parts of the study area is explored. The complete data set, divided into main groups, is available from the author.

SAMPLING STRATEGY AND SAMPLING

A major goal of the pilot project in the Tampere–Hämeenlinna area was to develop a sampling strategy serving two main purposes: i) a production of geochemical and petrological data allowing a delineation of regional differences and similarities in geochemistry, petrogenesis, metallogeny and areal distribution of different rock types and ii) a production of geochemical background values for rocks, which would assist the interpretation of regional till geochemical data. The sampling strategy was based on 1:100 000 bedrock maps, where rock types are divided into six main groups: (1) granitoids, (2) mafic plutonics, (3) felsic volcanics and gneisses, (4) mafic volcanics and amphibolites, (5) sedimentary rocks (including mica gneisses and migmatites) and (6) "others" for rocks not included in other groups (e.g. metasomatic rocks). Intermediate volcanics are not distinguished in bedrock maps and are included in either mafic or felsic volcanic groups. On the basis of the bedrock maps, areal distributions (area-%) were calculated for the main rock groups and separated for 100-km^2 squares. The number of samples of a particular rock group to be collected per square was determined according to this area-%. One sample was taken for each group exceeding 5% in areal distribution, and a second sample was taken for volcanics and mafic plutonics when they exceeded 20% and for granitoids and sedimentary rocks when they exceeded 50% in areal distribution. The higher threshold for granitoids and sedimentary rocks was intended to reflect their larger and more homogeneous bodies than volcanics and mafic plutonics. Actual sampling sites were selected so that all main rock types (>5% area-%) in one 1:100 000 bedrock map were included, and so that sampling sites were as evenly distributed as possible.

This sampling strategy reduces the number of samples, and thus the cost of the sampling needed to obtain an approximation of regional geochemical features. The sampling density varied according to the complexity of lithologies shown in bedrock maps, from two samples per 100 km^2 in areas containing only one main rock group up to 6–8 samples per 100 km^2 in areas containing a diversity of rock types. The point-like nature of the sampling must be emphasized: open small-scale variation occurs within the different formations, but information is obtained from one sample in one outcrop only. As a means of determining the degree of reliability of these single samples, in 45 cases a duplicate formation sample was taken about 200–1000 m away from the original sampling site, from an outcrop marked in the bedrock map as of identical lithology. In 39 cases the duplicate formation sample was confirmed to be from the same rock type and only these samples were included. Comparison of these duplicate formation samples with sample pairs (normal–duplicate, see below) from the original outcrop showed that, in about 70 per cent of cases, the information was the same and the samples were regionally representative (Sandström 1996). This means that broad regional differences and similarities, as also areal correlations, can be verified and correlated with the more detailed studies.

The sampling sites, selected as discussed above, were first studied in terms of rock types, primary features, deformation, metamorphic features, textures, alteration and contact relations. The lithologically most homogeneous part of the outcrop was selected for sampling. Sampling was done mainly with a mini-drill with diamond bit, or occasionally with a sledge hammer. Each sample comprised four subsamples from the same lithological unit, if detection of unit boundaries was possible (sometimes this was impossible,

e.g. in some migmatites). The sampled area varied from 10-cm wide turbidite beds to an area of about 2 m² for homogeneous granite. In the case of turbidites, the whole Bouma A, AB or ABC was sampled, avoiding the D-E. A composite sample was taken from veined migmatites and pelitic rocks when the layering was < 5 cm and a more homogeneous unit was not available. The sledge hammer sampling caused heterogeneity in the samples by guiding the sampling to the broken edges of outcrops. Mini-drill sampling enabled the sample to be taken from the most suitable part of the outcrop and is to be preferred in the future course of the project. The sampled unit was then classified as plutonic, volcanic, dyke or sedimentary rocks or as rock of unclear origin such as schist, gneiss, skarn and amphibolite. The classification was extended by a more-detailed subdivision into rock types. Studies of chemical composition and thin sec-

tions and remapping of some outcrops led to a refining of some classifications.

Duplicate samples were taken to evaluate the sampling precision. Ideally, the duplicate samples were to be taken from the same rock unit about 1–2 m away from the sampling site proper. Unfortunately, there was some deviation from this, and some duplicate samples were taken too far away, sometimes from different rock units. These samples were discarded. As noted above, to check the variation within the same rock type as presented on the bedrock map, a duplicate formation sample was taken as well. Since this was a pilot study, some modifications were made during the sampling stage, which introduced some scatter into the descriptions and the analytical data. These features, along with the analytical procedures, are discussed in more detail by Sandström 1996.

ANALYTICAL METHODS

The main analytical work was done in the laboratories of the Geological Survey of Finland (GSF). The sample preparation, analytical methods and the precision of the element determinations are discussed in detail by Sandström (1996); only the analytical methods are referred to here, and only briefly. Major elements (except Fe) and S, Cl, V, Cr (see below), Ni, Zn, Rb, Sr, Y, Zr, Nb, Ba and Pb were determined by XRF method, Fe by FAAS method, $C_{Tot.}$ by Leco CR–2 carbon analyser, F by ion selective electrode, aqua regia leachable Li and Cu by ICP-AES method, and aqua regia leachable Au, Pd, Te, As, Ag, Bi, Sb and Se by GAAS. The Cr values are background corrected values ($Cr_{Det.}$-30 ppm).

Samarium, La, Th, Sc, Co and U were determined by neutron activation at the Techni-

cal Research Centre of Finland. The precision and accuracy of the method have been reported by Rosenberg et al. (1982). Some in-batch drift variation (e.g. for Sc) has been observed (Sandström 1996), producing scatter. Although this may affect individual sample correlations to some degree, it should not affect group comparisons, as the samples are more or less evenly distributed in the analysing sequence. Samples, excluding duplicate "formation" samples, were also analysed in the XRAL laboratories in Canada, for B and Be by DCP emission spectrometry method, for Ga, Nb, Sn, Ta, Th and Bi by ICP-MS method, for Hg by cold vapour method and for CO_2 by classical wet chemistry. $C_{Graf.}$ was calculated from the $C_{Tot.}$ and CO_2 data.

GENERAL GEOLOGY OF THE STUDY AREA

The study area is situated in southern Finland, in the central part of the Fennoscandian Shield, and lies entirely within the Palaeoproterozoic Svecofennian domain (Fig. 1). The area has been covered by 1:100 000 scale regional bedrock mapping, which is described in eight map sheets with accompanying explanatory texts (except 2142): 2113 Forssa (Neuvonen 1954a, 1956), 2114 Toijala (Matisto 1973, 1976a), 2123 Tampere (Matisto 1961, 1977), 2124 Viljakkala–Teisko (Simonen 1953, 1952), 2131 Hämeenlinna (Simonen 1949a, 1949b), 2132 Valkeakoski (Matisto 1970, 1976b), 2141 Kangasala (Matisto 1964,

1976c), 2142 Orivesi (Laitakari 1986). The main geological features, as depicted in Fig. 2, support a division into five areas, and several subareas, delineated mainly by lithological features. The five main areas are North of the Tampere Schist Belt, Tampere Schist Belt, Mica gneiss–migmatite Belt, Hämeenlinna Schist Belt and Microcline granite Complex. Only a brief description of the main rock types is given here, and only in special cases are the separate samples of the study referred to. As all the sedimentary and volcanic rocks are metamorphosed, the prefix 'meta' has been dropped.
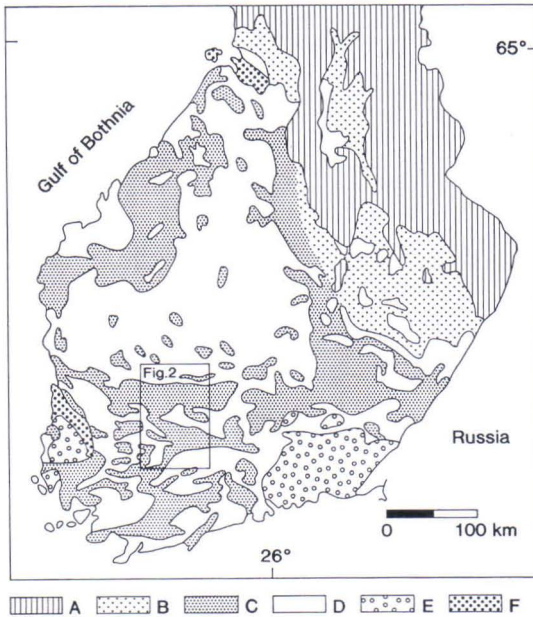
Fig. 1. Simplified geological map of southern Finland, after Simonen (1980b). A. Archaean rocks; B. Karelian schists; C. Svecofennian schists, gneisses and migmatites; D. Svecofennian plutonic rocks; E. rapakivi granites; F. Jotnian sedimentary rocks. The study area is outlined (see Fig. 2).
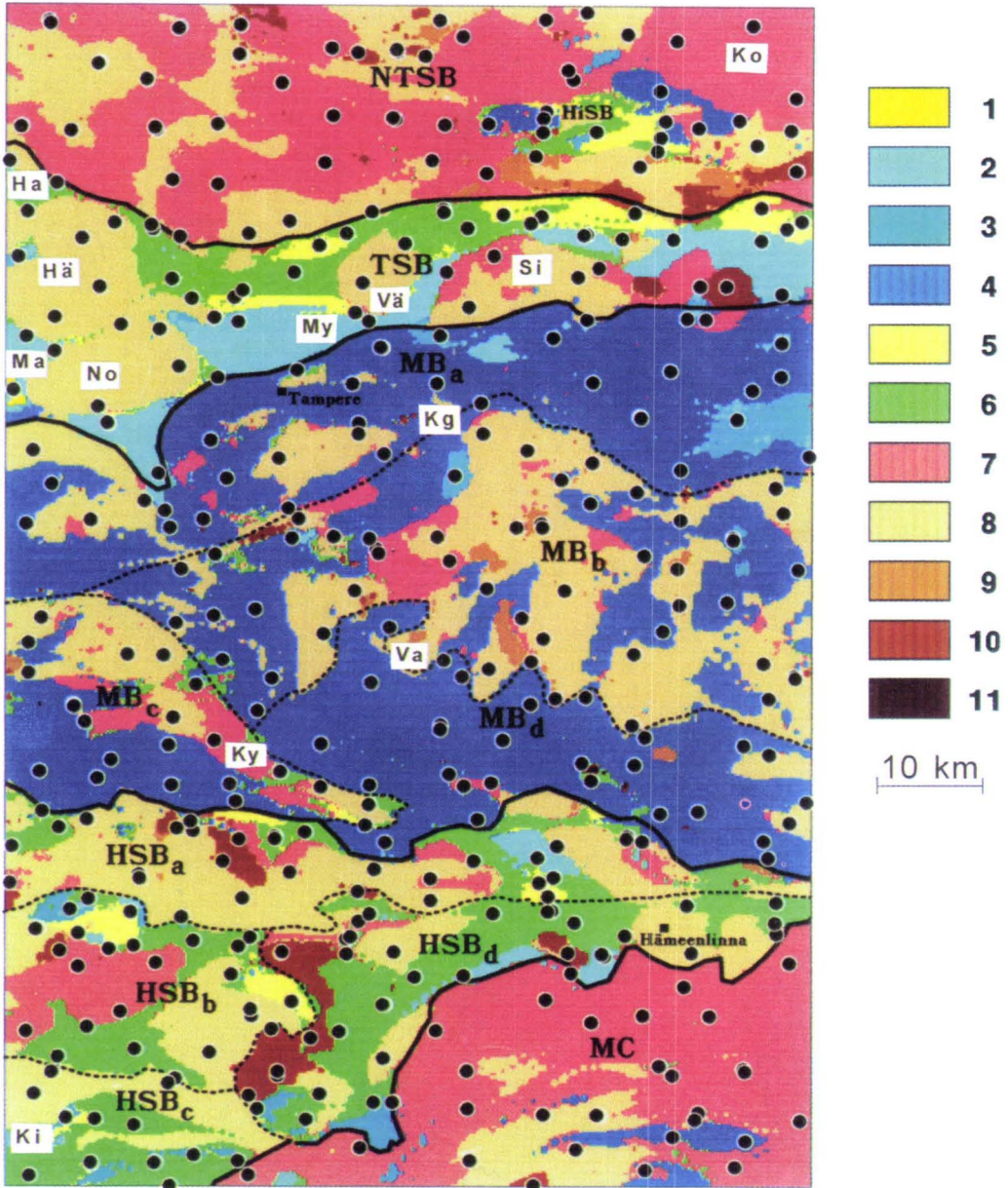
Fig. 2. Geological map of the study area: a slightly simplified version of the digital map, compiled and redrawn by Tiainen from the published 1:100 000 bedrocks maps of the area (Simonen 1949, 1952; Neuvonen 1954, Matisto 1961, 1964, 1970, 1973; Laitakari 1986). NTSB – North of the Tampere Schist Belt, HiSB – Hirsilä Schist Belt, TSB – Tampere Schist Belt, MB – Mica gneiss–migmatite Belt, HSB – Hämeenlinna Schist Belt, MC – Microcline granite Complex. Ha – Haveri formation, Hä – Hämeenkyrö pluton, Kg – Kangasala, Ki – Kiipu volcanic association, Ko – Koppelojärvi granite, Ky – Kylmäkoski granitoid complex, Ma – Mauri arkose, My – Myllyniemi formation, No – Nokia pluton, Si – Siitama pluton, Va – Valkeakoski, Vä – Värmälä pluton. The locations of the cities Tampere and Hämeenlinna are shown. 1 – arkose, 2 – greywacke/mica schist, 3 – mica gneiss, 4 – mica gneiss–migmatite, 5 – quartz-feldspar gneiss/felsic volcanics, 6 – mafic–intermediate volcanics/amphibolite, 7 – granite, 8 – granodiorite, 9 – quartz diorite, 10 – diorite/gabbro, 11 – peridotite.

Structure and metamorphism

The structural evolution of the Tampere Schist Belt (TSB) and the Mica gneiss–migmatite Belt (MB) has been studied by Campbell (1980), Nironen (1989b), Kähkönen (1989), Kähkönen & Nironen (1994) and Kilpeläinen et al. (1994), and the structural evolution of the Hämeenlinna Schist Belt (HSB) by Hakkarainen (1994). Structural interpretations differ, especially as regards the number of deformation stages distinguished and the correlations between areas. Here I follow the tectonometamorphic evolution interpretation presented by Kilpeläinen at al. (1994), but the reader is also referred to Koistinen et al. (submitted).

The earliest structures are the layer-parallel schistosity and compositional banding related to horizontal D1 deformation. In the TSB, schistosity related to D1 deformation is only found locally. In general, there is a correlation between the intensity of D1 and metamorphic grade. The second-generation folds were developed during N–S compression (D2) and have preserved their attitude as a major syncline in the TSB, but two conjugate plastic foldings (D3 deformation) have turned the D2 structures in the MB, often with the formation of dome-basin interference structures, and at least in part also with folding of the metamorphic isograde surfaces.

According to Kilpeläinen et al. (1994), the metamorphism took place at 470°C and 3–4 kbar in the central parts of the TSB syncline, and at higher temperature (570°C) at similar pressures at the margins of the syncline, near to the migmatite area (MB). Metamorphic reactions and migmatization in the MB begun progressively during D1 with an increase in temperature and decrease in pressure in the course of the D1–D2 deformation. Some rare observations (Vammala area) indicate that the early stage of metamorphism may have taken place at 7–8 kbar, but the highest temperature (670°C) was reached at 5–6 kbar. An abundant occurrence of aqueous fluids is inferred during tonalitic migmatization (D1–D2), and granitic migmatization characterizes the D3 stage. An important observation is that the progressive metamorphism is related to D1 in the MB and to D2 in the TSB, further implying that the temperature and age of metamorphism and the onset of structural evolution increase as a function of depth (Kilpeläinen et al. 1994).

According to Hakkarainen (1994), structural evolution in the HSB was as follows: the D1 event was an E–W oriented isoclinal to open folding with initially subhorizontal fold axes, and the D2 event was regionally a non-penetrative asymmetrical shear folding; the D3 event occurred locally and is defined by large subhorizontal open folds, and D4 comprises NW–SE to NE–SW oriented shear zones.

The numerous aeromagnetic lineaments indicate the occurrence of many fault and/or thrust surfaces in the Microcline granite Complex (MC). The occurrence of hypersthene and a garnet–cordierite–microcline–sillimanite association indicates high grade and, at least locally, nearly granulite facies metamorphic conditions.

North of the Tampere Schist Belt (NTSB)

The area North of the Tampere Schist Belt (NTSB) consists predominantly of plutonic rocks, with the small Hirsilä Schist Belt (HiSB) in the east composed of mica gneisses, veined gneisses, mafic and intermediate volcanics, amphibolites and felsic gneisses (Laitakari 1986). Mica gneiss samples of this study did not show clear sedimentary features,

apart from the blastoclastic plagioclase. Horn-
blende and andesine are not uncommon and
their presence indicates a close genetic link
with volcanics, and an epiclastic volcanic
origin is proposed. The occurrence of pumice
fragments and amygdales in some volcanic
samples indicates a pyroclastic origin, at least
for them.

The plutonic rocks form the southern part of
the Central Finland Granitoid Complex
(CFGC) and are characterized by a volumi-
nous occurrence of granites. A massive, coarse-
grained variety dominates, but even-grained
granites occur as well (Simonen 1952).
Slightly foliated quartz diorites and granodi-
orites are also widely distributed and they
contain hornblende and biotite as main mafic
minerals with some relict pyroxene. Diorites
and gabbros occur as small bodies and frag-
ments in granitoids, and within them ultraba-
sic olivine-, pyroxene- and hornblende-bear-
ing peridotites occur as small lenses (ibid.).
Age data is available only for the Koppelo-
järvi granite (1879±14 Ma, Patchett & Kouvo
1986), situated in the NE corner of the study
area (Fig. 2).

Classification into diorites and gabbros in
this study is based mainly on field observa-
tions and should be considered tentative. Di-
orites, in particular, gradually change to ma-
fic quartz diorites and monzodiorites, and, in
many cases, samples described as diorite–
gabbro in the bedrock map, turn out to be
quartz monzodiorites when examined in thin
section. There is a close association between
mafic plutonics and intermediate granitoids
seen in the common comingling and breccia

features and abundant granite–aplite dykes in
gabbros and diorites. Age relations are not
always clear, but the comingling nature of
many samples and the abundant occurrence of
mafic enclaves in granitoids indicate a similar
age for the mafic plutonics and granitoids.
Diorites have a similar mineralogy of plagi-
oclase (andesine), hornblende and biotite.
Quartz and K-feldspar are found in small
amounts and the main accessories are coarse
sphene, apatite, epidote and, in one sample,
zircon. Hornblende gabbros contain, besides
plagioclase and hornblende, also biotite and
chlorite, and pyroxene locally.

Forty-nine samples from the NTSB repre-
sent intermediate to felsic plutonic rocks. The
occurrence of mafic enclaves is common, and
evidence for comingling is often seen, espe-
cially in quartz diorites and granodiorites.
Three quartz monzodiorites, four quartz dior-
ites and 18 granodiorites make up the interme-
diate granitoids. Granodiorites contain both
hornblende and biotite, and chlorite is abun-
dant in some samples as an alteration product.
Granite samples in this study include four
samples from the Koppelojärvi granite. The
sample near the assumed contact is a feldspar
porphyry and other samples are porphyritic
granites. One thin section from the Koppelo-
järvi granite contains orthoclase with abun-
dant perthite and myrmekite and thus differs
from the normal microcline in the western
NTSB granites (Simonen 1952). The other
granites contain biotite and, to a lesser extent,
hornblende, but varieties containing only bi-
otite are common as well.

Tampere Schist Belt (TSB)

Ever since the time of Sederholm (1897),
the well-preserved and well-exposed volcan-
ic-sedimentary TSB has been a key area for
studying the evolution of Svecofennian su-
pracrustals (see Kähkönen 1989, Nironen

1989a, Kähkönen et al. 1994 for references).
The tentative generalized stratigraphic
scheme of the central TSB (Kähkönen et al.
1994) differs slightly from that proposed by
Simonen (1980). Kähkönen et al. (1994) con-

sidered the tholeiitic volcanics of the Haveri Formation to be the lowermost unit, followed by the Myllyniemi turbidites with volcanic interbeds. The arc-type volcanics and related sedimentary rocks form the main volcanic association (a term used in this study). Overlying this is Veittijärvi conglomerate, with the mafic volcanics at Takamaa as the uppermost unit. The U–Pb zircon ages of volcanics (1904–1889 Ma) confirm the occurrence of two volcanic units separated by the Veittijärvi conglomerate (Kähkönen et al. 1989).

The available Sm–Nd isotopic data (ε_{Nd} from -1 to 0, Huhma 1987) from three greywackes and one phyllite, and the detrital zircon data from greywackes (Huhma et al. 1991, Claesson et al. 1993), indicate a mixed Archaean and prevailing Palaeoproterozoic source for these TSB sediments. The occurrence in the Ahvenlampi conglomerate of Archaean granitoid cobble with minimum U–Pb zircon age about 2.55 Ga is in agreement with these results (Kähkönen & Huhma 1993). The occurrence of plutonic clasts (1.88–1.89 Ga, Nironen 1989a and references therein) in conglomerates high in stratigraphy shows a very rapid recycling and erosion of arc material at this level. The stratigraphic position of the Mauri arkose has not been resolved, but the dominant provenance of uplifted granites and clastic zircons of 1.9 Ga age (Matisto 1968) indicates that it is high.

The sedimentary rocks in the TSB were studied in detail by Seitsaari (1951) and Simonen & Kouvo (1951), following up the early work of Sederholm (1897). These studies and the available bedrock maps with explanatory texts (Simonen 1952, 1953, Matisto 1961, 1977, Laitakari 1986) have provided the basis for later studies incorporating new methods for sedimentary environmental analysis (Ojakangas 1986, Rautio 1987, Leveinen 1990, Kähkönen & Leveinen 1994). The TSB sedimentary rocks are interpreted to represent mid-fan turbidites of submarine fans deposited in a forearc basin with palaeocurrents mainly from the east (Ojakangas 1986). Higher in the stratigraphy, there are rocks bearing signs of fluvial environment (Kähkönen & Leveinen 1994). The general trend in the central TSB is towards younger rocks from the boundary of the MB in the south to the volcanic dominated stratas in the north, but there are many breaks and possibly repetitions of strata due to folding (syncline) and faulting (see Kähkönen 1989, Kähkönen 1994, Kähkönen & Leveinen 1994). Apart from quartz, plagioclase and micaceous matrix, the greywackes also contain volcanic rock fragments of various composition, plutonic rock fragments, sedimentary rock fragments (slate and minor quartzite) and microcline (Simonen & Kouvo 1951, Simonen 1952, Ojakangas 1986, Kähkönen & Leveinen 1994). The occurrence of quartzite pebbles in some conglomerates and of quartzite clasts in greywackes (Seitsaari 1951, Ojakangas 1986), together with the detrital zircon data (see above), show that the source material for the greywackes contained an older basement component.

The TSB volcanics are dominated by medium-K to high-K calc-alkaline intermediate pyroclastic rocks with general resemblance to mature island arc or continental margin rocks (Kähkönen 1987, 1989, 1994). Shoshonites are not uncommon in the central TSB. While the general stratigraphic scheme (see above) seems justified, the exact stratigraphical correlation of the various volcanic units is unresolved and possibly will remain obscure due to the interfingering nature of the different units. The Ti-rich basalts of the Haveri Formation show local pillow structures and also deviate from the general geochemical trends in the TSB in having initial arc stage, enriched Mid-Ocean Ridge Basalt (EMORB) or marginal basin geochemical affinities (Mäkelä 1980, Kähkönen 1989). Kähkönen & Nironen (1994) confirmed the marginal basin basalt affinity for the Haveri Formation and suggested that it records the change from a

restricted, shallow extensional basin to a larger arc-related basin environment.

The plutonic rocks of the TSB comprise the Hämeenkyrö (1885±2 Ma, Nironen 1989a), Värmälä (1878±3 Ma, ibid.; see also Kähkönen et al. 1989), Nokia and Siitama plutons. The Nokia and Siitama plutons, which are surrounded by sediments, occur south of the main volcanic association and are characterized by abundant schist xenoliths; the Nokia batholith also contains inherited zircons (Nironen 1989a). The most abundant variant of the Nokia pluton is porphyritic granodiorite with abundant K-feldspar which contains abundant inclusions, especially plagioclase, and often has an orthoclase centre which gradually changes to tricline microcline at the margin. A rapakivi-like texture has also been observed (Matisto 1977). The Hämeenkyrö pluton has been studied in detail by Front (1981) and Nironen (1989a), and a multiply intruded zoned origin has been observed with rocks ranging from marginal tonalite through prevailing granodiorite to monzogranite.

Metamorphic mafic dykes and subjotnian mainly olivine diabases are common, especially in the Orivesi area (Aro & Laitakari 1987; Laitakari 1987). Shear zones are postulated to act as north and south boundaries in the TSB (approximately coinciding with the area boundaries in Fig. 2) (Nironen 1989b). The southern shear zone is a south dipping thrust with uplift of the higher grade rocks (ibid.). The main metallogenic features are the now exhausted Ylöjärvi Cu–W mine in tourmaline–quartz breccias cutting the supracrustals near the eastern contact of the

Hämeenkyrö pluton (see Nurmi et al. 1984 for references) and the exhausted Haveri Cu–Au mine in the Haveri Formation (Stigzelius 1944, Mäkelä 1980, Kähkönen & Nironen 1994). There are other Au-occurrences in the volcanics in the TSB (Luukkonen 1994), among which Kutemajärvi is an operating gold mine.

The sedimentary rock samples from the TSB are mainly greywackes with turbidite structures, but some finely laminated mudstones and Mauri arkose (one sample) occur also. Locally the blastoclastic texture is both well preserved and totally destroyed. Volcanics are mainly pyroclastic rocks, and the only sample from the Haveri Formation is a pillow-like lava. Some massive volcanics can be of lava origin (also partly sills), but pillow lavas are not found outside Haveri. This is in agreement with observations made by Kähkönen (1989). Amygdaloidal structures are common, and carbonate and epidote are common minor minerals and accessories. Locally, these rocks are sheared and partly altered, as seen in one sample rich in coarse muscovite flakes and another with abundant tourmaline.

The Hämeenkyrö pluton samples are granodiorites, containing both hornblende and biotite. The sampling outcrops in the Nokia and Siitama plutons contain mafic and intermediate enclaves locally, and samples have abundant biotite and are normally devoid of hornblende, and thus they differ mineralogically from the Hämeenkyrö pluton. An abundant occurrence of sulphide patches characterizes these plutons. The quartz monzodiorite east of the Siitama pluton occurs in the same zone and is probably associated with it.

Mica gneiss–migmatite Belt (MB)

The MB comprises about half the study area and is composed mainly of mica gneisses/migmatites and granitoids. It belongs to the tonalitic migmatite zone, but more granodioritic and granitic leucosomes are found as well. The MB has been divided into subareas on the basis of lithological differences (differences in the amount of granitoids and volcanics) and

aerogeophysical maps.

The eastern part of the MBa is characterized by the occurrence of well-preserved grey-wackes (Matisto 1964, 1976c). These are locally very thick (up to 10 m), and according to Matisto (1976c) they are partly conglomerates with quartz and feldspar mineral aggregates and phyllite, gneiss and possibly plutonic rock fragments. An important feature is the occurrence of partly blastoclastic quartzite with abundant plagioclase and K-feldspar (more accurately subarkose) associated with diopside gneiss and limestone depicting a peaceful evolution stage during sedimentation (ibid.). Mica gneisses are characterized by black schist and tuffitic intercalations and by numerous calcareous concretions. Limestones and skarnrocks have also been encountered in the Nokia (Matisto 1977) and Valkeakoski areas (Matisto 1976b). The preservation of greywackes is due to the mineral composition and massive and competent character, as the more pelitic layers are typically strongly deformed and also migmatized.

The MBb is characterized by the voluminous occurrence of granitoids, diorites and gabbros (Matisto 1961, 1964, 1970, 1973), while the MBc is characterized by the Kylmäkoski granitoid complex, the Kylmäkoski Ni-mine, amphibolites and mafic volcanics (Matisto 1973). The MBd, which is the eastern continuation of the MBc, contains in addition some amphibolites and mafic volcanics (Matisto 1970, 1973). Graphite- and sulphide-bearing schists and gneisses are common in both subareas, and well-preserved schists are found near the HSB.

Granodiorites, the predominant plutonic rocks in the MB, exhibit a gradual transition to both quartz diorites and granites. They are locally strongly foliated near the contacts and intrude the surrounding schists (Matisto 1976a, 1976b, 1976c, 1977). Pegmatites are not uncommon and locally they contain rare minerals such as beryl and tantalite (see references in Matisto 1976c, Lahti 1981). Dior-

ite, gabbros and more uncommonly peridotites occur as small intrusions and fragments either in schists and gneisses or in granitoids. Granodiorites contain porphyritic variants with locally occurring rapakivi-like texture, and variants with hypersthene. Granites occur as small bodies in other granitoids and in schists. The largest occurrences are one granite in the MBb and the granitic part of the Kylmäkoski granitoid complex in the MBc (Fig. 2).

Apart from tuffitic intercalations, volcanic rocks are rare in the central and northern MB. Uralite–plagioclase porphyries and amphibolites are found mainly as small dykes and fragments in schists and granitoids. Pillow-like structures occur in the southwestern part of the subarea MBc (Fig. 2) and agglomeratic and amygdaloidal structures occur locally in the southern part of the MB (Matisto 1976a). Also found are metadiabases with cutting and conformable relations to schists and granitoids, and a metadiabase with pillow lava structures intruded by aplites and pegmatites (Matisto 1976b). The main metallogenic features are the numerous Ni-indications and the now exhausted Kylmäkoski Ni–Cu mine hosted by mafic plutonics (Papunen 1985). Au-mineralizations in granitoids are found in the Pirkkala–Valkeakoski areas (Rosenberg 1990, 1992).

MBa samples with clear greywacke structures are all from the eastern part, but metamorphic recrystallization has destroyed all primary features on microscopic scale. These rocks are now quartz- and feldspar-rich (mainly plagioclase) gneisses with both biotite and muscovite. Muscovite occurs mainly as an alteration product of K-feldspar. The other mica schist and mica gneiss samples from the eastern part of the MBa are mostly from massive, homogeneous and probably thick units of massive greywacke origin. The mica gneisses and veined gneisses from the western part of the MBa are mostly psammitic rocks veined by tonalitic–granodioritic to

more rarely pegmatitic leucosome.

Only one sample from the MBb is of clearly turbiditic origin, and the mica gneiss samples are psammitic to silty rocks with simple mineralogy (normally quartz–plagioclase–biotite±garnet); but more pelitic rocks characterized by variable occurrence of muscovite, sillimanite and cordierite are not uncommon. In many cases the preserved psammitic fragments float in a migmatitic and more pelitic matrix. Concretions are very common. Some veined gneisses contain granitic to granodioritic leucosome, which seems to come from the surrounding granitoids. In veined gneisses of more silty-pelitic origin, the leucosomes seem to have originated in 'in situ' differentiation. These are thin leucosomes with very thin melanosomes. In general there seem to be more rocks of silty to pelitic character in the MBb than in the MBa.

One greywacke and the mica gneisses and veined gneisses in the MBc are similar to the rocks considered above. They are mainly psammitic rocks which occur in pelitic veined gneisses. Some pelitic mica gneisses and migmatized black schists are also found. The most preserved sedimentary rocks in the MBd are two greywackes, one thinly laminated pelite and three black schists. One of the greywacke samples contains labradoritic plagioclase. The more preserved mica schists and gneisses (both psammitic and more pelitic) occur mainly in the southern part of the MBd. Locally they also contain K-feldspar and muscovite (partly as pseudomorphs of relict Al-silicate), but normally the mineralogy is a simple one of quartz, feldspar and biotite.

There are no volcanic samples from the MBa, and the two samples from the MBb discussed with volcanic rocks are hypabyssal dykes. One dyke cuts metamorphic veining, contains strongly deformed granodiorite inclusions and comingles with non-foliated granodiorite. Both dykes contain plagioclase, amphibole, biotite, quartz and abundant apatite (long prisms) and zircon.

Five samples from the MBc are of possible volcanic origin. One sample shows comingling with feldspar porphyry and is similar to the samples from the above-mentioned dykes. In the same area Matisto (1976) has described metadiabases that cut gneisses and granodiorites and that contain abundant apatite and zircon and so resemble the hypabyssal dykes. Plagioclase porphyritic rock occurs near a contact with mica gneisses and the Kylmäkoski granitoid complex, but the nature of this sample is obscure (hypabyssal or true volcanic rock). Amygdaloidal mafic lava breccia or pillow lava, an amygdaloidal basalt in association with crystal tuffs, and an altered (chlorite, clinozoisite, carbonate) and sheared rock of possible tuff origin are the other volcanics in the MBc.

Garnet-bearing felsic rock from the MBd shows a massive nature, but the biotite streaks are interpreted to indicate a volcanic origin. One amphibolite sample is from an association characterized by agglomerates (Matisto 1970), and another is a fine-grained and homogeneous rock that gradually becomes more diabase- and gabbro-like. It is either a hypabyssal intrusion or a thick lava flow.

Both gabbros and diorites were sampled in the MB. Gabbros contain plagioclase-cumulus locally and in one case orthopyroxene-cumulus with hornblende, clinopyroxene and biotite as intercumulus phases differing from sample to sample. In one sample, garnet was found as idiomorphic grains. Quartz diorite and granodiorites from the western part of the MBa contain abundant biotite, and also abundant sulphide patches, and are thus similar to Nokia and Siitama rocks. These are locally strongly foliated and also sheared, and locally contain mafic enclaves. Alteration is a common feature, especially around joints (muscovite and also chlorite). Hornblende is found locally, with apatite, sphene and zircon as main accessory minerals. A small heterogeneous granite body in schists contains, in addition to biotite, also muscovite, garnet and

tourmaline. An aplite granite and a pegmatitic granite (muscovite+biotite) occur among schists in the eastern part of the MBa.

The MBb is characterized by abundant granitoids. The three quartz diorites and a quartz monzonite contain both hornblende and biotite, and one quartz diorite contains garnet and another pyroxene. The most abundant group is granodiorites (19 samples), with about the same number of porphyritic and even-grained variants. Granitoids are locally strongly foliated, deformed and sheared and contain abundant mafic to intermediate mafic enclaves. Clear sedimentary schist inclusions were found in two samples. Plagioclase is commonly altered to sericite and saussurite, and amphibole and biotite to chlorite. Sul-phides occur often, as do tourmaline-bearing pegmatite veins. In three of the four granite samples, granite occurs in association with other granitoids; in the fourth, it occurs as a pegmatite dyke in schists.

The major plutonic feature in the MBc is the Kylmäkoski granitoid complex (Fig. 2), which based on the aeromagnetic map of the area (not shown) seems to cut, at least partial-ly, the main tectonic features. It is composed of granodiorite (mainly porphyritic), granite and numerous gabbro and volcanic inclusions. As stated above, at least some of these volcan-ic fragments are quickly cooled, comingled mafic magma. Similar mafic dykes cut meta-morphic veining, indicating the late- or post-kinematic nature of the complex.

Hämeenlinna Schist Belt (HSB)

The HSB is differentiated from the MB by a lithological change from sediments to plu-tonic and volcanic rocks (Fig. 2), but it is not clear whether the boundary is a purely litho-logical one or whether there is a tectonic break. The HSB has been divided into four subareas. The HSBa is separated from the other HSB subareas by the Hämeenlinna shear zone (Hakkarainen 1994), and the other sub-areas are separated from each other by pluton-ic rocks.

Volcanic rocks predominate, most of them being mafic porphyries and amphibolites with local amygdaloidal, breccia and agglomeratic structures, but there are also intermediate and felsic variants, partly pyroclastic and partly sedimentary in origin (Simonen 1948,1949, Neuvonen 1956, Matisto 1976a, 1976b). Ba-saltic uralite-plagioclase porphyries are abun-dant in the Hämeenlinna area and have been interpreted by Simonen (1949) as lava flows. There is variation from porphyritic via ophitic texture to typical gabbro texture, which indi-cates a close association between porphyries and mafic plutonics, and the boundaries be-tween volcanics and diorite–gabbro are thus locally gradational (Neuvonen 1956). Local-ly, the phyllites and mica schists show bed-ding and graded bedding and contain anda-lusite, cordierite, and in pelitic layers also garnet and staurolite. Impure limestone has been found in the HSBc (Neuvonen 1956). Hakkarainen (1994) divides the volcanics in the HSB into lower Forssa group and upper Häme group. The extrusives in the Forssa group are rhyolites to dacites on unknown basement, followed by andesites and basalts with pillow structures and autobrecciation. The Häme group, in turn, is characterized by predominant basalt to andesitic lava flows with interlayered pyroclastics erupted in an E–W trending fissure system.

The local stratigraphy in the different areas of the HSB has been discussed by Neuvonen (1954b) and Hakkarainen (1994). The rela-tionships between the different domains are unclear, and interfingering and the complex nature of volcanic units with many volcanic centres (see Neuvonen 1954b, Hakkarainen 1994) hinders unit by unit correlation. A ten-

tative generalized scheme based on these studies is nevertheless as follows: unknown basement or greywackes (lowermost); bimodal basalt–rhyolite/dacite with interfingering carbonates and pelites as the lowermost rocks in the Forssa group; andesites underlain locally by voluminous greywackes; the uppermost rocks in the Forssa group, locally basaltic in composition; the Häme group fissure system beginning with pelites and sulphide precipitation in isolated anoxic basins and volcanic conglomerates, and then volcanic breccias and pillow lavas, and in the central part pyroclastics showing subaerial features. The U–Pb zircon age 1888±11 Ma (Vaasjoki 1994) recorded for a dacitic volcanic in the Koijärvi area in the eastern part of the HSBb (Fig. 2) is the only available age from volcanics. According to Neuvonen (1954b), this Koijärvi unit is at the uppermost level, but Hakkarainen (1994) interpreted the area to have been juxtaposed by faulting to the same level as the Häme group. Although the exact stratigraphic position of this felsic unit is not known, in a general sense it is correlated with the Häme group.

Granodiorites and quartz diorites are common in the HSB and are locally strongly foliated. Microcline-rich granites and granodiorites occur in the western part of the subarea HSBb (Fig. 2). The Aulanko (Hämeenlinna) granodiorite (1886±14 Ma, Patchett & Kouvo 1986) (Fig. 2) cuts the surrounding schists (Simonen 1948) underlying the Häme group. This verifies the approximately 1885–1890 Ma age suggested for the Häme group. Diorites are the most voluminous mafic plutonics, but gabbros and peridotites are not uncommon. As noted above, these change, in some cases gradually, to volcanics and also lie in a close association with granitoids. Apart from the volcanogenic Kiipu Zn-prospect in dacitic to rhyolitic pyroclastic rocks (Mäkelä 1980) and some W- and Au-prospects, only some small occurrences of sulphides in volcanics and iron-magnesium metasomatic rocks have

been found (Simonen 1949, Neuvonen 1956).

A greywacke (turbidite), a thinly laminated andalusite-bearing mica schist, and a sheared and brecciated quartz-feldspar schist (mylonite) were sampled in the HSBa. The turbiditic greywacke from the HSBb contains coarse porphyroblast pseudomorphs, and a mica gneiss sample from the same subarea is characterized by late coarse muscovite flakes. An andalusite mica schist and two quartz-feldspar gneisses were sampled in the HSBc. Mica schists with ghost-like bedding of 1 to 5 cm pelite and sandier 1 to 2 cm thick units characterize the HSBd sediments underlying the Häme group. These schists are locally rich in cordierite porphyroblasts and also contain K-feldspar (microcline), relict andalusite and coarse flakes of muscovite. Migmatized mica gneisses (partly veined gneiss) occur in the southern part of the HSBd.

Two samples from the western part of the HSBa (Fig. 2) of probable volcanic origin are partly migmatitic rocks of heterogeneous nature, characterized by thin banding of diopside and amphibole-bearing layers. Most of the other samples from this area are mafic and intermediate pyroclastic rocks. The HSBb volcanics are mainly pyroclastic rocks, but some massive partly UR-porphyritic amphibolites may be massive pyroclastics, lava rocks or hypabyssal rocks cogenetic with mafic plutonics. Alteration is not uncommon and, for example, one mafic volcanic is totally altered and contains carbonate, talc, epidote, chlorite and sericite/muscovite, along with some relict hornblende grains. The volcanic rocks of the HSBc are likewise characterized by abundant pyroclastic rocks, but one sample is of possible hypabyssal origin and another is from a mafic volcanic dyke cutting across the surrounding volcanics. The HSBd is characterized by massive UR-porphyries, which at least in part change gradationally to mafic plutonics via ophitic texture to typical gabbro texture (Neuvonen 1956). It seems therefore that these porphyries are mainly massive lavas and

pyroclastic rocks (see Hakkarainen 1994), but hypabyssal variants are not uncommon. The HSBd samples of this study are mainly mafic rocks with both massive and more clearly pyroclastic variants.

The mafic plutonic samples in the HSB represent both diorites and gabbros. One sample was from the homogeneous UR-porphyrite area of the bedrock map, but was interpreted as fine- to medium-grained diorite (hypabyssal/lava). The HSB granitoid samples include quartz diorites, granodiorites and granites. The mafic and intermediate granitoids have abundant mafic enclaves and both hornblende (sometimes lacking) and biotite. In the western part of the HSBb there is an extensive area of granite with microcline porphyroblasts containing plagioclase inclusions (Neuvonen 1956). Three porphyritic granodiorite samples are from this 'granite' pluton. An important feature is the lack of mafic enclaves. One granite sample is from a small microcline granite occurrence, which possibly contains ghost inclusions of granodioritic rocks (Neuvonen 1956).

Microcline granite Complex (MC)

The MC is characterized by the occurrence of late-kinematic granites with an interpreted age of about 1.84–1.82 Ga, and possibly 1.84–1.81 Ga (age data in Korsman et al. 1984, Huhma 1986, Suominen 1991). Older gneissose granodiorites associated with gneisses and small gabbro lenses are found in the southern part of the MC. The hornblende gneisses and pyroxene gneisses have relict textures indicating a volcanogenic origin (Simonen 1949). In addition to the predominant high grade coarse-grained garnet–cordierite–microcline veined gneisses, there are mica gneisses with textures indicating a sedimentary origin. At present there are no indications of economic mineralizations in the MC.

The migmatites in the MC contain abundant 2–30 mm granitic leucosomes with 1–3 mm melanosomes (stromatic). The mineralogy is quartz, microcline, plagioclase, biotite, ± cordierite, ± garnet, ± sillimanite and accessory magnetite. Magnetite seems to be concentrated in cordierite-rich parts. The paragenesis in these samples is indicative of nearly granulite facies conditions, but the exact nature is obscure. Evidently most of the leucosomes are in situ, but intrusive veins are not uncommon. One critical question is: What are the proportions of the different components and are these rocks partly restites. One sample of probable volcanic origin bears amphibole-rich streaks, suggesting a tuff origin.

Older granitoids (six samples) in the MC are deformed in various degree and vary from slightly foliated to gneissic granodiorite. They are characterized by mafic enclaves and abundant granite dykes. Granitization around dykes and joints is another common feature, as is the occurrence of a small amount of sulphides in thin shear bands. The most abundant granitoid type in the MC is microcline granite, divided among normal even-grained, pegmatitic, porphyritic, garnet-bearing and muscovite-bearing variants (Simonen 1949). Except for one sample, all are characterized by the absence of mafic enclaves and only schist inclusions are found. The exception is a sample near to the contact of the HSB, where UR-porphyrite inclusions occur.

There are 19 microcline granite samples, of which 14 represent the normal variant with abundant microcline and a small amount of biotite. Three samples represent the porphyritic variant, and one of these contains abundant muscovite. Garnet in the form of grain aggregates occurs in one sample, and abun-

dant sillimanite with garnet, biotite and mus-covite characterize another. An almost unde-formed quartz monzodiorite, dated at 1812±2 Ma (Vaasjoki 1995), was found in the micro-cline granite area. If, as seems to be, the quartz monzodiorite is comingling with the

granite, at least some of the granite must be of contemporaneous age. Both hornblende and biotite occur, and coarse-grained sphene, ap-atite and zircon are characteristic features of this rock.

GEOCHEMISTRY OF SEDIMENTARY ROCKS

Factors controlling the composition of sedimentary rocks

An interpretation of the composition of the provenance area (source rock composition) is central to most studies dealing with the geo-chemistry of sedimentary rocks. Although the chemical composition of clastic sediments is essentially controlled by the lithology of the provenance area, the composition of any par-ticular sedimentary rock is also controlled by weathering, sedimentary sorting (grain-size effects) and compositional changes during post-depositional processes, including dia-genesis, metamorphism and migmatization. The petrography of greywackes has also been used to predict provenance (e.g. Dickinson & Suczek 1979), but the greywacke matrix prob-lem and the effects of diagenesis and meta-morphism in the mineralogy in most cases prevent a reliable interpretation. This is seen in the possibility of a post-depositional break-down of K-feldspar in Kaleva greywackes (Kohonen 1994). In the following, the effect of weathering is briefly discussed, and then sedimentary sorting, the influence of tectonic environment and the elements most reliable for an interpretation of the source rock com-position. The influence of post-depositional changes is the most difficult and controversial question and only the effects of migmatiza-tion are considered here.

The effect of weathering on the chemical composition depends on the amount of labile components in the source rocks, the duration of the process, the climatic environment and the erosion rate. The effects of weathering are

insignificant in tectonically active areas (es-pecially in arid areas) with high erosion rates, but will show up more clearly in a passive tectonic setting (especially in humid areas) with a low erosion rate. Complex recycling sedimentary histories with increased effects of weathering are more common in passive tectonic settings but not impossible also in other tectonic settings.

Grain-size effects are very important, be-cause the finer fractions, which are enriched in clay minerals, are also enriched in most trace elements and show more pronounced effects of weathering (e.g. McLennan et al. 1990). Grain-size fractioning also play a cen-tral role in dividing the different provenance components into fractions. Volcanic rocks tend to produce finer grain-size material than do coarse-grained granitoids, and thus sands and their associated muds may represent dif-ferent source components, with sand being enriched in granitoid components and mud in volcanic components. The geochemistry of sand–mud pairs also reflects the environment. For example, the grain-size distribution in volcanic environment is close to unimodal and may produce more or less similar geochemical fingerprints in a sand–mud pair. In contrast, the bimodal grain-size distribution characteristic of granitoid-dominated environment will proba-bly produce considerable geochemical diver-gence in sand–mud pairs (see data in McLen-nan et al. 1990). The degree of sorting varies in turbidites, and, in particular, the composi-

tion is affected by the greater amount of mud chips in some samples. Poorly sorted mass flows can also be expected to show a more mixed composition. In many cases the source will be a recycled sedimentary provenance, which in an extreme situation may produce a greywacke with mud-originated geochemistry from a metamorphosed pelite.

In their study of geochemical, petrographic and grain-size variations within single turbidite beds, Korsch et al. (1993) found great geochemical variation between coarse and fine fractions. With decreasing grain-size they noticed a decrease in SiO_2 contents, an enrichment in TiO_2, Al_2O_3, K_2O and Na_2O contents, and an increase in the abundances of most trace elements (Ce, Cr, Cu, Ga, La, Nb, Ni, Pb, Rb, Sc, Th, U, V, Y, Zn, Zr). Although the enrichment factor varies from one element to another, the Th/Sc ratio remains nearly constant (see below).

The tectonic setting of a depositional basin is related with the provenance that provides the sediment detritus, and thus tectonic setting is considered to correlate with the composition of sedimentary rocks (Valloni & Maynard 1981, McLennan et al. 1990), and chemical compositions have also been evaluated as a means of interpreting the tectonic setting of ancient sedimentary rocks (e.g. Bhatia 1983; Bhatia & Crook 1986). One major problem in regard to such interpretations is that any greywackes associated with the tectonic setting of deposition may have a totally different source, especially in trench sedimentation. This has been seen in the Java Trench sediments, which are not derived from the arc but probably were transported by the Ganges rivers (Moore et al. 1982).

Thorium, Sc and REEs are among the most useful elements in deducing the average source composition, while other trace elements, such as Cr, Ni, Co and Ba, are considered much less reliable because they are more easily affected by weathering, dissolution, transport, deposition and diagenesis (e.g. McLennan et al. 1990). Thorium is considered highly incompatible and Sc relatively compatible, and both elements are transferred quantitatively to terrigenous sediments during sedimentation (Taylor & McLennan 1985). The Th/Sc ratio accordingly has been used to monitor the average source composition, and in some cases there is no grain-size effect on the ratio, as noted above. On the other hand, the sand–mud pairs of McLennan et al. (1990) often had different Th/Sc ratios, with the muds normally having either comparable or significantly lower Th/Sc ratios, indicating a more mafic source.

Although chromium may be enriched in shales due to its adsorption on clay minerals during weathering or deposition, in general the Cr/Th ratio appears to reflect the differences in source composition (Condie & Wronkiewicz 1990). Most of the sedimentary samples in this study showed the effects of only moderate weathering and chromium could reliably be used in the interpretation of source variation.

Although the discussion here is very brief (see McLennan et al. 1990 for a detailed discussion), it should be clear that the geochemical history of sedimentary rocks can be highly complicated. The effects of chemical and biogenic sedimentation (sulphides, carbonates and organic matter) during basinal evolution may complicate the picture still more. The effect of the factors controlling the geochemistry of sedimentary rocks and the interpretation of provenance components for the studied sedimentary rocks are discussed below.

Classification

In this study, sedimentary rocks comprise all sampled rocks that show sedimentary structures in outcrop scale and/or blastoclastic texture in microscopic scale, and mica gneisses and migmatites that have an interpreted sedimentary origin. In many cases, grading is visible in the outcrop, but the texture in thin section is totally metamorphic. The occurrence of graphite and concretions was used as an indication of sedimentary derivation in massive structureless mica gneisses and migmatites. Although most of the samples discussed in this section are almost certainly sedimentary, some of the SG1 rocks (see below)

could be volcanoclastic in origin. The sedimentary rocks have been divided into eight groups (SG1–SG8), primarily on the basis of chemical composition and especially the occurrence of the more conservative elements Th, Sc and Cr (see previous section). The lithological nature and regional characteristics have also been taken into account. The locations of samples of the different groups are shown in Fig. 3, and some general characteristics are set out in Table 1. Table 2 reports major and trace element concentrations, mainly as arithmetic means, for groups, subgroups and some single samples. The values of ore-related elements are presented and discussed in Lahtinen and Lestinen (1996).

The sedimentary group 1 (SG1) is interpreted to be composed mainly of arc-derived material from a local source, and is characterized by low CIA values (Chemical Index of Alteration, Nesbitt & Young 1982) and wide compositional variation (Table 1). Group SG2 includes five samples of generally rather mafic source but otherwise differing from each other. Groups SG3–SG7 are basement-related groups and most of the sedimentary rocks that were sampled fall into these groups (Fig. 3). The detrital zircon data from the TSB (Huhma et al. 1991, Claesson et al. 1993) show the SG3–SG7 rocks to have a mixed Archaean and Palaeoproterozoic source. SG3 rocks are mainly psammitic rocks with the source dominated by felsic components, as seen in high Th/Sc and low Ti/Zr ratios. SG4 is also characterized by psammitic rocks, but the mafic component is greater, as expressed in lower Th/Sc and Th/Cr and higher Ti/Zr ratios. SG5 is mainly composed of migmatites (veined gneisses) and has chemical compositions close to SG4 (Table 1) but differing in lower SiO_2 contents and higher Ti/Zr ratios and especially in a larger amount of graphite and sulphides (Table 2). SG6 samples are pelites, pelitic mica
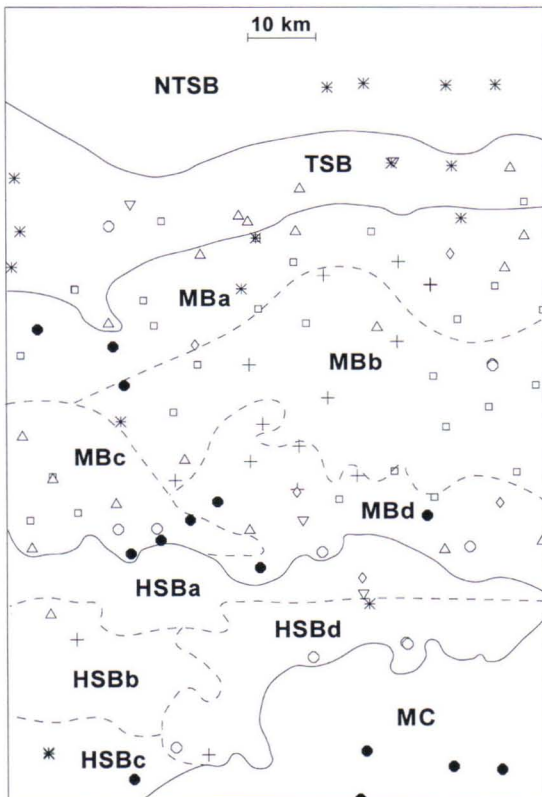

Fig. 3. Sample locations of sedimentary rocks in the study area. For more detailed lithology see Fig. 2. Asterisks – SG1, open diamonds – SG2, open upright triangles – SG3, open squares – SG4, crosses – SG5, open circles – SG6, filled circles – SG7, open inverted triangles – SG8.

Table 1. Major chemical and lithological characteristics of sedimentary groups in the Tampere–Hämeenlinna area.

Group	N	$SiO_2\%$	K_2O/Na_2O	CIA[1]	Th/U	Th/Sc	Th/Cr	Ti/Zr	Grw	Pel	Mgn	Mig
SG1	16	56.6–74.8	0.5–2.0	51.0–58.7	2.1–4.6	0.3–1.2	0.04–1.04	9.0–35.4	3	1	7	5
SG2	5	53.9–62.8	0.9–1.8	54.5–67.1	3.0–4.0	0.2–0.4	0.02–0.08	25.8–62.8	1	1	1	2
SG3	19	66.7–72.0	0.7–1.3	55.8–61.5	3.0–6.1	0.8–1.5	0.11–0.24	8.9–16.7	9		2	8
SG4	28	65.7–69.0	0.8–1.2	56.8–60.0	3.4–6.4	0.5–0.8	0.09–0.14	16.6–20.5	8	1	6	14
SG5	15	62.8–65.5	0.9–1.3	57.7–60.2	3.5–5.5	0.5–0.6	0.08–0.12	20.9–26.7			2	13
SG6	11	56.3–64.6	1.5–3.4	63.1–68.5	3.0–4.6	0.5–0.8	0.08–0.11	22.0–37.3		3	5	3
SG7	14	58.5–63.8	1.0–2.2	56.9–68.5	4.0–7.7	0.6–1.1	0.12–0.16	20.4–35.5		1		13
SG8	4	60.4–-63.3	1.3–1.9	59.3–64.0	3.3–6.5	0.5–0.7	0.08–0.18	21.7–27.5	4			

Note: 10th and 90th percentiles are used for the range, except for groups SG2 and SG8 where total range is used. Grw – greywacke; Pel – pelite/siltstone; Mgn – mica gneiss; Mig – migmatitic mica gneiss or mica gneiss fragment in migmatite.
[1] Chemical Index of Alteration (Nesbitt & Young 1982).

gneisses and migmatites with higher CIA values. The migmatites of interpreted pelitic origin characterize SG7 and, though compositionally similar to SG6, their higher Th/Sc and Th/Cr ratios indicate a more felsic source. Group SG8 comprises four mafic greywackes that do not fall into any of the above groups and are considered one by one.

The groups SG3–SG7 partly overlap and in some cases exhibit a gradational change from one to the other. Although the classification of some specific sample may be questioned the groups show distinct geochemical and also lithological characteristics, which support the proposed grouping. After a summary of the major and trace element concentrations and the effects of migmatization, these groups, with their subgroups, are discussed below; the differences in source components are considered and probable tectonic settings are proposed.

Interpretation of major and trace element concentrations

There are two main disadvantages in basing an interpretation solely on the major element data. In the case of SiO_2, TiO_2, Al_2O_3, FeO and MgO, normal source variation and grain-size variation (mainly quartz-dilution) give rise to similar trends (e.g. Fig. 4). In the case of CaO and less clearly Na_2O and K_2O, vectors are different.

The SG1 samples mostly follow the average trend for the TSB volcanics, while the other sedimentary groups tend to follow the inferred grain-size trend. The psammite groups (SG3 and SG4) are overlapping in their geochemical fields, but clearly differ from the more pelitic groups SG6 and SG7. The SG3 sample from the MBd with an exceptionally high CaO value (S8911060 in Table 2) contains metamorphic labradoritic plagioclase. The low Na_2O and mature origin comparable with other SG3 samples do not favour high Ca in clastic plagioclase and thus the high Ca-content of the plagioclase is probably due to the metamorphic recrystallization of carbonate-bearing greywacke.

The groups SG3–SG7 show an increase in trace elements Cr, Nb, Ni, Rb, V, Zn and decrease in Sr and Zr along the inferred grain-size trend (Sr, Zr, Cr in Fig. 5, other data not shown). The same trend is seen in the differences between group means (Table 2). The Ba
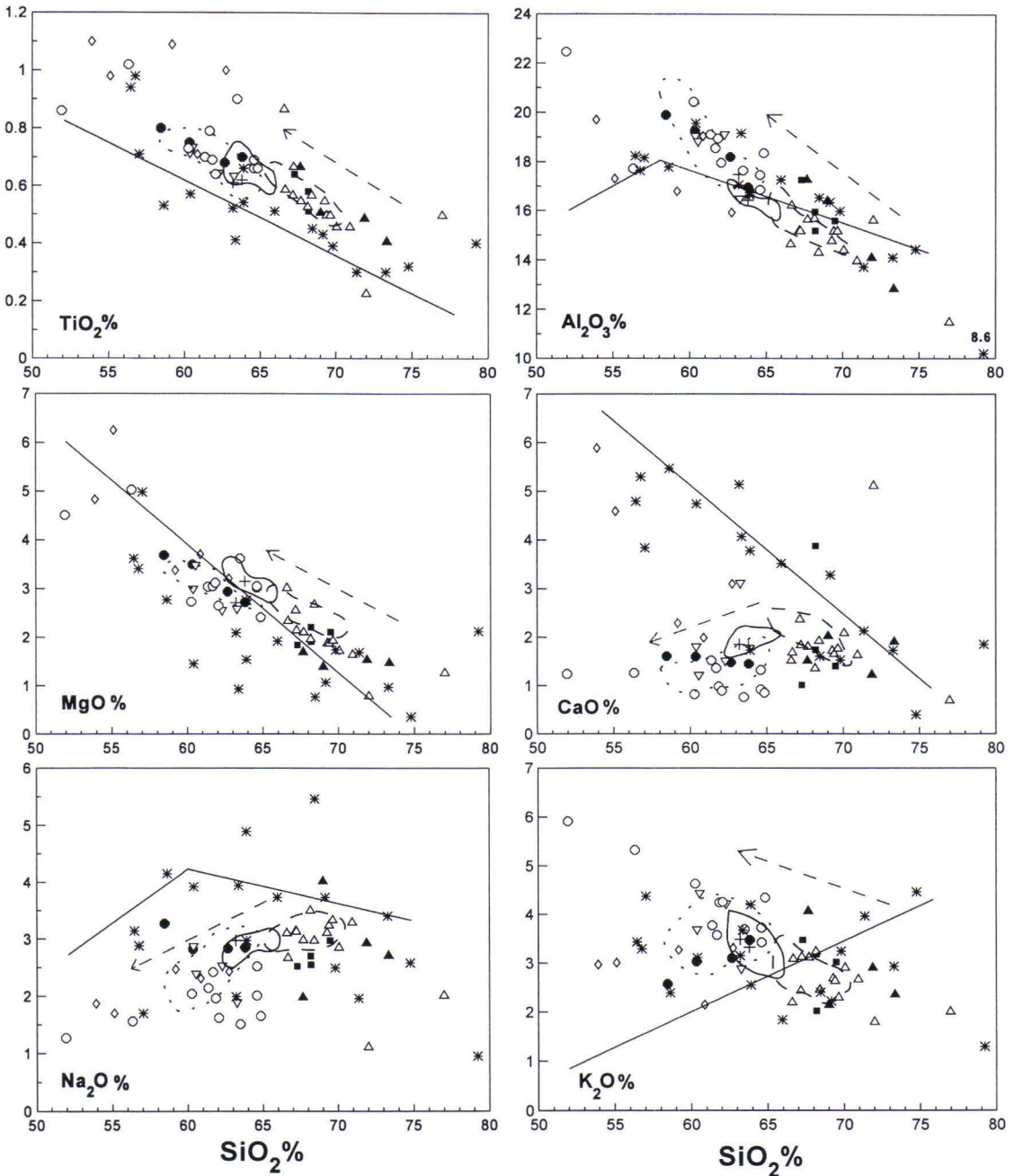
Fig. 4. Harker-type selected major element (%) variation diagrams for sedimentary rocks in the Tampere–Hämeenlinna area. Data from this study. FeO is total Fe as FeO. Asterisks – SG1, open diamonds – SG2, open upright triangles – SG3 excluding TSB, filled triangles – SG3 samples from the TSB, filled squares – SG4 from the TSB, crosses – SG5 from the HSB, open circles – SG7, filled circles – SG7 from the MC, open inverted triangles – SG8. Dashed line – main field of SG4 samples, solid line – main field of SG5 samples, dotted line – main field of SG6 samples, straight line – average differentiation trend of the TSB volcanics (data from this study), dashed arrow – inferred grain-size trend based on Korsch et al. (1993) and results of this study.

Table 2. Average chemical composition of metasedimentary rocks in the Tampere–Hämeenlinna area. Compositions are reported for groups and subgroups and some single samples.

Group	SG1	SG1	SG1	SG2	SG3	SG3	SG3	SG3	SG3
Subgroup[1]	MA	low-Cr	high-Cr		HSBb	MBd	MB	MB/M	TSB
N	1	7	5	5	1	1	4	8	5
SiO_2	74.78	64.93	58.56	58.38	76.99	72.02	68.48	68.44	70.35
TiO_2	0.32	0.51	0.74	0.98	0.50	0.23	0.56	0.56	0.49
Al_2O_3	14.43	17.52	17.69	17.76	11.53	15.66	14.94	15.15	15.36
FeO	1.63	3.96	6.81	7.92	3.55	2.17	4.53	4.63	3.45
MnO	0.04	0.12	0.13	0.14	0.06	0.06	0.09	0.08	0.07
MgO	0.36	1.40	3.51	4.28	1.29	0.81	2.15	2.19	1.59
CaO	0.40	3.44	4.64	3.57	0.72	5.14	1.82	1.79	1.66
Na_2O	2.58	3.95	2.97	2.16	2.03	1.13	3.13	3.13	2.84
K_2O	4.46	2.94	3.21	2.94	2.03	1.82	2.96	2.66	2.96
P_2O_5	0.05	0.20	0.31	0.21	0.14	0.07	0.18	0.14	0.15
CO_2	0.01	0.17	0.19	0.03	0.00	0.02	0.06	0.03	0.02
$C_{Graf.}$	0.00	0.02	0.09	0.18	0.01	0.00	0.09	0.04	0.12
S	<0.01	0.06	0.01	0.18	0.01	0.01	0.03	0.05	0.02
F	0.02	0.07	0.13	0.11	0.01	0.02	0.07	0.07	0.06
CIA^2	59.9	53.8	53.3	58.6	63.9	54.7	57.3	58.2	59.3
Ba	1070	1040	982	430	293	1210	616	569	726
Cl	37	82	102	109	31	35	45	81	40
Cr	10	24	135	141	163	32	95	89	64
Nb	12.1	12.0	11.9	9.6	8.2	19.6	9.6	9.7	11.5
Ni	20	22	47	66	54	26	42	49	37
Rb	123	87	116	136	87	66	121	107	109
Sr	90	559	735	194	122	627	240	228	283
V	43	79	181	211	92	34	110	113	89
Y	29	21	19	24	21	22	24	24	24
Zn	30	78	109	139	75	55	71	83	71
Zr	186	180	156	153	263	211	283	231	203
Co	5	7	18	21	-	3	11	12	9
La	36.6	32.8	32.6	24.1	27.9	41.3	45.6	40.5	37.7
Sc	11.5	14.5	25.6	25.1	13.5	4.8	15.0	14.4	12.3
Th	10.8	7.9	6.9	7.4	11.6	13.2	15.8	15.1	14.3
U	3.3	2.4	1.9	2.2	2.9	3.3	3.4	2.7	3.6

Major elements (wt%), S (wt%) and Ba–Zr (ppm) analysed by XRF, $C_{Tot.}$ by Leco-analyser and F by ion selective electrode at the GSF laboratory; Co–U by neutron activation at the Technical Research Centre of Finland; CO_2 by wet method at XRAL in Canada. $C_{Graf.}$ calculated from $C_{Tot.}$ and CO_2.

[1] MA – Mauri arkose (S8910941); low-Cr /high-Cr – excluding HSB samples; HSBb – sample S8911086; MBd – sample S8911060; MB – Mica gneiss-migmatite Belt; MB/M – migmatitic mica gneiss or mica gneiss fragment in migmatite; TSB – Tampere Schist Belt; HSBd – sample S8911102; MC – Microcline granite Complex.

[2] CIA = molecular ratio of $(Al_2O_3/(Al_2O_3+CaO+Na_2O+K_2O)) \times 100$ (Nesbitt and Young 1982).

and Y values are scattered but with somewhat higher values normally found in the pelitic groups SG6–SG7. Likewise the sulphur values are scattered but show a trend coinciding with the grain-size trend. This is not a true grain-size trend, however, but a composite effect of sulphide formation and slow sedimentation rate (smaller grain size). The occurrence of a sulphide component will change the concentrations of many sulphur-related trace metals. On the other hand, the only small increase of Ni (10–30 ppm) in sulphide-bear-

Table 2 (continued).

Group	SG4	SG4	SG4	SG5	SG5	SG6	SG7	SG7	SG8
Subgroup[1]	TSB	MB	MB/M	HSBd	MB			MC	
N	4	10	14	1	13	11	10	4	4
SiO_2	68.29	68.09	67.09	63.81	65.07	61.19	61.68	61.32	61.64
TiO_2	0.56	0.57	0.59	0.62	0.60	0.76	0.71	0.73	0.68
Al_2O_3	15.99	15.02	15.54	16.42	16.28	18.68	18.27	18.56	18.32
FeO	4.04	4.67	4.87	6.34	5.54	6.86	6.38	6.83	6.60
MnO	0.10	0.09	0.09	0.08	0.09	0.08	0.10	0.10	0.09
MgO	2.02	2.46	2.52	3.15	2.88	3.29	3.07	3.21	2.88
CaO	2.01	1.93	2.07	1.83	2.04	1.08	1.64	1.54	1.89
Na_2O	2.69	3.16	2.95	2.85	2.95	1.88	2.43	2.94	2.40
K_2O	2.92	2.66	2.87	3.32	3.16	4.26	3.80	3.04	3.78
P_2O_5	0.16	0.16	0.14	0.15	0.17	0.13	0.13	0.10	0.16
CO_2	0.02	0.09	0.04	0.01	0.04	0.02	0.02	0.04	0.02
$C_{Graf.}$	0.11	0.08	0.04	0,68	0.22	0.51	0.64	0.00	0.20
S	0.05	0.03	0.05	0.04	0.11	0.33	0.57	0.03	0.07
F	0.07	0.06	0.07	0.13	0.10	0.11	0.08	0.21	0.12
CIA^2	61.7	57.7	57.5	58.0	58.6	66.9	63.1	63.6	61.9
Ba	493	568	595	588	581	636	651	389	580
Cl	44	47	93	66	124	65	148	219	84
Cr	81	96	99	215	89	151	123	123	118
Nb	11.0	9.0	9.7	10.3	10.0	13.5	14.2	15.7	12.8
Ni	47	54	54	75	58	86	77	74	64
Rb	112	101	119	147	125	180	152	249	153
Sr	196	228	236	229	209	149	200	140	182
V	108	119	124	149	136	188	163	148	132
Y	24	22	23	22	21	26	27	30	27
Zn	79	75	85	142	108	170	141	138	125
Zr	187	189	188	178	174	173	185	145	169
Co	12	13	14	15	17	18	16	18	18
La	32.1	32.0	32.6	34.1	31.0	38.3	42.1	34.5	34.5
Sc	15.5	16.0	17.1	21.2	18.6	24.6	19.5	23.8	21.2
Th	10.9	10.8	11.5	13.4	9.9	13.9	16.9	16.4	13.0
U	2.6	2.3	2.6	2.4	2.3	3.7	3.4	3.0	2.8

ing (1–2% S) black schists relative to pelitic rocks with S about 0.1–0.3% indicates that most of the Ni variation is due to variation in ferromagnesium mineral content. The same is true for other sulphide-related elements (Co, Zn) occurring in ferromagnesium silicates (combined grain-size and source variation), although it is clear that sulphide precipitation produces minor input. The organic carbon component (at present graphite) also shows a trend partly coinciding with the grain-size trend (Fig. 6), but the correlation is poorer than for the sulphur data. The black schist samples exhibit an increase in Zn, Ni, Ag, Pd, Mo, B and Te and a weaker increase in As, Sn, Sb and Bi (Lahtinen & Lestinen 1996). Since these samples also have high sulphur contents, some of these elements may have been bounded at least partly in the sulphide fraction. The black schist samples also have higher V values (not shown) due to vanadium accumulation in carbonaceous rocks (e.g. Breit & Wanty 1991).
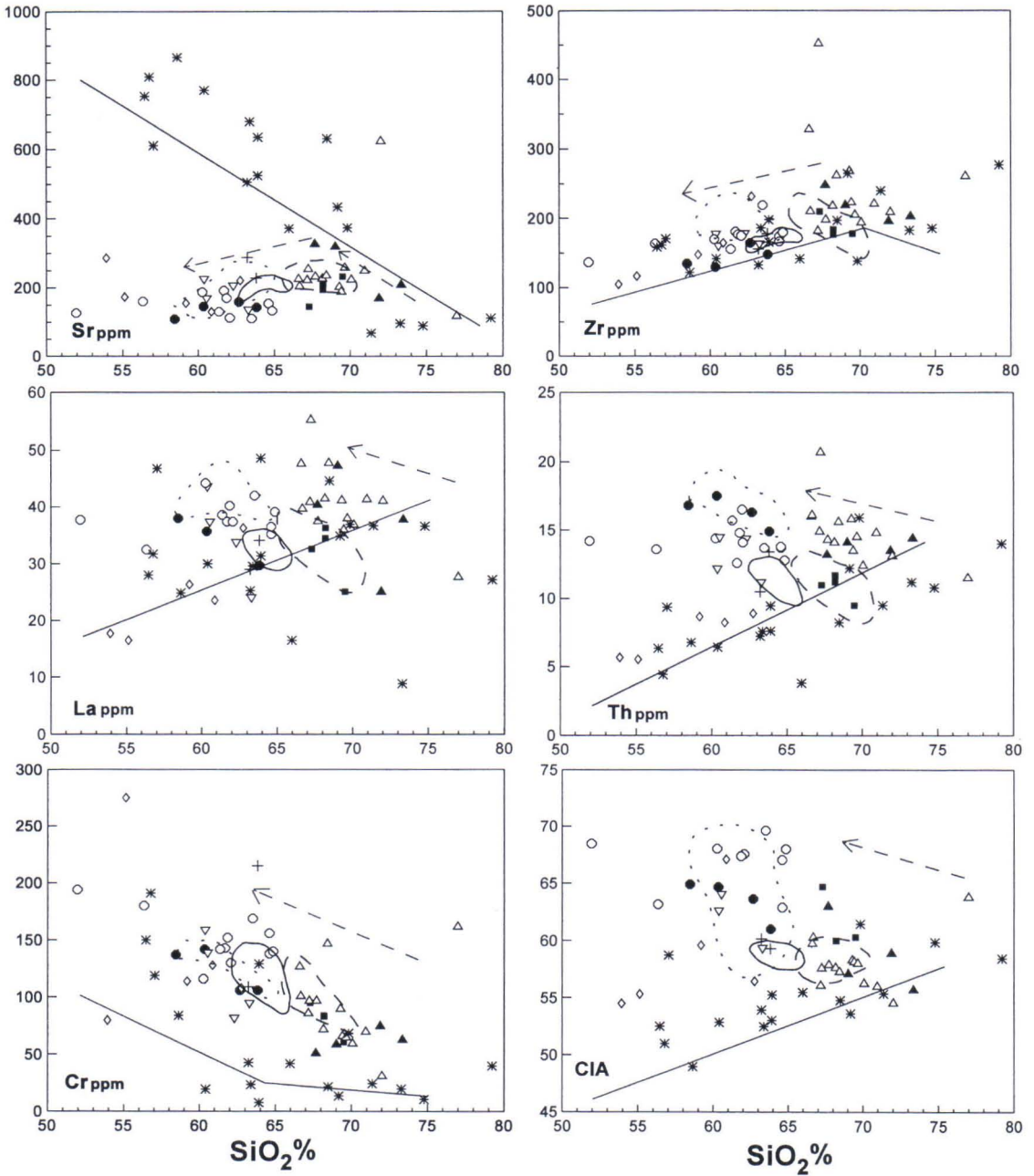
Fig. 5. Harker-type selected trace element (ppm) and CIA-value (Nesbitt and Young 1982) variation diagrams for sedimentary rocks in the Tampere–Hämeenlinna area. Data from this study. See Figure 4 for symbols.

Effects of migmatization

The MB is characterized by upper amphibolite facies tonalitic migmatites, with more granitic leucosomes found locally. The MC migmatites contain granitic leucosomes, with a mineral paragenesis indicative of high grade, possibly granulite facies conditions. Except for the lower CO_2 and $C_{Graf.}$ and higher Cl, the average compositions of veined gneisses and mica gneiss fragments in migmatites are exactly the same as in the non-migmatized samples in the tonalitic migmatite zone (MB). The chlorine data are noteworthy because they indicate an increase in chlorine during migmatization (Fig. 7) and agree well with the interpretation of a prominent fluid phase during

migmatization in the MB (Kilpeläinen et al. 1994). The low B values in migmatites indicate a loss during migmatization.

The fluorine data do not show either depletion or enrichment during migmatization in the MB. The graphite data (Fig. 6) are somewhat problematic because there is variation in the primary levels of C_{Graf}, but the trend to lower $C_{Graf.}$ values with higher Cl values indicates some loss of graphite during migmatization. The low CO_2 contents of the MB gneisses, with generally lower values in migmatites and abundant occurrence of concretions, indicate that carbonate has been locally common in these rocks, but carbon dioxide has been
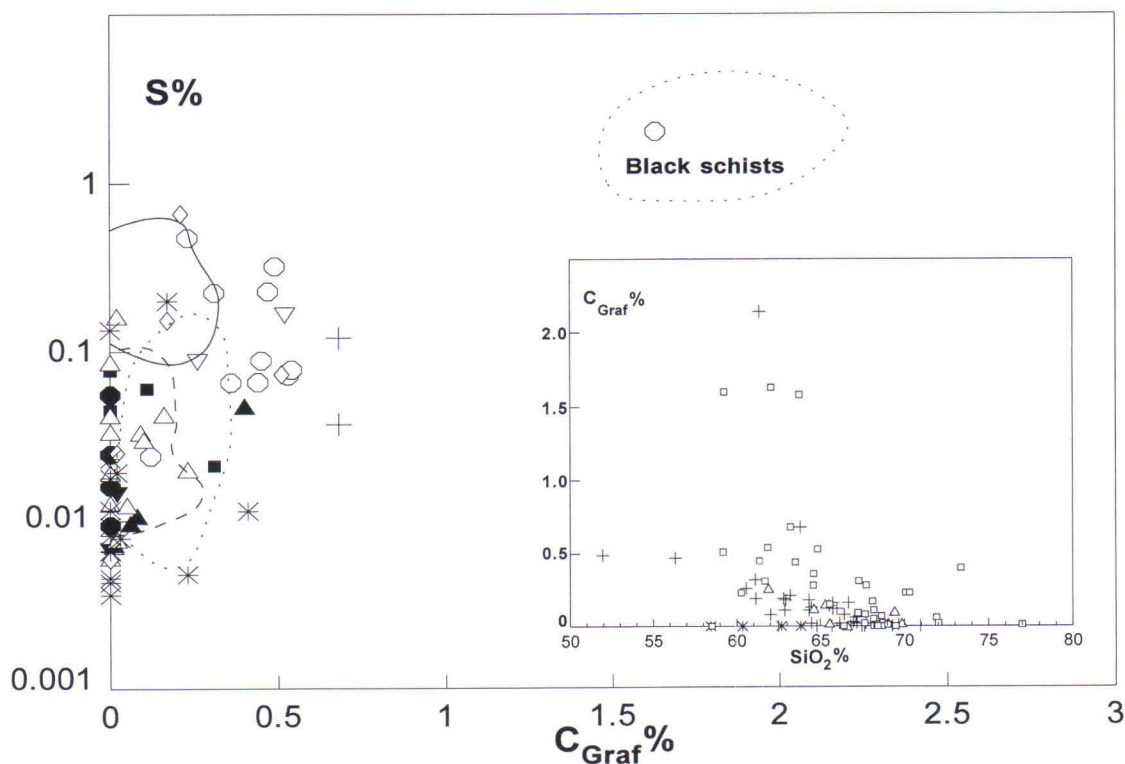

Fig. 6. $C_{Graf.}$–S and $C_{Graf.}$–SiO_2 (insert) diagrams for sedimentary rocks in the Tampere–Hämeenlinna area. Data from this study. Only samples from groups SG3–SG7 are shown in the insert figure. See Figure 4 for symbols in the main figure. Symbols in the insert figure: open squares – greywackes, pelites and mica gneisses, open triangles – mica gneiss fragments in migmatites, crosses – migmatites, and asterisks – migmatites from the MC.

lost during metamorphism. Otherwise there is
no clear indication of great chemical change
during migmatization in the MB. The scatter
in Rb values (Fig. 7), and also in some sul-
phur-related trace elements, indicates a redis-
tribution of these elements, but there are no
observable trends.

Along with higher Cl values, the migma-
tites in the MC have clearly lower values of
S, B, Cu, As, Bi, Sb, Ag?, Au?, Te?, Pd? and
Ba? (Lahtinen & Lestinen 1996), and three
samples have higher values of Rb (Fig. 7). All
these samples are totally devoid of graphite
(Table 2) and the three Rb-rich samples also

have high F (Fig. 7). One sample deviates
with 'normal' levels of Rb and F. The diffi-
culty in interpreting the MC samples is the
lack of primary precursor material and the
possibility that different processes have oper-
ated in the migmatites. For example, partly
restitic material may later have been imprint-
ed with fluids (Rb and Sn). The high level of
LIL elements (K, Rb, Th, U, and La) does not
favour a high level of restite, as these ele-
ments normally are enriched in the first melts.
The sample with lowest SiO_2 also shows low
K_2O, and this could be interpreted as due ei-
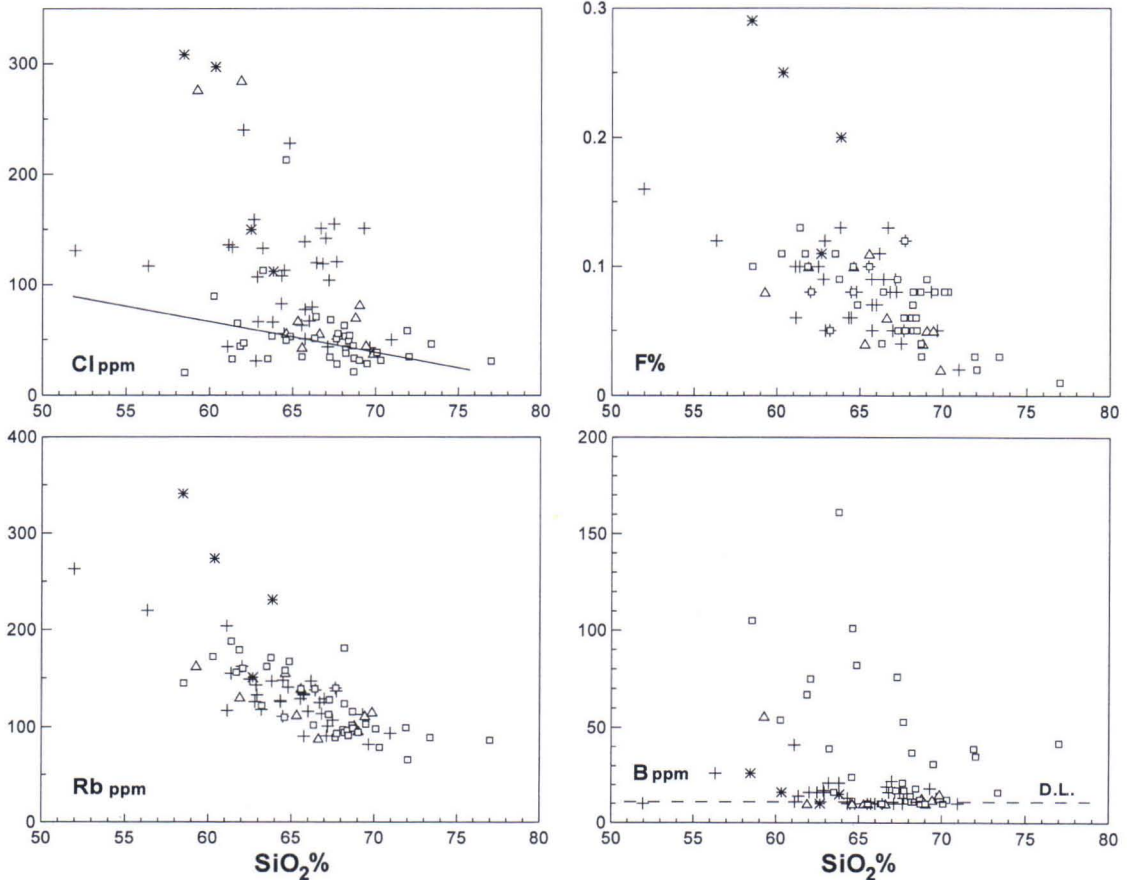ther to a small loss of melt from the veined

Fig. 7. Harker-type selected mobile trace element variation diagrams for groups SG3–SG7 in this study. See insert in Figure 6 for symbols. D.L. is the detection limit of B.

gneiss or to a higher proportion of melanosome.

The model proposed for the geochemical features in the MC migmatites is a combination of loss of some elements (C, S, B, Cu, As and Bi) into a fluid phase during migmatization or earlier, and a gain of Cl, F and possibly also Rb and Sn from the fluid phase. The high Rb could point to fluid phase expelled from microcline granites, but the F values are higher than the normal level of microcline granites (<0.05% F), although the nature of the last expelled fluids is not known. The increase of F in more anhydrous restite biotites (Patiño Douce & Johnston 1991) during melting is one possibility, but then these samples should have a very large restitic composition (not favoured). A difference in precursor material cannot be excluded. The occurrence of Cl and F in the fluid phase during migmatization is an interesting possibility. In particular, the high values of F could indicate a genetic link to fluids derived from mantle-derived alkaline WPB-type melts. The F and Cl most probably are situated in biotite and we need to know whether there are different generations of biotite and which generation bears the high F and Cl. The interpreted loss of graphite has probably changed the fluid phase to more CO_2-rich, which may be partly responsible for nearly granulite facies metamorphic conditions and for the crystallization of magnetite.

Description of sedimentary rocks

SG1 (arc-related rocks)

SG1 rocks can be divided into three subgroups: HSB gneisses, low-Cr rocks (including Mauri arkose) and high-Cr rocks. The two samples from the HSBc (SiO_2 71.4% and 73.3% in Figs. 4 and 5) are either slightly altered volcanics or epiclastic rocks of volcanic derivation. The HSBd sample is a sheared rock and has low Al_2O_3, Na_2O and K_2O and high FeO (not shown) and MgO contents (SiO_2 79.2%, Fig. 4). The other SG1 samples are characterized by normally lower TiO_2 and MgO and higher CaO and Na_2O compared with other groups (Fig. 4). They also have higher Ba, Sr and P_2O_5 abundances at similar SiO_2 values (Table 2) and the values of the Chemical Index of Alteration (CIA) are rather low (Fig. 5) indicating rapid erosion. They follow the source variation trends and the Th/U ratios (Figs. 4–5, 8) are lower than the upper continental crust value of 3.8 (McLennan et al. 1990).

Both the low- and the high-Cr groups (Figs. 5, 8 and 9) are geochemically related to high-K calc-alkaline and/or shoshonitic rocks, possibly mainly to volcanics. The Mauri arkose (see Table 2) has a granite source with 1.9 Ga zircons (Matisto 1977), indicating origin mainly from the TSB-related granitoids, and the low Cr relative to V differentiates it from groups SG3–SG7 (Table 2). These features support an origin comparable to the other SG1 rocks, the main difference being the more granitoid-dominated source in the Mauri arkose. The source of the SG1 rocks has varied from mafic to more felsic, as seen in Figs. 4–5 and 8, especially in the Sc–Th relation. The wide variation in chemical composition, the similarity with the TSB volcanics and the low degree of weathering indicate a rapid erosion of arc material as well as a rapid deposition in arc-related basins without any strong mixing in large river–delta systems.

The NTSB SG1 samples are all of low-Cr group, but more samples are needed to verify the absence of other sedimentary rock types from the NTSB. There are four SG1 samples in the MB, of which two occur near the boundary of the TSB and MBa. The easternmost of these two samples has exceptionally low Cr (8 ppm at SiO_2 63.9% in Fig. 5) and a graphite content of 0.17% C. The greywacke-like mi-

cagneiss from the MBb is of low-Cr type. The
third SG1 sample in the MBa is a migmatitic
gneiss of high-Cr type with high P_2O_5 (0.37%)
and $C_{Graf.}$ of 0.41%. Although this sample may
have a partially tuffitic origin (detrital-like
zircon indicates the occurrence of more felsic
component), the occurrence of rocks with a
geochemical link to high-K calc-alkaline and
shoshonitic rocks in the MB indicates that the
TSB and MB have had a common history.

SG2

As seen in Figs. 4–5 and 8, the rocks of this
group give indication of a more mafic source
than do the rocks of other groups (excluding

SG1 in part). Because these samples also dif-
fer from one another, they are considered here
one by one. The migmatite from the MBd
(S8911001; SiO_2 53.9% and Th 5.7 ppm) may
be a tuffaceous layer in SG4 sediments, but
the $C_{Graf.}$ of 0.17% indicates the occurrence of
a sedimentary component. The easternmost
SG2 sample in the MBd (Fig. 3) is a gneiss
(8910978; SiO_2 55.1% and Th 5.6 ppm) char-
acterized by very high Cr content (275 ppm)
indicating a primitive mafic source, but the
$C_{Graf.}$ of 0.21% confirms the sedimentary ori-
gin. Both samples to some extent follow the
general source variation trend and have high
CaO (Figs. 4). And both can be considered as
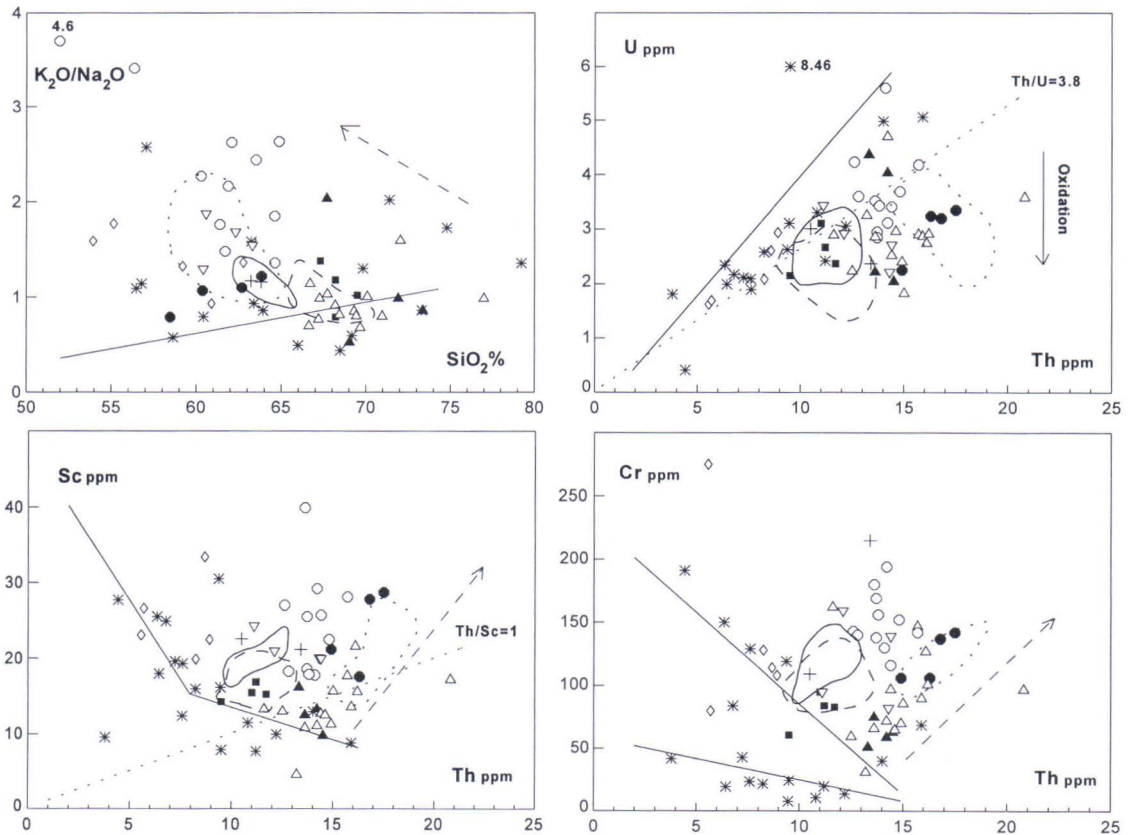tuffaceous rocks with a high proportion of

Fig. 8. K_2O/Na_2O–SiO_2, U–Th, Sc–Th and Cr–Th diagrams of sedimentary rocks in the Tampere–Hämeenlinna area. Data from this study. See Figure 4 for symbols. Dotted straight line in the Sc–Th diagram is the average crustal ratio from McLennan et al. (1990).

mafic volcanic source. The greywacke SG2 sample in the MBa (SiO_2 59.2% and Th 8.7 ppm) deviates from the SG3–SG7 samples in having higher TiO_2 (1.09%), V (302 ppm) and Sc (33.4 ppm) indicating a mafic component with tholeiitic character. The elevated $C_{Graf.}$ of 0.51% may slightly increase the V level but is not responsible for the enrichment of Ti.

The pelite sample from the HSBa (8911008; SiO_2 60.9% and Th 8.2 ppm) is an andalusite micaschist. The pelitic character is seen as high CIA value (67.1), but the low La, Th and Th–Sc relation (also Th/U ratio) suggest a source enriched in mafic component. The veined gneiss from the MBa (S8910847; SiO_2 62.8% and Th 8.9 ppm) is geochemically rather similar to the SG5 migmatitic gneisses, but the lower Th and slightly higher TiO_2 (1.00%) indicate a more mafic origin. The elevated CaO (3.10%) and clearly higher P_2O_5 (0.37%) are probably due to a volcanic component or a sedimentary phosphate component, but an outside leucosome component with high P_2O_5 and TiO_2 cannot be totally excluded.

SG3–SG7 (basement-related sediments)

The SG3 rocks are characterized by relatively high Th and La contents at SiO_2 66.6–77.0% (Fig. 5), and their Th–Sc and Th–Cr (Fig. 8) relations indicate a source enriched in felsic components. The Th/Sc ratio is normally greater than the upper crustal value of 1 (Taylor & McLennan 1985), but if the inferred trend in grain-size variation holds, the ratio will also decrease with decreasing grain-size and so with the amount of clay minerals. The same pattern is seen in the Th–Cr relation (Fig. 8) and Th–Ni relation (data not shown), and indicates that the ratios are highly dependent on grain-size variation. The HSBb greywacke (Table 2) differs from other SG3 samples in having the highest SiO_2, CIA value and Cr and low Th. The lower Th can be explained by the quartz dilution (grain size),

but the high Cr indicates a more Cr-rich source or heavy mineral enrichment. These differences, and the occurrence of this sample in the HSB, suggest a different origin from the other SG3 samples. If the interpretation of carbonate dilution as discussed above is correct, the greywacke from the MBd (Table 2) should also have rather high silica and CIA value. This sample, too, is considered to have a different origin from the other SG3 rocks.

The K_2O/Na_2O ratio describes the behaviour of two highly mobile elements and must be considered somewhat unreliable. The normal values of 0.7–1.3 (Table 1, Fig. 8) in the SG3 group show fairly limited variation on the other hand. Some TSB samples exhibit a deviation to slightly higher ratios in the K_2O/Na_2O–SiO_2 diagram (Fig. 8). The scatter in the U–Th data may be partly due to uranium loss during migmatization or to an enrichment of uranium in organic sedimentation, since two black schists show low Th/U ratios. Although present day weathering may also cause some uranium loss, this is not considered to be significant since the groups show clear differences in Th and U abundances (Table 2) signalling original differences. Many of the SG3 samples have Th/U ratios distinctly higher than the average continental upper crust value of 3.8 (McLennan et al. 1990), and although the above-mentioned processes may have produced some variation, the higher ratios are interpreted to indicate the oxidation of U during sedimentation and the presence of a recycled sediment component.

The geochemistry of sedimentary rocks has sometimes been used in tectonic setting discrimination of sedimentary basins (Bhatia & Crook 1986), but there would seem to be great variation in the geochemistry even in similar tectonic settings (see McLennan et al. 1990). The normal variations in the Th/Sc (0.8–1.5), La/Sc (2.0–3.7) and Ti/Zr (9–17) ratios for SG3 samples are intermediate between Bhatia & Crook's (1986) ratios for continental island arc and active continental margin. The MBd sam-

ple (Table 2) is the only sample with ratios (Th/Sc=2.8, La/Sc=8.6 and Ti/Zr=6.5) close to passive margin setting. The indicated quartz-rich nature and high interpreted CIA value for this sample point to more intensive weathering. As discussed above, the grain-size variation may have an effect on the Th/Sc, La/Sc and Ti/Zr ratios and the values of these ratios should be considered with caution, especially in rocks that contain Archaean detritus. Taken together, the ratios point to a source enriched in felsic rocks, and the rather low CIA values to only a minimal degree of weathering. There are some indications of sediment recycling (Th/U ratio), seen also in the detrital zircon data and Sm–Nd studies (Huhma 1987, Huhma et al. 1991, Claesson et al. 1993).

The SG4 samples resemble the SG3 samples geochemically, and in their major element data the two sets of samples are almost indistinguishable (Tables 1–2, Fig. 4). However, the lower La, Th, Zr and in general higher MgO, Sc and Cr (Table 2, Figs. 5 and 8) indicate a more mafic source for the SG4 samples. A more mafic source is also evident in the normal variation of the Th/Sc (0.5–0.8), La/Sc (1.7–2.4) and Ti/Zr (16–20) ratios, which are close to Bhatia & Crook's (1986) values for continental island arc. The TSB samples have slightly elevated K_2O/Na_2O ratios and CIA values (Table 2 and Figs. 5 and 8) and possibly slightly lower MgO and Cr values relative to other SG4 samples, and in that respect they resemble the SG3 samples. The similarity with the SG3 samples could indicate a similar source, but with more mafic component in the SG4 samples. There is no clear elevation in Sr and P_2O_5 concentrations compared with SG3 samples, however, and this does not favour a mafic component from the high-K calc-alkaline to shoshonite mafic volcanics of the TSB, which are enriched in these elements. Hence the mafic component must be either the more sparse low-K to medium-K mafic volcanics in the TSB or else

there has been a change to a more mafic source during erosion of the "basement".

The SG5 group is characterized by abundant veined gneisses and, although it is difficult to interpret the original grain-size from metamorphosed and migmatized samples, this group seems to be more silty or pelitic in origin than the SG3 and SG4 groups. The SG5 group is geochemically coherent and similar to SG4, but the CIA values are slightly higher and SiO_2 values lower (Table 2, Fig. 5). In both groups the Th and La fields are similar and partially overlapping (Fig. 5), but the SG5 samples tend to have higher C_{Graf}, S, Ni, Co and Zn values. The S–C_{Graf} diagram (Fig. 6) does not show a linear trend for the SG5 samples, and they also have low graphite contents relative to the S level. This may be due to depletion of graphite and a lesser depletion of S during migmatization (p. 31), or due to a different depositional environment from the sulphur- and graphite-enriched groups SG6–SG7. The ranges of the Th/Sc (0.5–0.6), La/Sc (1.4–1.8) and Ti/Zr (20–26) ratios are indicative of a slightly more mafic source for the SG5 than SG4, but more generally the different values, especially the higher Ti/Zr ratios for SG5 rocks, are due to grain-size variation. While the SG5 group is interpreted to be geochemically similar to SG4, some samples represent a more mafic source. The more distal character (more pelitic nature) and the lower SiO_2 values characteristic of chemical and organic sedimentation in the SG5 must thus be mainly responsible for the differences. The two SG5 samples from the HSB differ from the other SG5 samples in having higher C_{Graf} and lower S (Fig. 6) and these samples are considered as a subgroup of SG5. The HSBd sample (Table 2) is characterized by high Cr and is correlated with the Cr-rich SG3 sample from the HSBb (Figs. 5 and 8).

The SG6 samples are pelites, pelitic mica schists, gneisses and veined gneisses, plus one black schist. The pelitic nature is ex-

Geological Survey of Finland, Bulletin 389
Geochemistry of Palaeoproterozoic supracrustal and plutonic rocks...

37

pressed in the high CIA and K_2O/Na_2O values (Table 2, Figs. 5 and 8). As seen in Figs. 4–5 and 8, the SG6 samples also deviate strongly from the average differentiation trends of the TSB volcanic source. According to proposed grain-size trends, at least the SG6 samples from the TSB and MBb could be classed with groups SG4 and SG5 as more pelitic rocks from approximately the same source. It is not clear, however, whether the samples from the HSB and the MBd can be correlated with these groups or whether different processes have produced their more or less similar chemical compositions. The normally lower MnO and also lower CO_2 values of SG6 samples compared with samples of other groups with similar SiO_2 (data not shown) are not explained but could be due to a more reducing environment (higher graphite content) during slow sedimentation.

The SG7 samples comprise one pelite, three black schists, abundant veined gneisses of pelitic nature and a subgroup of migmatites from the MC. There is great variation in the K_2O/Na_2O and CIA values (Figs. 4–5 and 8), which at least partly is due to the migmatitic nature. The high Th/U value in some samples (Fig. 8) may be due to the loss of U during migmatization (especially in the MC samples), but high values also occur in rocks with little indication of migmatization. The SG7 sample with low Th/U ratio (Fig. 8) is a black schist, and here the low ratio may be due to the sedimentation of uranium with organic material. The SG7 samples are geochemically very similar to the SG6 samples; only the Sc–Th and Cr–Th relations are different (Tables 1–2, Fig. 8) indicating a more felsic source for the SG7 samples. The migmatites from the MC are classified with the SG7 rocks on the basis of apparent geochemical similarity which points to broadly similar precursor material.

SG8 (mafic greywackes)

This group consists of four mafic greywackes that do not fit into any group and are discussed one by one. The eastern SG8 sample from the TSB (S8910802T; SiO_2 62.3% and Th 14.3 ppm in Figs. 4–5 and 8) has high K_2O/Na_2O and Th/U ratios (1.7 and 6.5, respectively) with values of Th/Sc (0.72), La/Sc (1.69) and Ti/Zr (22) indicating a relatively mafic source. The lower Cr (Figs. 6 and 7) could indicate mixing in of a small amount of arc-derived material (SG1) with SG4 material.

The western SG8 sample (S8910926; SiO_2 60.4% and Th 12.1 ppm in Figs. 4–5 and 8) occurs stratigraphically high in the main sedimentary association of the TSB, possibly intermingled with the lower parts of the main volcanic association. It has geochemical characteristics comparable with SG5–SG6, but the elevated P_2O_5 (0.21%) and Sr (223 ppm) relative to high CIA value (62.5) indicate mixing in of a small amount of arc-derived material.

The SG8 sample from the HSBa (8911108; SiO_2 63.3% and Th 11.1 ppm in Figs. 4–5 and 8) is geochemically very similar to the SG5 samples, except for higher CaO (3.09%), lower Na_2O (1.87%) and lower La. The fact that the SG2 pelite to the north is highly mafic suggests that there may be a pronounced mixing of group SG5–SG6 material with mafic volcanics to produce these SG8 and SG2 samples.

The SG8 sample in the MBd (S8911006; SiO_2 60.6% and Th 14.4 ppm in Figs. 4–5, 8) is slightly migmatized mica gneiss, with primary bedding still visible. The geochemical features are similar to those of the pelitic group SG6. Two main possibilities for the origin of this sample are the mixing of group SG6–SG7 pelites with mafic volcanic material (tuffaceous layers occur in the same outcrop) or a cannibalistic recycling of SG6 material.

Correlation with other studies

One problem with a study like this is the isolated nature of the sampling sites and the lack of stratigraphical correlation. A detailed study of the geochemistry of sedimentary rocks in the TSB with stratigraphical control of most samples is available, however (Kähkönen & Leveinen 1994), and this was used as the basis for the general 'stratigraphical' correlation in this study.

There are two profiles across the central TSB, the Näsijärvi and Pulesjärvi profiles, which are described briefly in the following. The lowermost Vaarinniemi greywackes of the Myllyniemi formation in the Näsijärvi profile are characterized by elevated P_2O_5 and Sr and are derived from mature arc. The next, Alasenlahti member is characterized by high silica greywackes, and then there is a change to lower silica Jukonniemi and Kupinniemi members, which are characterized by a variable increase of P_2O_5 and Sr. The Tuuliniemi formation is characterized by mudstones, while the volcanics-associated upper Tervakivi and Kolunkylä greywackes and mudstones are characterized by elevated P_2O_5 and Sr. The Ahvenlampi conglomerates and greywackes in the Pulesjärvi profile are stratigraphically comparable to the Alasenlahti greywackes, but the Ahvenlampi rocks have slightly lower SiO_2 and CIA. Both the Ahvenlampi and Alasenlahti greywackes contain abundant quartz clasts (including quartzite) and may be richer in granitoid clasts than other Myllyniemi greywackes (Kähkönen & Leveinen 1994). The Tervakivi formation is also found in the Pulesjärvi profile, and above this formation occur Pulesjärvi and Pohtola volcanic and sedimentary rocks.

From the chemical composition of the TSB greywackes, Kähkönen & Leveinen (1994) interpreted them to be from "pooled active margins" including continental arc basins, back arc basins, strike slip basins, continental collision basins and forearc basins of evolved arcs. The Ahvenlampi and Alasenlahti grey-wackes are more like trailing edge sediments, whereas the Pulesjärvi greywackes have low SiO_2 comparable to primitive island arc greywackes. However, trace element data for the greywackes indicate an association with an evolved arc and a source enriched in potassic volcanic rocks or shoshonites. The lack of prominent Eu-depletion shows that intracrustally differentiated rocks were not abundant in the source area. Kähkönen & Leveinen (1994) also interpreted the REE data to exclude the Archaean TTG type; however, an occurrence of TTG type mixed with HREE-enriched volcanics could perhaps satisfy their data. Luukkonen (1994) has also presented data for sedimentary rocks in the TSB and proposed a general continental island arc origin.

The results of the present study for sedimentary rocks have been compared as far as possible with the results of Kähkönen & Leveinen (1994). Because most of their samples were from the base of turbidite beds, and most of our composite samples (four samples) represented the whole Bouma A, AB and ABC, SiO_2 values were higher in their results. The analytical methods were different as well, probably producing some scatter and complicating the interpretation. Th, Sc, REE and Cr (in moderately weathered samples) are the most stable elements (p. 24) and the Th–Sc and Th–Cr relations were used as major indicators in our study. The lack of Sc and Cr data in Kähkönen & Leveinen (1994) prevents a direct comparison. Despite these few difficulties, however, some useful conclusions can be drawn. Most of the samples in the Alasenlahti and Ahvenlampi groups are comparable with the SG3 samples. The higher SiO_2 and CIA of the Alasenlahti greywackes than of the Ahvenlammi greywackes are reminiscent of the deviating SG3 TSB samples in Fig. 5, and support the idea that there are two slightly different subgroups among the SG3 rocks in the TSB. Kähkönen & Leveinen (1994) under-

stood the higher values to reflect the slightly greater amount of sericite/muscovite in the Alasenlahti greywackes. Our SG4 samples are geochemically similar to the samples of the Jukonniemi member, and the SG5 samples are similar to the samples of the Kupinniemi mem-

ber. The SG1 samples resemble those of Tervakivi and Pulesjärvi and the SG6 and SG7 samples exhibit some similarities with the mudstones of the Myllyniemi formation. The lack of trace element data (Sc, Cr) for the Myllyniemi samples prevents a more detailed comparison.

Source characteristics and tectonic setting

There are a number of difficulties in interpreting the geochemical data of sedimentary rocks. Sorting effectively separates minerals into different grain-size classes, and hydrodynamic conditions (eg. laminar versus turbulent) influence sorting trends. Most sedimentary rocks are not first-cycle sediments but are derived from the erosion of sedimentary rocks or unconsolidated sediments (e.g. Blatt et al. 1980). When older sediments are metamorphosed in high grade, their average grain-size is increased, and greywackes derived from them may have a geochemical composition similar to that of the preceding mud rock. Sediment recycling also effectively mixes different source characteristics and it may be difficult to ascertain the evolutionary path of such rocks. The lithostratigraphic correlation of sedimentary rocks is complicated by the different nature of proximal and distal deposits and the occurrence of these deposits in disparate parts of the depositional basin. There is also a difference in the depositional environment, with chemical and biogenic sedimentation associated with low-energy rocks. The preservation potentials of sedimentary rocks during basin evolution vary from place to another.

The age population of detrital zircons from the base of a 3.5-m-thick greywacke unit (turbidite) in Vihola in the TSB (Kouvo & Tilton 1966) was recently evaluated by single zircon ion microprobe method (Huhma et al. 1991). There were nine zircons, varying in age from 1907±15 Ma to 1997±16 Ma, one zircon of age 2316±29 Ma and three Archaean zircons (about 2.7 Ga). The exact stratigraphic position of this greywacke is unclear, but probably

the Vihola greywackes can be correlated with felsic greywackes of the Myllyniemi formation. A greywacke from Siiviikkala, in the northern part of the Myllyniemi formation, also dated by ion microprobe, shows detrital zircon ages from 1926±30 Ma to 2039±12 Ma (10 zircons) and from 2.77 to 3.44 Ga (6 zircons). This sample thus differs from the Vihola sample in having an abundant early Archaean component. Apparent U–Pb zircon ages of 2.2–2.3 Ga from other metasediments in the TSB and in the Kangasala area (MB) confirm the widespread occurrence of this type of mixed zircon population. The Nd depleted mantle model ages of 2.2–2.4 Ga from metasediments in the TSB (Huhma et al. 1991, Huhma 1987) are in agreement with this, as is the occurrence of Archaean granitoid cobble in the Ahvenlampi conglomerate with minimum U–Pb zircon age about 2.55 Ga and Nd model age T_{DM} of 2.76 Ga (Kähkönen & Huhma 1993).

All these studies show the occurrence in the source area of a 1.91–2.0 Ga component (2/3) mixed with an Archaean component (1/3). However, although the detrital zircon data indicate the approximate proportion of zircons (mainly from granitoids, Claesson et al. 1993), they do not give the proportion and age of the volcanic component (especially mafic). The apparent recycled nature of most metasediments means that, at least in part, they contain older sediments. The nature of the mafic component, which is detailed in Fig. 9, shows similar relations for groups SG3–SG7 and points to a more or less similar source. The main exceptions are the SG3 and SG5 samples from the HSB (Table 2) which are Cr-

rich. The SG1 and most of the SG2 samples differ in the mafic component and in general point to a more evolved Cr- and Ni-poor source. The V–Cr diagram is interesting in that it clearly separates the basement-related sedimentary rocks from the felsic–intermediate igneous rocks in the study area. The Cr- and Ni-rich nature of groups SG3–SG7 indicates a contribution from primitive Archaean (komatiite) and/or Palaeoproterozoic (>1.91 Ga) mafic detritus.

The geochemistry of greywackes has frequently been used to estimate the tectonic setting of sedimentary rocks (Bhatia & Crook 1986). The trace element levels and ratios of

the SG1 sediment samples are very different, and use of the discrimination ratios alone would place them in quite different tectonic settings, as seen in the Sc–Th relation in Fig. 8. As discussed by McLennan et al. (1990), however, there are also some general trends. Sc and Cr versus Th diagrams (Fig. 10) were set up to compare the results for the basement-related groups SG3–SG7 with the results for modern deep-sea turbidites (Mc Lennan et al. 1990) and Palaeozoic turbidite sequences of eastern Australia (Bhatia & Crook 1986). The overlapping nature of modern deep-sea turbidites from different tectonic settings is seen especially in the Cr–Th relation. The SG3–
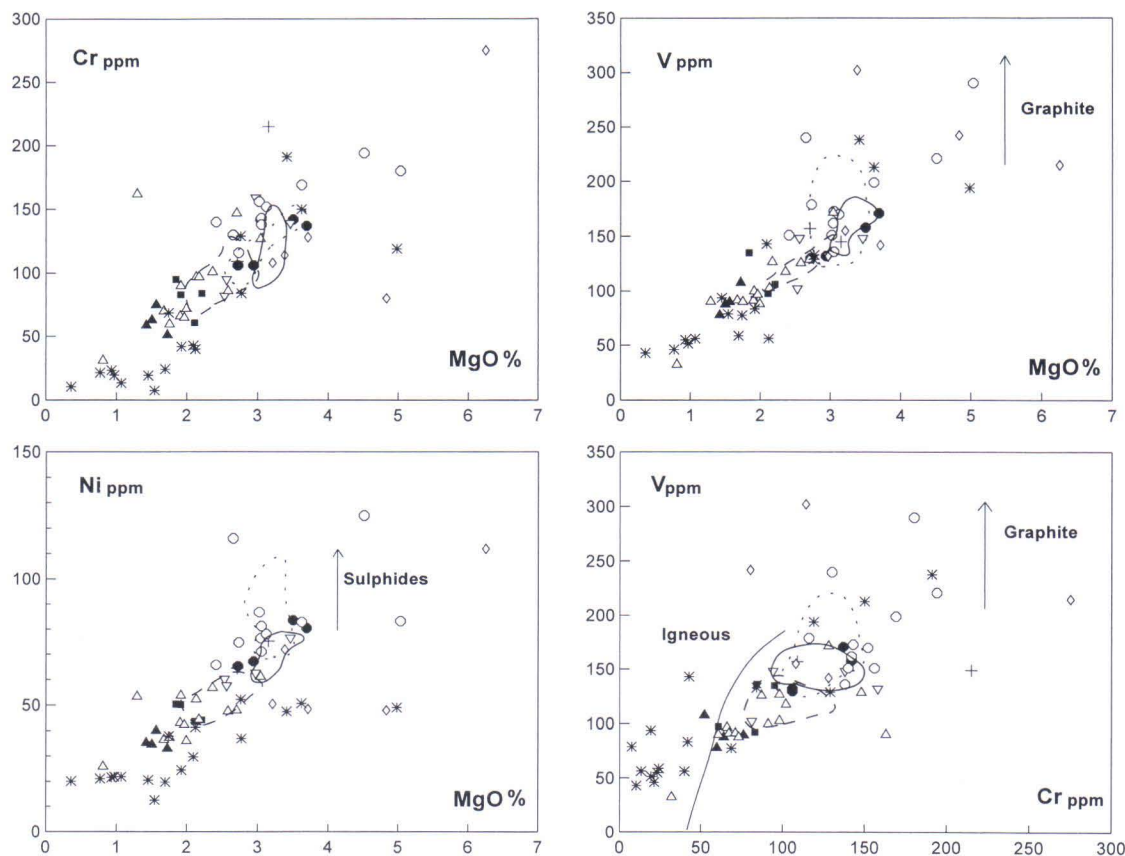

Fig. 9. Cr–MgO, V–MgO, Ni–MgO and V–Cr diagrams for the sedimentary rocks in the Tampere–Hämeenlinna area. Data from this study. See Figure 4 for symbols. Igneous field covers the intermediate and felsic igneous rocks (>60% SiO_2) in this study and clearly separates them from the basement-related sedimentary rocks (SG3–SG7).

SG7 rocks are comparable to turbidites from Continental Arc basins and the Back Arc basin of Japan (not separately indicated in Fig. 10), which are representative of mature arc type with older basement.

An interesting feature of the SG3–SG7 samples is the elevated level of all three indicator elements (Th, Cr, Sc; Fig. 10). Perhaps this is due to a bimodal source, with highly mafic rocks (very low Th and high Sc and Cr) associated with enriched felsic rocks (high Th and low Sc and Cr), and at the same time a lack of intermediate rocks. Another possibility is the depletion of quartz from the sedimentary record, producing higher values of all three elements. In the case of an Archaean component, Jatulian quartzites could be the reservoir for the depleted quartz component. The quartzites (for example, at Tiirismaa) in the Svecofennian of southern Finland and the quartz-rich rocks in the MBa and HSB also could have acted as reservoirs.

Another approach to determining the source composition is to assume that the average present composition of the rocks to some extent correlates with the average source composition. Figure 11 shows the results of normalizing se-

lected elements of SG3–SG7 rocks to late-Archaean (3.5–2.5 Ga) upper continental crust (restoration model, Condie 1993). The presently available data indicate 3.4 Ga age (Claesson et al. 1993) for the oldest component in these sediments, and about one third of the felsic source is late Archaean in age, at least in the TSB. The early Proterozoic upper crust model (Condie 1993) is also shown in Fig. 11, and the main differences relative to the Late Archaean upper crust are slightly higher levels of elements from K to Sc and much lower levels of Cr, Co and Ni. There is also a difference in the La, Sm and Y levels due to fewer rocks with high La/Yb (TTG) in early Proterozoic time.

The SG3–SG7 average follows a similar trend to the late Archaean model for elements Nb–Y but at higher level, and it differs from the early Proterozoic upper crust model in not showing relative La depletion or Sm and Y enrichment. The low Sr value is due to weathering (e.g. Nesbitt et al. 1980) and the high Sc and V indicate a higher proportion of mafic component. The Cr and Ni levels are intermediate between the late Archaean and early Proterozoic models, suggesting the mixing of Archaean komatiite source with less primitive
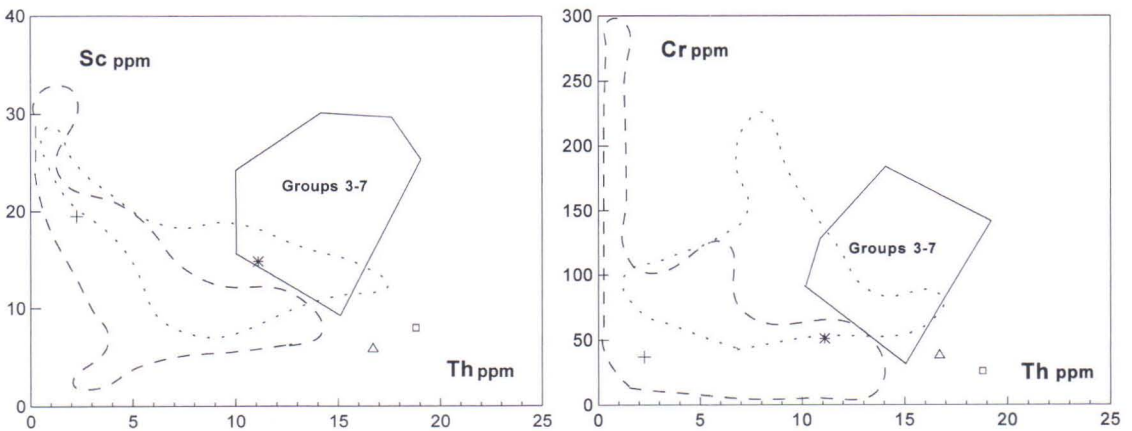

Fig. 10. Sc–Th and Cr–Th diagrams showing the fields of SG3–SG7 sedimentary rocks of this study. Dashed fields – modern deep sea turbidite sands, dotted fields – comparable muds; both from McLennan et al. (1990) The mean values of Palaeozoic greywackes from eastern Australia (Bhatia and Crook 1986): cross – oceanic island arc, asterisk – continental island arc, open square – active continental margin, open triangle – passive margin.

Palaeoproterozoic mafic source. The Rb and Th levels, in turn, suggest enrichment of a felsic component. Rb and Ba are considered to some extent to be concentrated relative to K and fixed in clays during weathering (Nesbitt et al. 1980). This could in part explain the behaviour of Rb, but Ba behaves differently and appears at lower level than K. Th is considered reliably to characterize the source composition (e.g. McLennan et al. 1990), and although not as heavily enriched as Rb it shows clear enrichment relative to Ba. Biotite contains both Ba and Rb, but K-feldspar is the most important Ba mineral in granitic rocks, with plagioclase considerably less important (Puchelt 1972). Th and Zr are decoupled in

the SG3–SG7 rocks, which means that zircon controls only a small portion of Th in them. Possibly the main part of Th occurs in ferromagnesium minerals and monazite inclusions within them, with subsequent attachment to clays during weathering (Rogers & Adams 1969).

Two possible models, separate or combined, are considered feasible to account for the Ba deficiency: K-feldspar has been selectively enriched in arkositic rocks during evolution of the recycled sedimentary component or Ba has been selectively leached, during weathering or during diagenetic/metamorphic destruction of the K-feldspar. The behaviour of Ba during weathering is normally considered to be conservative (e.g. Nesbitt et al.
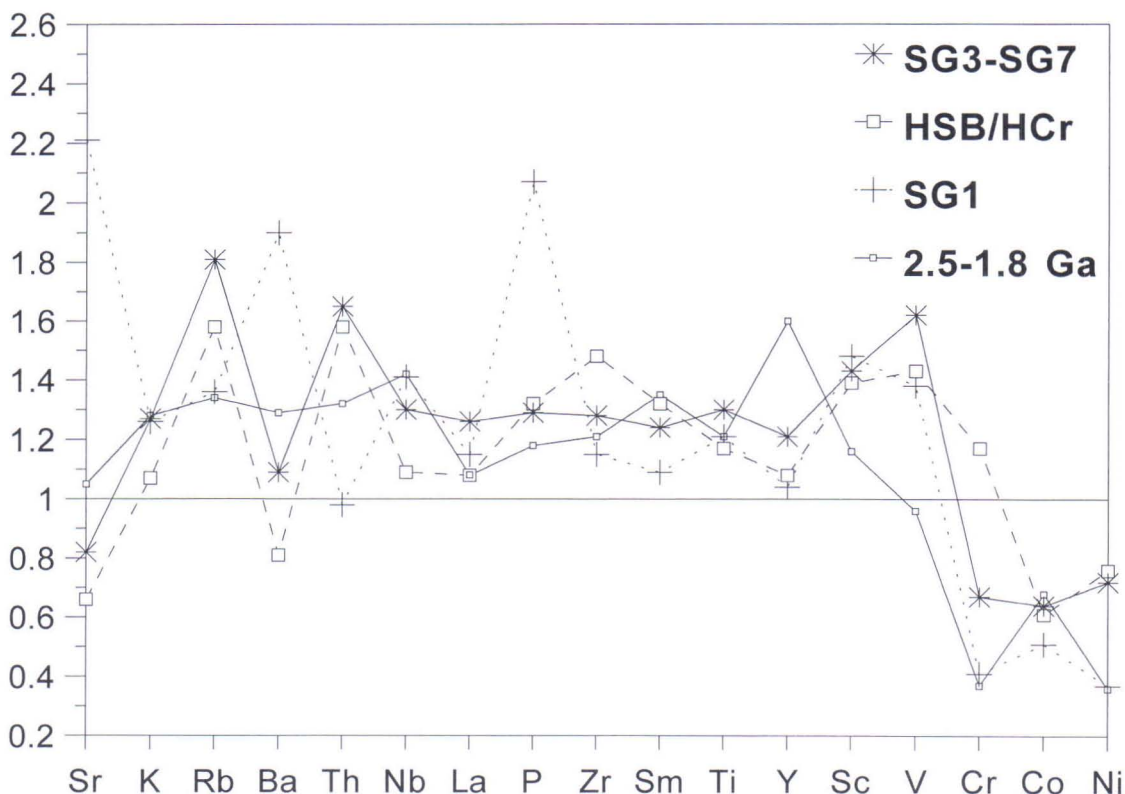

Fig. 11. Major and trace element distributions in basement-related sedimentary rocks (av. of SG3–SG7), in high-Cr sedimentary rocks in the HSB (av. of two samples)(HSB/HCr) and in arc-related sediments (av. of SG1) of this study. Results are normalized to the late Archaean restoration model (3.2–2.5 Ga) for the average chemical composition of juvenile upper continental crust (Table 4 in Condie 1993). The normalized values of the early Proterozoic (2.5–1.8 Ga) upper continental crust restoration model (ibid.) are included.

1980), but both Ba increase and Ba decrease have been observed in weathering products (ibid., Puchelt 1972). The possible slight Ba deficiency in sedimentary rocks in general (Condie 1993) could indicate depletion of Ba relative to Rb. The enrichment of Ba relative to Rb and Th in some pelagic sediments associated with recycled oceanic crust contributes to Ba enrichment in subduction-related magmas (Hawkesworth et al. 1991) and in heterogenous mantle component (EMI, Weaver 1991), probably producing mass balance of Ba. Although the nature of Palaeoproterozoic pelagic sediments is unknown, the Ba enrichment in the proposed enriched mantle component in late Svecofennian rocks (Lahtinen 1994b, this study) argues for a similar enrichment in Palaeoproterozoic pelagic sediments.

Detrital zircon data and the above considerations indicate an Archaean to Palaeoproterozoic source with high proportion of recycled component for the SG3–SG7 rocks. Bimodal felsic and mafic sources have been dominant and an Archaean komatiite source with primitive Palaeoproterozoic mafic component is responsible for elevated Cr and Ni values. The Ba depletion, Th–Sc and Th–Cr relations and the high level of both felsic and mafic source related elements (Figs. 8, 10 and 11) indicate a depletion of quartz and possibly also K-feldspar. This depletion probably occurred in the pre-2.0 Ga component and it could indicate the preservation of more proximal deposits in the crust and the origin of the recycled >2.0 Ga component in distal deposits.

The average of two high-Cr HSB samples (samples HSBb and HSBd in Table 2) is also shown in Fig. 11. The Sr–La and Sc–V relations show a similarity with the SG3–SG7 average, but whether the higher Zr is due to the heavy mineral influence or source effects is unclear. The high Cr and the decoupling of Cr and Ni could indicate a greater amount of the Archaean component or the occurrence of fine-grained detrital chromite. The SG1 average shows similarities with the early Proterozoic upper crustal model (Fig. 11), but the high levels of Sc and V, and especially the high levels of Sr, Ba and P, point to a source enriched in mafic–intermediate high-K calc-alkaline and/or shoshonite rocks.

Regional correlations

The occurrence of SG3–SG5 samples and also SG1 samples in the MB, especially in the northern part, indicates similar histories for the MB and TSB. The south dipping thrust (Nironen 1989b) is not, therefore, a major suture separating two different areas but more likely is a partly overturned reactivated fault separating volcanic arc and forearc basin (trenchward dipping backstop) as described in the configurations of modern forearc regions by Ingersoll (1988), or alternatively it is a back thrust. The occurrence of SG1 sediments in the northern part of the MB shows the influence of the evolved island arc volcanism in the TSB, but it is not clear whether these samples are correlated with the SG1 sediments occurring high in the stratigraphy or with the lowest Vaarinniemi formation where one sample (1–B-YK/91, Table 2 in Kähkönen & Leveinen 1994) contained high abundances of CaO, Sr and P_2O_5.

The MB has a complex deformation history with a lack of clear marker horizons. The proposed suture (p. 95) may divide the MB into different blocks, but overthrusting and the possible occurrence of pre- to syn-rifting, pre-collisional and syn-collisional sediments hamper the interpretation. The sediments in the MBa, MBb and the northern part of MBc are correlated with the TSB sediments. Some of the HSB sediments show different geochemical characteristics and the abundant occurrence of SG6–SG7 rocks in the MC and HSB and in the southern part of the MB indicate somewhat different evolution histories for these areas.

GEOCHEMISTRY OF VOLCANIC ROCKS

Factors controlling the composition of volcanic rocks

As discussed above, the provenance of sedimentary rocks and the tectonic environment of deposition are not easy questions to resolve. The major problem is the possibility of long transport distance, on the order of a few thousand kilometres. The volcanic rocks, on the other hand, sample the underlying crust and mantle, and the geochemistry of volcanic, especially mafic volcanic rocks, can be used to infer the tectonic setting. In many cases discrimination diagrams have nevertheless proved to be misleading, leading to false conclusions. The geochemistry of mafic volcanic rocks is controlled by the interaction of several factors, the most important being the mantle type, the possible presence of a sub-

duction component, fractional crystallization, mixing, contamination and compositional changes during post-depositional processes. A review of all factors affecting the chemical composition of volcanic rocks is beyond the scope of this paper but a short discussion is presented of the effect of the above-mentioned factors, especially on mafic rocks. Post-depositional processes are not included but their effects are considered for some individual samples and groups. First the types of volcanic rocks in different tectonic environments are briefly discussed.

The most voluminous volcanics are mid-oceanic ridge basalts (MORB), which are effectively recycled to the mantle via subduc-
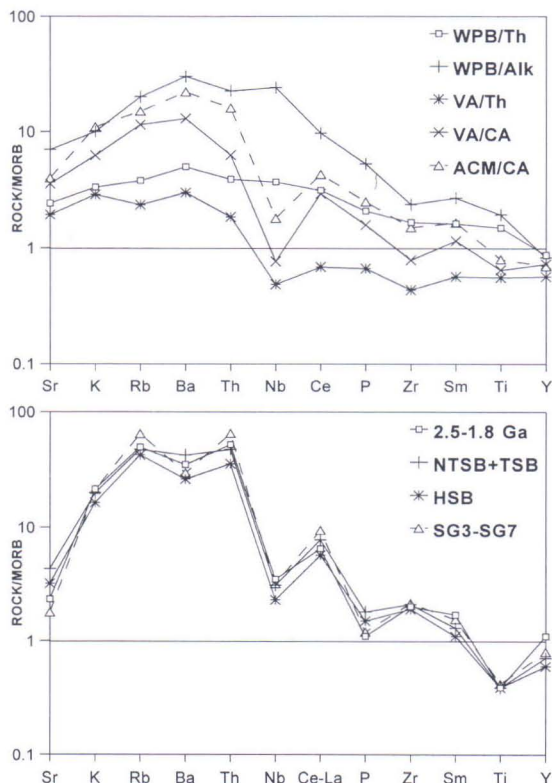

Fig. 12. Mid-ocean ridge basalt-normalized (Pearce 1982) trace element patterns for basalts in different geotectonic environments (upper) and for some possible contaminants (lower) during the ascent of mafic magmas. La has been used instead of Ce for NTSB+TSB, HSB and SG3–SG7 results. The normalizing value of La (3.8 ppm) is interpolated from the Ce value of Pearce (1982). WPB/Th – tholeiitic within-plate basalt, WPB/Alk – alkaline within-plate basalt, VA/Th – tholeiitic volcanic arc basalt and VA/CA – calc-alkaline volcanic arc basalt (all data from Table 1 in Pearce 1982). ACM/CA – calc-alkaline active continental margin basalt (approximate trend adapted from Figure 8 in Pearce 1983 for Central Chile calc-alkaline basalts). 2.5–1.8 Ga – restoration model for average chemical composition of juvenile early Proterozoic upper continental crust (Table 4 in Condie 1993), NTSB+TSB – average chemical composition of GG2 granitoids in the NTSB and TSB, HSB – average chemical composition of GG2 granitoids in the HSB, SG3–SG7 – average chemical composition of basement-related sedimentary rocks.

tion. Within-plate basalts (WPB), or ocean island basalts (OIB), also occur in oceanic environment where they often follow hot-spot traces. Their fate is not clear, but evidently oceanic plateaus are sometimes capable of resisting subduction and are accreted to form continental crust (e.g. Ben-Avraham et al. 1981). Most MORB are depleted in large ion lithophile elements (LILE) and especially K, Rb, Cs, Sr, Ba, U, and light REE, and are referred to as normal mid-ocean ridge basalts (NMORB). Transitional MORB (TMORB) are undepleted, and enriched MORB (EMORB) are enriched in LILE and in some high field strength elements (HFSE) such as Nb and Ta (Pearce 1982). EMORB generally occur near seamounts or oceanic islands and are associated with long-lived hot-spots. Oceanic WPB are enriched in LILE and HFSE (Fig. 12), but, as discussed below, different source components show variable composition.

WPB also occur in areas underlain by continental crust as exemplified by the voluminous continental flood basalt (CFB) magmatism triggered by the emplacement of a mantle plume or by lithospheric extension (e.g. Carlson 1991, Hawkesworth & Gallagher 1993). The eruptive products are often removed by erosion, but their subsurface expressions, especially magmatic underplate, may represent a significant addition to the crust. Some CFB show geochemical similarities with their oceanic counterparts, while others bear indications of a different source, possibly related to distinctive source regions in the subcontinental lithosphere (e.g. Hawkesworth & Gallagher 1993) or in sublithospheric enriched layer 'perisphere' in the lower part of the thermal boundary layer (Anderson 1994).

Destructive plate margin magmatism is one major crust forming process. Tholeiitic basalts and basaltic andesites characterize the primitive island arcs (PIA) in oceanic environment. The amount of andesites and especially dacites and rhyolites generally increases in going from PIA to more mature conti-

nental island arcs and active continental margins (ACM) (e.g. Gill 1981). Figure 12 shows patterns for destructive plate margin volcanics, where the characteristic feature is LILE enrichment attributed to the occurrence of a subduction component and about the same level of Nb, Zr, Ti and Y, thus forming the negative Nb anomaly characteristic of arc rocks (e.g. Pearce 1982). The ACM example also shows higher HFSE values with inclined trend representing an enriched subcontinental lithospheric component associated with a subduction component.

Mantle types and subduction component

The major component of basaltic magmas is a melt derived from the mantle. The major reservoir is the upper mantle, which contains both convecting asthenosphere and subcontinental lithospheric mantle. The lithosphere, including crust and subcontinental lithospheric mantle, is here considered as the part of the earth where heat is transferred mainly by conduction and that moves as a tectonic plate, providing a coherent reservoir isolated from the convective asthenosphere (e.g. Hawkesworth & Gallagher 1993). Mantle plumes may originate at the core–mantle boundary (e.g. Griffiths & Campbell 1990) or at the upper to lower mantle boundary (mesosphere boundary layer) (Allégre & Turcotte 1985, Weaver 1991). The present-day OIB (WPB) sources, which at least partly are related to mantle plumes, have remained isolated in the mantle for periods of 1–2.5 Ga (Chase 1981) and, according to Ringwood (1990) have been accumulated within and near the 650-km discontinuity. Anderson (1994) has nevertheless questioned this, arguing that the enriched components are stored in the shallow mantle, where they contaminate the depleted plume component. Consensus does not exist, therefore, on the location of the enriched source. The character of the asthenosphere is particularly crucial; is it homogeneous and depleted

as normally assumed, or do enriched mantle and depleted mantle co-exist in the shallow mantle, with small fraction melts sampling EM preferentially (Leeman & Harry 1993).

In this paper the concept enriched mantle (EM) is used to refer to a heterogeneous mantle with prevailing depleted mantle (DM) component containing a variable amount of streaks of variably enriched component. This type of EM characterizes areas overlain by continental crust, regardless of the actual location either in subcontinental lithosphere or in sublithospheric enriched layer. The enrichment in mantle plumes may have either deep or shallow source, but the mantle plumes should be seen as large volumes of magma and hot-spot trace (Hawkesworth & Gallagher 1993). In general these features are also valid for the Palaeoproterozoic time, although the possible hot-spot traces are difficult to track down due to later tectonic movements.

Several mantle endmember components have been proposed on the basis of isotopic heterogeneities (Zindler & Hart 1986): depleted MORB mantle (DMM), high U/Pb mantle component (HIMU), enriched mantle components (EMI and EMII), with two additional components — bulk silicate earth (BSE) and prevalent mantle composition (PREMA) — considered as mixtures of other components. Pure DM melts (MORB) show low LILE and are used as the normalizing composition in Fig. 12. The enriched component is primarily composed of ancient recycled basaltic oceanic crust, and after passing through subduction zone processes carries the trace element and isotopic signature of dehydration residue (Weaver 1991). Pure HIMU are derived from such a source and are characterized by an enrichment in HFSE relative to LILE and LREE, low Rb/Sr, and high U/Pb and Th/Pb. In particular, the Nb–Ta enrichment is a unique feature related to HIMU originated magmas (ibid.). In the EMI, ancient pelagic sediment with high LILE/HFSE, LREE/HFSE, Ba/Th and Ba/La ratios and low U/Pb

ratio contaminate the HIMU source, and in the EMII, the contaminant is ancient terrigenous sediment with high LILE/HFSE and LREE/HFSE ratios, but lacking relative Ba enrichment, and with higher U/Pb and Rb/Sr ratios (ibid.).

The above-described trace element patterns are based on the study of young OIB (WPB), and their validity for Palaeoproterozoic time is open to question. Moreover, the sedimentary rocks of this study show clear Ba depletion (Fig. 12), which would suggest Ba enrichment in pelagic sediments to balance the Ba cycle. These mantle endmembers and their mixtures are considered to characterize Palaeoproterozoic just as they do present time, although their time-integrated isotopic characteristics have probably not had sufficient time to develop to extreme values, at least not in areas overlain by relatively young continental crust (<0.5 Ga). The general term EM is used here, and only occasionally are proposals made for the most dominant component. The WPB patterns in Fig. 12 do not represent any single endmember, but show the enriched nature and inclined trend from Nb to Y. In part this pattern may be due to lower degrees of mantle melting and crystal fractionating, but the proposed endmembers normally have lower Zr/Nb and La/Nb ratios compared with NMORB (Weaver 1991), and the Y values in Fig. 12 are still lower than in MORB, indicating that the degree of melting is about the same and that the inclined trend also characterizes the source. Of course, a great amount of garnet in the source residue lowers the melt Y values.

The subduction component includes chemical contributions from subducted sediments and altered oceanic crust (e.g. Hawkesworth et al. 1994), and most likely is transported into the mantle wedge via aqueous or silicate fluids. The subduction component is considered to be responsible for the characteristic depletion in Nb, Ta, Zr, and Ti relative to LILE and LREE (Fig. 12) and the depletion has alternatively been ascribed to residual

HFSE-rich phases in the source (Green & Pearson 1987, Ryerson & Watson 1987), a large-scale HFSE-depleted source (Salters & Shimizu 1988), melting phenomena (McKenzie & O'Nions 1991), arc magma-mantle interactions (Keleman et al. 1990), and HFSE retention in the subducting slab (Tatsumi et al. 1986). Although consensus exists on the importance of fluids and/or hydrous melts in arc magma genesis, the degree of interaction between the mantle wedge and subduction component is not well resolved. Hawkesworth et al. (1991) estimated that only 15% of the Sr and 10% of the Th in an average low Ce/Yb arc composition were derived from subducted material. This could indicate the scavenging of some elements by hydrous fluids from the slab and/or the mantle wedge. The problem of the relative contributions of the subduction component, scavenged elements and the mantle melt composition is especially acute in areas underlain by subcontinental lithospheric mantle enriched by earlier events. The ACM example in Fig. 12 shows a mixed pattern intermediate between the PIA and WPB patterns.

Baker et al. (1994) argue that the heterogeneous distribution of H_2O in the mantle in arc settings results in the production of a spectrum of mantle melts ranging from wet (calc-alkaline) to dry (tholeiitic), where the wet primary magmas may be of high-SiO_2 nature (up to 58%). The tholeiitic parental liquid might also evolve to a calc-alkaline liquid line of descent by reacting with ultramafic wall rocks (Keleman 1990). In general, the source area of destructive plate magmas is characterized by dominantly DM in PIA to heterogeneous EM in continental island arc and ACM, with variable amounts of H_2O and enriched components in different areas and even in single arc segments. The magmatism is initiated by the release of subduction component, but the nature of this component (fluid/hydrous melt) and its composition vary with the nature of the subducted material, which may be dominated by altered oceanic crust, pelagic sediment or terrigenous sediment. The subduction angle combined with the thermal regime may perhaps also affect the nature and composition of the subduction component. The effect of the subduction component is probably most pronounced in situations where the mantle is highly depleted in certain trace elements (Hawkesworth & Ellam 1989).

Fractional crystallization, magma mixing and crustal contamination

The other factors affecting the composition of mafic magma are fractional crystallization, magma mixing and crustal contamination. The predominant crystallization assemblage in basaltic magmas is olivine ± clinopyroxene ± plagioclase (Pearce 1983), although other minerals also are important as briefly discussed below.

Meen (1990) has proposed that coprecipation of olivine, plagioclase, augite, and low-Ca pyroxene in magmas at the Moho beneath continental crust produced enrichment in K_2O with only slight enrichment in SiO_2, so that, at least in part, the variation in K_2O/SiO_2 is related to crustal thickness. Experimental investigations on the role of H_2O in producing a calc-alkaline differentiation trend from high-alumina basalts (HAB) have shown that H_2O lowers the temperature of appearance of crystalline silicates, enabling the earlier precipitation of Cr-spinel and magnetite, and stabilizing very calcic plagioclase, but at the same time reducing the total proportion of plagioclase in the crystallizing assemblage (Sisson & Grove 1993a). Hornblende can form as a near liquidus mineral in wet sodic basalts, but does not appear until the liquidus reaches andesitic composition in moderately sodic basalts. This means that the absence of hornblende in basalts with low-to-moderate Na_2O contents cannot be taken as evidence for the absence of H_2O in the melt (ibid.). High-An plagioclase can also be a crystallizing phase in more refractory melts with abnormally high CaO/Na_2O values (>8). Apart from

producing the silica enrichment and calc-alkaline differentiation trend, magmas with high H_2O contents will become saturated with and then exsolve aqueous fluid upon approaching the surface, and they will grow crystals at shallow depths, accounting for the abundant phenocrysts in low-MgO HABs and basaltic andesites (Sisson & Grove 1993b).

Olivine and orthopyroxene have low mineral/melt partition coefficients for the elements shown in Fig. 12 and, thus, their crystallization only changes the level, and not the pattern. Plagioclase crystallization lowers the relative level of Sr, and clinopyroxene can account for the small relative negative change in Y, Ti and Sm. Magnetite crystallization can account for depletion of Ti, and to a lesser extent Nb, and apatite crystallization produces strong depletion of P. Amphibole affects K and HFSE, and the occurrence of sphene as a crystallizing phase in high-Ti rocks will produce strong Ti and Nb depletion. Thus, before magnetite or amphibole starts to crystallize, the patterns of mafic magmas (Fig. 12) do not change in any great degree. The situation is different, however, for the wetter basaltic magmas (see above) and for intermediate and felsic melts precipitating these phases. The calc-alkaline andesites are widely considered to originate through fractional crystallization from a basaltic parent due to fractional crystallization containing magnetite as crystallizing phase (e.g. Gill 1981), but a more siliceous parent magma is also possible (see above).

Magma mixing, another way in which the magma composition is changed, has been invoked to explain the genesis of calc-alkaline rocks (e.g. Koyaguchi 1986). Magmas with similar amounts of SiO_2 mix more easily, while the mixing of mafic and felsic melts occurs only where the proportion of mafic magma is large and the mafic magma is not quenched (Sparks & Marshall 1986). The contamination of mafic magmas due to bulk assimilation or to assimilation in combination with fractional crystallization (AFC) is not uncommon (e.g. Brandon et al. 1993) and the effects of the contamination may be difficult to interpret, especially if the contaminant is not a highly differentiated old crust but a juvenile mafic crust. A particular problem associated with contamination is the possible decoupling of major and trace elements, where the precipitation of fractionating minerals increases with only minor change in silica, but substantial changes occur in trace elements (O'Hara 1980). The possible contaminants in the study area are the basement-related sediments and the medium-K to high-K granitoids in the NTSB+TSB and HSB, which at least in part are interpreted to represent melts derived from the lower-middle crust. These contaminants exhibit similar patterns, but a pronounced Ba depletion characterizes the sedimentary rocks. If depleted lower crust were a contaminant the effects of contamination would be slightly different: for example, Rb and possibly U would be lower.

Classification of the volcanic rocks

There are two major volcanic belts in the study area, the TSB (including HiSB) and the HSB, each with distinct characteristics. Continuous SiO_2 variation from 53 to 73% (excluding the Haveri basalt) characterizes the TSB samples, while basalts and basaltic andesites predominate in the HSB (Fig. 13). The HSB calc-alkaline rocks are predominantly basaltic andesites and andesites, and the amount

of felsic rocks is less relative to the TSB. High Th/U ratios characterize the TSB samples, and ratios are low in the HSB samples, even in the separated calc-alkaline group (Fig. 13). The TSB is characterized by high-K to very high-K rocks, and the HSB by medium-K volcanics. These features, and the general calc-alkaline nature of the TSB compared with the mostly tholeiitic HSB, indicate a different origin for these

two belts, as will be discussed below in the context of the different rock groups.

The pyroclastic rocks in the Tampere–Hämeenlinna area are associated with outgassing and synvolcanic fluid circulation and this, together with the not uncommon alteration effects complicates the interpretation of the geochemical data. Except for a few samples to be discussed below, there is no clear evidence for metamorphic effects, though some alteration effects may be associated with retrogressive metamorphic events concentrated in fault and shear zones. Some samples, especially ones in amygdaloidal and pumice-bearing rocks, exhibit an elevated carbonate component. The sulphur data and the elevated contents of certain trace elements (Li, As, Sb, Au, Te) (Lahtinen & Lestinen 1996), indicate mineralization effects in many of the samples. In many cases, therefore, the present geochemical composition of the rocks gives only a general idea of the original magma composition. Geochemical MORB-normalized spidergrams modified from Pearce (1982) were calculated, but tantalum data were not included due to poor analytical reliability, and La was used instead of Ce. Pearce's spidergram was developed for basalts, whereas most of the NTSB and TSB volcanics are more evolved, judging from the SiO_2 contents, and some tholeiitic HSB subgroups show no or only slight SiO_2 enrichment during differentiation. For these reasons, the spidergrams are only used to point out major differences or compare individual samples.

The volcanic rocks are divided into eight geochemical groups and a number of subgroups on the basis of their geochemical nature. The sample locations are shown in Fig. 14. Classification is not based on any single element or ratio. Instead, the levels and ratios of elements, especially Rb, Ba, Th, Nb, La, Zr, Ti, Y, Ni and Cr, are considered against the levels of silica and potassium, and the tholeiitic or calc-alkaline nature is taken into account in a general way. Altered samples are classified, many of them only tentatively, however, by

considering how alteration may have changed the original composition. Like all groupings, this grouping of volcanics involves an element of subjectivity in the interpretation of the processes affecting the individual samples.

Volcanic group 1 (VG1) comprises tholeiitic basalts of rather primitive DM–EM origin. Groups VG2–VG3 lack iron enrichment but are considered tholeiitic on the basis of the high FeO/MgO ratio relative to SiO_2; however, a few samples are transitional to calc-alkaline rocks. VG2 volcanics show geochemical characteristics compatible with a WPB origin from predominantly EM-type mantle, but there is indication of a subduction component in some samples, and these are gradational to group VG3. In VG3 rocks a higher pro-
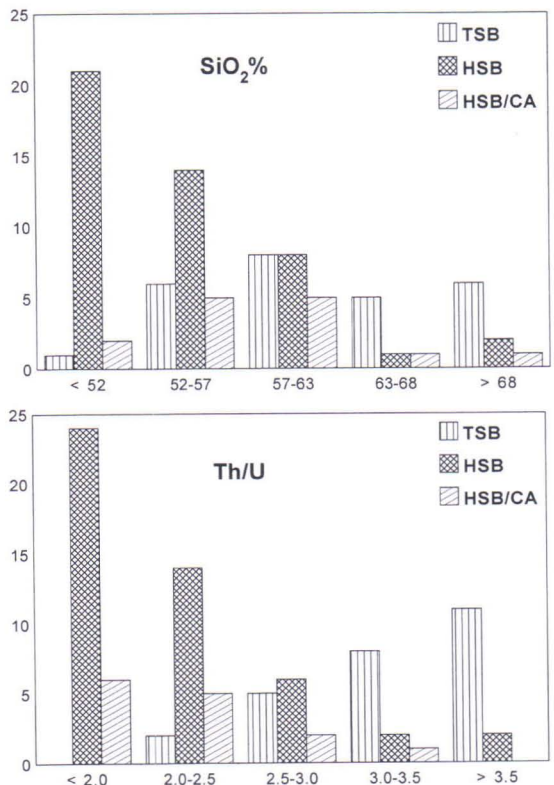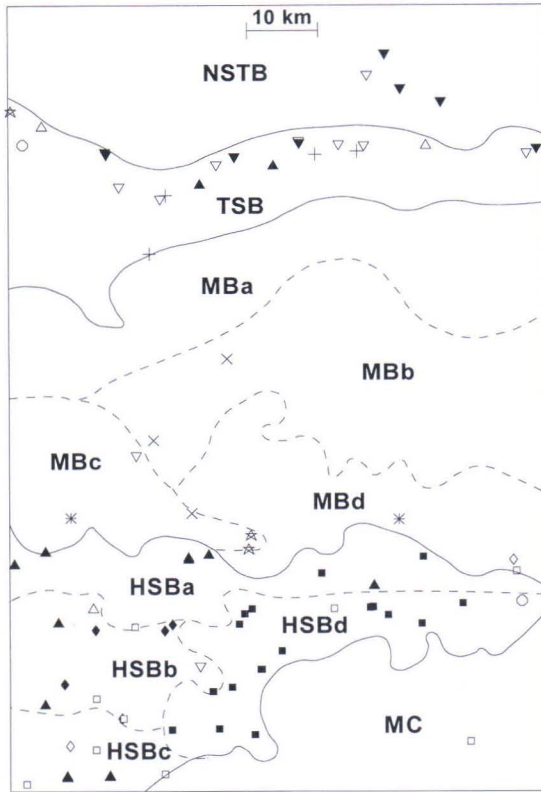

Fig. 13. Histograms of SiO_2 and Th/U ratio for metavolcanics in the TSB (including HiSB) and HSB. Data from this study. TSB – all volcanic samples in the TSB and HiSB, HSB – all volcanic samples in the HSB, and HSB/CA – calc-alkaline volcanics in the HSB.

Fig. 14. Sample locations of the volcanic rocks. See Figure 2 for more detailed lithology. Asterisks – MORB-affinity volcanics (VG1), stars – EMORB–WPB affinity volcanics (VG1), open squares – VG2, filled squares – VG3 main group, filled diamonds – VG3 intermediate group, diagonal crosses – VG4, filled upright triangles – VG5 basalts, basaltic andesites and andesites, open upright triangles – VG5 dacites and rhyolites, filled inverted triangles – VG6 basaltic andesites and andesites, open inverted triangles – VG6 dacites and rhyolites, crosses – VG7, open diamonds – VG8, open circles – volcanic greywackes.

portion of DM-type mantle component is associated with the subduction component. VG4 rocks are hypabyssal dyke rocks of alkaline WPB affinity. Group VG5 comprises low- to medium-K calc-alkaline rocks, and VG6 medium-K to high-K calc-alkaline rocks. Shoshonites characterize VG7, and two dacites of tholeiitic affinity are classified as VG8. Analyses of selected samples are shown in Table 3. Note that the total of oxides was calculated to 100% in Figs. 15–18, while the values used in Table 3 are values obtained in analysis. The ore-related elements are considered in Lahtinen & Lestinen (1996).

Description of volcanic rock groups

VG1

The five rocks of this group are tholeiitic basalts of rather primitive DM–EM origin and are divided into two subgroups; two are MORB-affinity and three EMORB–WPB affinity volcanics. The MORB-affinity low-K tholeiitic basalt 8911037 (SiO_2 49.3% in Figs. 15–18) of possible pillow-lava origin from the MBc has rather high TiO_2 and Y and low Al_2O_3, K_2O and La (Table 3). Geochemical features resemble MORB (Fig. 19), but the somewhat elevated Rb and Ba suggest slight contamination.

Sample 8911011 from the MBd (SiO_2 47.9%), with 17.9% MgO and 1300 ppm Cr and 420 ppm Ni, is the most mafic sample in this study. Low Na_2O+K_2O (0.81%) and TiO_2 (0.54%) values relative to MgO identify it as a picrite (komatiite) according to Le Maitre (1989). The geochemical interpretation is hampered by the low contents of Rb, Th and Nb, which are near to or below the detection limits. The Rb value has been interpreted from the INAA determination. According to Fig. 19, this sample has a very primitive IAT–MORB-like origin. The occurrence of graphite (0.11%), and the negative Ba- and positive La-anomalies like those of sediments, suggest a MORB origin with a small (about 1%) assimilated sediment component.

Relative to the two MORB-affinity volcanics the other three samples of group VG1 exhibit more enriched patterns (Fig. 19). The

amygdaloidal tholeiitic basalt 8911059 from the MBc (SiO$_2$ 48.7% in Figs. 15–18) has elevated carbonate content and rather high TiO$_2$ and Y, but compared with sample 8911037 it also has higher Al$_2$O$_3$, K$_2$O and Sr (Table 3). There is a small negative Nb-anomaly (Fig. 19). Otherwise the geochemistry is indicative of EMORB to primitive WPB affinity, though primitive island arc tholeiite (IAT) origin cannot be excluded.

Sample 8911061 from the MBc is strongly sheared and altered rock and may have gained SiO$_2$, but according to P$_2$O$_5$, Y and La data (not shown), it is similar to 8911059 or to the VG2 sample from the MBd.

Sample 8910927 (SiO$_2$ 50.0% in Figs. 15–18) is the only pillow lava and the only basalt from the TSB. It is characterized by high Ti and Zr (Table 3) and by medium-K tholeiitic character. Figure 19 shows a slightly negative Nb anomaly due to increase of Th, but otherwise the pattern is similar to that of sample 8911059 but at higher level for elements from La to Sc. The Th peak, also seen as high Th/U-ratio (4.9), is probably due to contamination and not a primary magmatic feature.

VG2

This group includes two basalts, two basaltic andesites, one trachybasalt and two basaltic trachyandesites (Fig. 15). Two altered samples are not included in Figs. 15–18. Most of the VG2 rocks share features with VG3 rocks, but the generally higher Zr and Y abundances point to a slightly different origin. The alkaline rocks also show high-K affinity (Fig. 16) and can be considered as a subgroup. The general trend for the subalkaline rocks (Fig. 19) is compatible with WPB origin, but whether there is a slightly negative Nb anomaly or a positive P anomaly is unclear. The highly differentiated nature evident in the low Cr and Ni values (Fig. 20), also in most mafic sample (Table 3), indicates extensive frac-

tional crystallization, which may be responsible for these anomalies. Although the occurrence of a small amount of subduction component cannot be excluded, an EM-type origin is proposed.

The HSBc dyke rock (8911137; SiO$_2$ 50.3% in Figs. 15–18) is a medium- to high-K basalt and to considerable extent resembles the VG4 alkaline dyke rocks. The highly differentiated nature of this sample is evident in the very low MgO, Ni and Cr and high Al$_2$O$_3$ levels (Table 3) for a basaltic rock. Figure 19 shows the enriched pattern, but the slightly negative Ba anomaly could indicate either crystallization of a Ba-bearing phase or a small amount of sediment assimilation or crustal contamination. The lapilli-tuff 8911066 is a high-K basaltic trachyandesite (SiO$_2$ 51.7%) with lower levels of Th, Nb and La (Fig. 19) compared with the dyke rock, but it is unclear whether this is a primary feature or due to K, Rb and Ba enrichment. Sample 8911120 is also a high-K basaltic trachyandesite (SiO$_2$ 55.3%) and has higher MgO, Cr and Ni (Figs. 17 and 20) than the two samples considered above. The enrichment of LILE and slightly negative Nb anomaly could indicate the presence of subduction component (Fig. 19), but the high levels of K, Rb and Th along with low Ba and high silica content are more compatible with crustal contamination than a subduction component.

The medium-K tholeiitic basaltic andesite 8911121 from the HSBc is strongly mineralized, and K, Rb and Ba appear to be depleted (Fig. 19) probably due to alteration. This sample is included in VG2 because it has geochemical characteristics closer to group VG2 than group VG3, but it should really be considered as a unique sample. Amphibolite 8911132 from the HSBb is a sheared rock with elevated Cl, F and S and depletion of Zn (data not shown). The Rb, Ba, Th values (data not shown) suggest a redistribution of these elements during shearing and alteration and the classification of the sample as VG2 is only

Table 3. Chemical composition of selected metavolcanic rocks in the Tampere–Hämeenlinna area.

Group	VG1	VG1	VG1	VG2	VG2	VG3	VG3	VG3	VG4
Subarea[1]	MBc	MBc	TSB	HSBb	HSBc	HSBd	HSBd	HSBb	MBb
Sample/S89[2]	11037	11059	10927	11142	11137	11151	11140	11093	11025
SiO_2	48.27	47.81	49.08	47.72	49.42	48.52	48.36	53.40	49.49
TiO_2	1.25	1.44	1.85	0.91	1.66	1.07	1.17	1.07	2.48
Al_2O_3	14.70	19.97	15.42	18.79	20.13	16.88	19.12	16.96	16.06
FeO	12.67	11.03	12.47	10.18	9.98	10.90	10.37	9.33	11.95
MnO	0.21	0.19	0.19	0.19	0.16	0.18	0.17	0.15	0.17
MgO	6.33	3.83	5.12	6.66	2.97	7.47	5.63	5.12	4.84
CaO	11.26	9.84	9.75	8.50	8.89	9.64	7.74	8.16	7.30
Na_2O	2.94	3.37	3.51	2.36	3.20	2.96	3.27	2.73	2.73
K_2O	0.18	0.63	0.47	0.95	1.30	0.66	2.18	1.23	2.09
P_2O_5	0.14	0.16	0.24	0.30	0.53	0.23	0.39	0.33	1.08
CO_2	0.03	0.40	0.03	0.02	0.02	0.02	0.23	0.04	0.05
F	0.01	0.02	0.03	0.05	0.06	0.02	0.09	0.07	0.21
S	0.04	0.01	0.03	0.01	0.14	0.01	0.03	0.06	0.09
Ba	45	198	140	296	414	232	432	414	515
Cl	71	79	685	56	72	69	77	83	575
Cr	125	41	34	25	2	196	55	128	109
Nb	4.0	7.6	7.9	9.9	34.5	7.6	8.9	10.4	39.5
Ni	83	35	53	33	16	52	40	51	44
Rb	9	10	11	22	57	15	51	43	61
Sr	158	335	210	641	371	385	600	437	522
V	427	368	471	250	245	310	300	252	258
Y	25	25	37	16	36	20	25	22	34
Zn	125	128	111	106	105	100	132	110	197
Zr	79	111	166	105	232	84	113	145	303
Co	53	38	26	33	23	38	31	25	29
La	4.3	9.5	10.1	12.0	24.2	8.6	13.4	15.4	44.6
Sc	53.1	40.0	50.9	40.5	39.5	51.1	39.3	35.0	25.5
Th	0.3	1.0	1.8	1.6	4.5	1.1	2.1	3.1	3.6
U	0.2	0.7	0.4	0.6	1.4	0.8	1.1	1.6	1.8

Major elements (wt%), S (wt%) and Ba–Zr (ppm) analysed by XRF and F by ion selective electrode at the GSF laboratory; Co–U by neutron activation at the Technical Research Centre of Finland; CO_2 by wet method at XRAL in Canada.
[1] See Fig. 2.
[2] Sample numbers are referred to in the text.

tentative. Hornblende-mica gneiss 8911115 (SiO_2 53.3% in Figs. 15–18) from the MC has indications of a tuff origin, and the low K and Rb (Fig. 19) are probably due to incipient melting.

VG3

The VG3 samples come almost entirely from the HSBd (Fig. 14). Nine of the samples are altered or show disturbed chemical composition and these are not included in Figs. 15–18.

VG3 samples are divided into three subgroups: main subgroup, intermediate subgroup and trachybasalts. The main differences relative to VG2 are the more pronounced occurrence of negative Nb anomaly and the less inclined trend from Zr to Y in the main VG3 subgroup (Fig. 19).

Most of the main subgroup samples are medium-K tholeiitic basalts with only limited SiO_2 variation in anhydrous values from 48% to 50% (Figs. 15–18). In Harker diagrams Zr and Y values are increased and MgO values

Table 3 (continued).

Group	VG5	VG5	VG5	VG6	VG6	VG6	VG6	VG7	VG8
Subarea[1]	TSB	HSBc	HSBa	NTSB	TSB	TSB	HSBb	TSB	HSBc
Sample/S89[2]	10884	11119T	11041	10860	10855	10830	11157	10966	11117
SiO_2	52.26	55.65	59.73	54.91	60.01	67.29	68.89	54.28	67.25
TiO_2	0.70	0.74	0.80	0.70	0.46	0.44	0.32	0.70	0.59
Al_2O_3	15.76	18.48	18.17	17.93	19.41	16.39	15.87	15.41	15.31
FeO	11.06	7.67	6.78	7.82	4.75	3.99	3.40	7.58	5.27
MnO	0.18	0.15	0.13	0.17	0.16	0.14	0.10	0.16	0.13
MgO	8.18	3.51	1.94	4.23	1.80	1.11	1.64	7.52	1.20
CaO	6.21	7.01	5.37	6.84	5.36	2.61	3.04	6.55	2.37
Na_2O	3.24	3.70	4.01	3.33	4.56	3.49	2.74	2.50	3.95
K_2O	0.71	1.60	1.53	2.12	1.74	3.42	2.92	3.37	2.49
P_2O_5	0.28	0.19	0.20	0.43	0.29	0.11	0.10	0.35	0.16
CO_2	0.09	-	0.40	0.07	0.04	0.38	0.32	0.02	0.27
F	0.06	0.04	0.03	0.11	0.08	0.13	0.08	0.04	0.13
S	<0.01	0.01	0.01	<0.01	0.01	0.01	0.24	<0.01	0.03
Ba	274	410	460	1000	1300	1320	411	827	644
Cl	55	40	137	99	93	47	76	36	349
Cr	188	72	18	69	17	35	22	482	10
Nb	6.7	8.8	6.8	4.3	7.6	13.2	11.4	9.6	13.9
Ni	56	59	17	31	20	22	25	138	16
Rb	16.8	33	39	46	45	67	88	95	54
Sr	728	343	374	1220	1080	288	126	664	197
V	253	152	129	213	94	39	49	194	42
Y	14	13	18	15	12	23	20	23	41
Zn	124	92	89	112	96	99	61	96	122
Zr	79	110	166	80	102	159	205	152	270
Co	36	26	15	21	9	4	6	27	-
La	17.8	14.4	17.2	22.7	30.4	36.9	21.4	26.3	26.8
Sc	44.5	25.5	13.5	29.2	15.9	15.6	8.1	27.2	20.6
Th	2.6	2.6	4.6	2.3	4.1	6.1	12.0	7.5	6.0
U	0.7	1.3	2.1	0.8	1.1	2.0	5.0	2.5	3.2

Fig. 15. Total alkali–silica (TAS) diagram (Le Bas et al. 1986) for most preserved volcanics in the Tampere–Hämeenlinna area. Data from this study. B – basalt, O_1 – basaltic andesite, O_2 – andesite, O_3 – dacite, R – rhyolite, S_1 – trachybasalt, S_2 – basaltic trachyandesite, S_3 – trachyandesite, T – trachyte and trachydacite. Asterisks – VG1, open crosses – VG2, open squares – VG3, crosses – VG4, open upright triangles – VG5 excluding the TSB samples, open circles – VG5 from the TSB, open inverted triangles – VG6 samples from the TSB and HiSB, filled inverted triangles – VG6 samples from the MB and HSB, open diamonds – VG7, diagonal crosses – VG8. Dashed line – boundary line by Irvine and Baragar (1971), dotted line – boundary line by Kuno (1966).
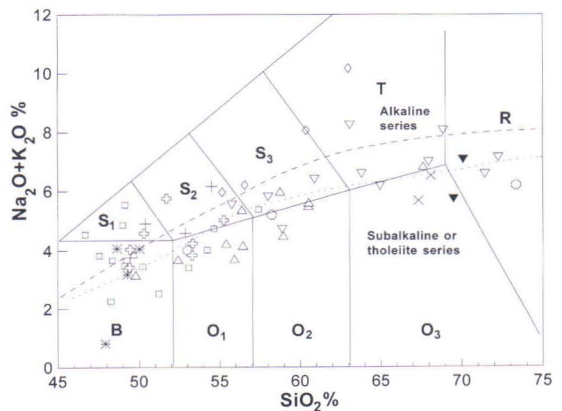
decreased. Increase in Nb and decrease in FeO and V are also noticed (data not shown). The Ni and Cr data (Fig. 20) are more scattered, but overall low values indicate a differentiated nature for these rocks. The chemical composition of sample 8911151, which has highest Cr value, is shown in Table 3. The pattern in Fig. 19 is interpreted to indicate an intermediate DM–EM origin associated with subduction component. Sample 8911076 (SiO_2 47.6%), which deviates to lower TiO_2 in Fig.

17, is the only main subgroup sample containing abundant magnetite (Lahtinen & Korhonen 1996); evidently magnetite has been a crystallizing phase depleting TiO_2 and possibly to some extent Nb.

The intermediate samples, forming a 'differentiation trend' in Figs. 15–18, are from the HSBb and HSBd. They are medium-K rocks, usually with lower FeO/MgO ratios than other VG3 samples. The three most mafic samples have a chemical composition similar to the main subgroup samples, but the lower TiO_2, Al_2O_3, La, Zr, Y and higher Ni and Cr indicate a slightly different evolution. The most primitive sample (8911144; SiO_2 49.8% in Figs. 15–18) has a pattern comparable to the main subgroup samples (Fig. 19). All the intermediate rocks show a pronounced negative Nb anomaly, but relative to the main subgroup there is a steeper declining trend from La to Y. This could be due to differentiation, but only Ti shows a decreasing trend, while P, La, Sr, Y show increasing trends relative to SiO_2 (Figs. 17–18), possibly indicating higher Zr/Y ratios in the parent magma for basaltic andesites and andesite, and a higher proportion of EM-type component. These high Zr samples are reminiscent of some VG2 intermediate rocks, with differences of deeper Nb anomaly and lower level of Y, however.

The three trachybasalts are from the HSBd, and differ from the main subgroup in higher K_2O, P_2O_5, Sr, La and Zr (Figs. 15–18), and in sample 8911140 also in higher F (Table 3). MgO, Ni and Cr are comparable to main subgroup levels, but Rb and Ba show slightly elevated abundances (data not shown). The trachybasalts, in fact, show a pattern intermediate between the VG3 main subgroup and VG2, but because of the deeper negative Nb and Zr anomalies relative to VG2 they are classified as a subgroup of VG3 (Fig. 19). They contain abundant magnetite (Lahtinen & Korhonen 1996) and probably magnetite has been a precipitating phase, causing the negative Ti anomaly and enhanced Nb anomaly.
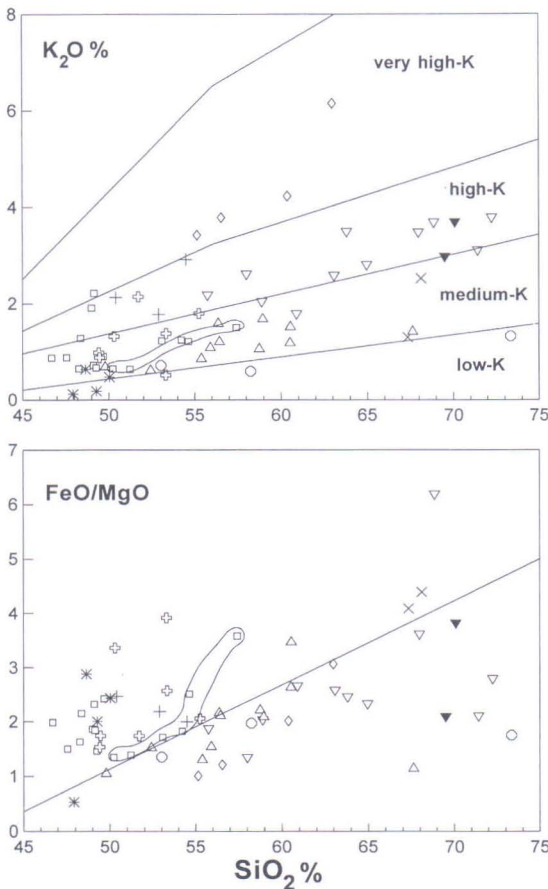

Fig. 16. K_2O–SiO_2 and FeO/MgO–SiO_2 diagrams for the best preserved volcanics in the Tampere–Hämeenlinna area. Data from this study. Oxide totals were recalculated to 100%. Boundary lines for K_2O–SiO_2 diagram are from Kähkönen (1989). The division between tholeiitic and calc-alkaline fields on the FeO/MgO–SiO_2 diagram is from Miyashiro (1974). See Figure 15 for symbols.

The high level of Rb could point to a small amount of crustal contamination.

Altered samples not included in the Harker diagrams are interpreted to be genetically related to the VG3 main subgroup. The patterns of three of the samples in Fig. 19 show a redistribution of mobile elements K, Rb, Ba and Th, which at least in part can be attributed to alteration, but otherwise they follow the main subgroup trend. Two altered andesites have been included among the VG3 intermediate samples and, for example, the strongly sheared and mineralized (S 1.7%) sample 8911132T is comparable to other intermediate

samples, except for the loss of Sr, K, Rb, and Ba during shearing and alteration (Fig. 19).

VG4

The three hypabyssal dyke rocks from the MB are geologically and geochemically related. They are high-K alkaline rocks, with the highest TiO_2, P_2O_5, Zr and La values of all volcanic rocks (Figs. 15–18), and also highest F-values (among volcanics) and high Cl-values, as seen in the representative sample in Table 3. These features, and the spidergram patterns in Fig. 21, show them to have an
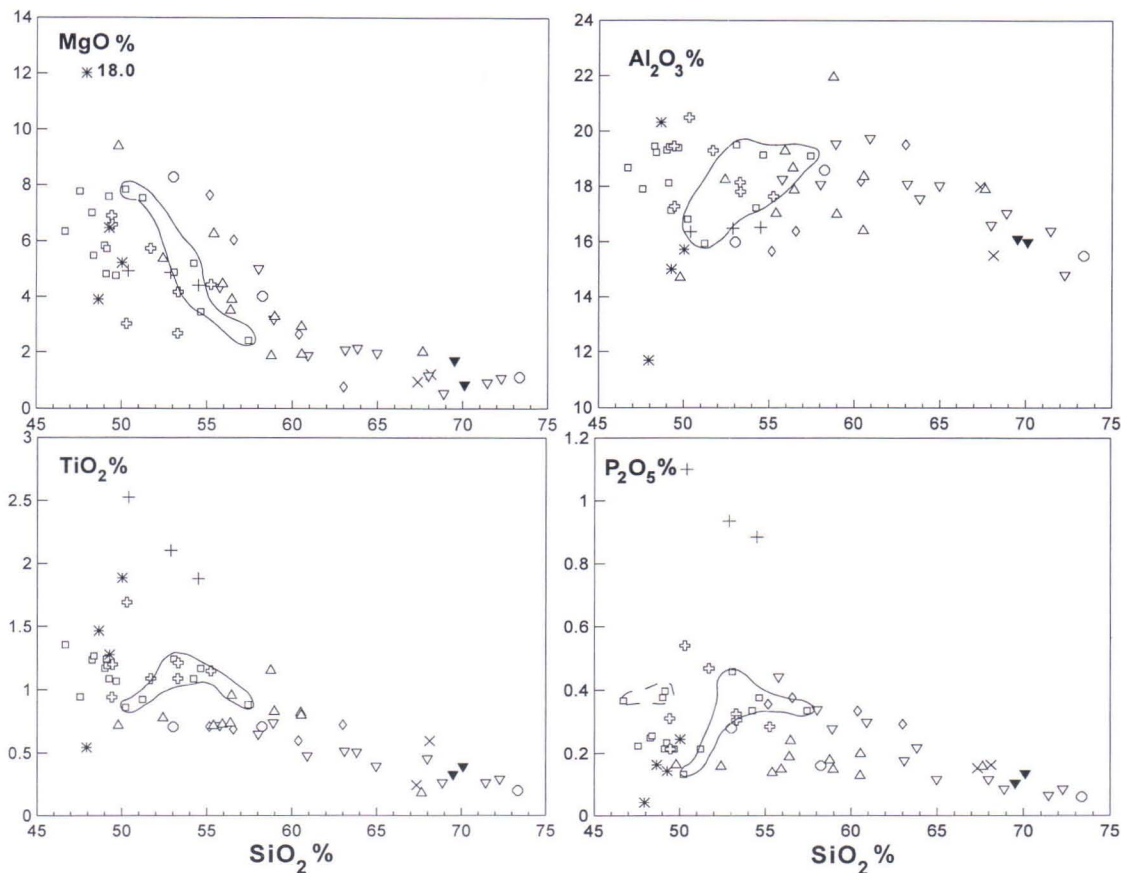

Fig. 17. Harker-type selected major element (%) variation diagrams for the best preserved volcanics in the Tampere–Hämeenlinna area. Data from this study. Oxide totals were recalculated to 100%. See Figure 15 for symbols. Solid line encloses the VG3 intermediate group samples and dashed line the VG3 trachybasalts.
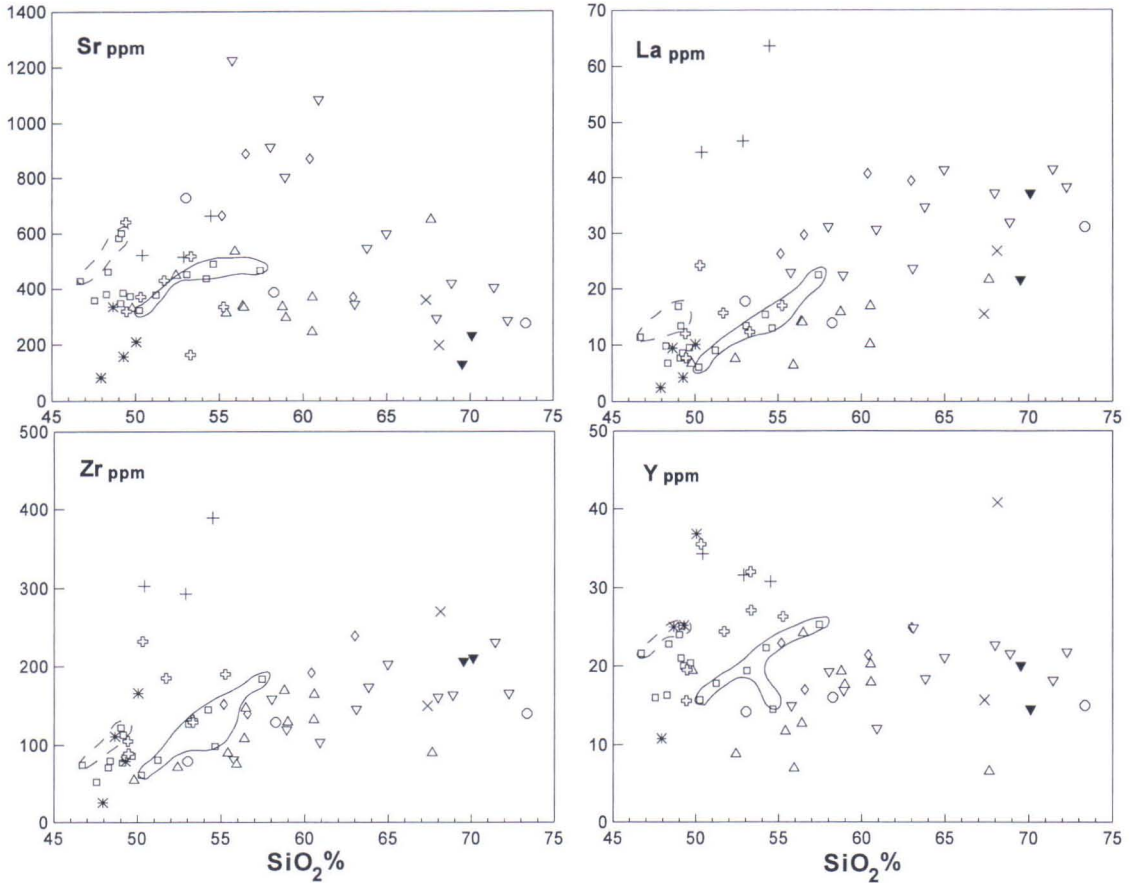
Fig. 18. Harker-type selected trace element (ppm) variation diagrams for the best preserved volcanics in the Tampere–Hämeenlinna area. Data from this study. Oxide totals were recalculated to 100%. See Figure 15 for symbols. Solid line encloses the VG3 intermediate group samples and dashed line the VG3 trachybasalts.

alkaline WPB character (e.g. Pearce 1982). There is a small negative Nb anomaly in the samples 8910960 and 8911057T, but it may be due to assimilation and/or crystallization of Ti-bearing phase and is not considered diagnostic of a subduction component. The dyke rocks have intruded migmatitic gneisses and are comingling with granodiorite; crustal contamination is thus one possibility, but the enriched nature and pattern do not favour a strong crustal component, and a small component is difficult to observe. The small amount of graphite in sample 8910960 (0.04% $C_{Graf.}$)

indicates a small assimilated sediment component.

VG5

There are 18 samples in this group, including five possibly altered samples not shown in Figs. 15–18. The chemical composition of representative samples is set out in Table 3. Most VG5 rocks are medium-K calc-alkaline rocks with lower TiO_2, Zr, Y and higher MgO, Cr and Ni compared with VG1–VG3 at similar SiO_2 values (Figs 17–20). VG5 rocks predominantly occur in the HSB, and the few TSB
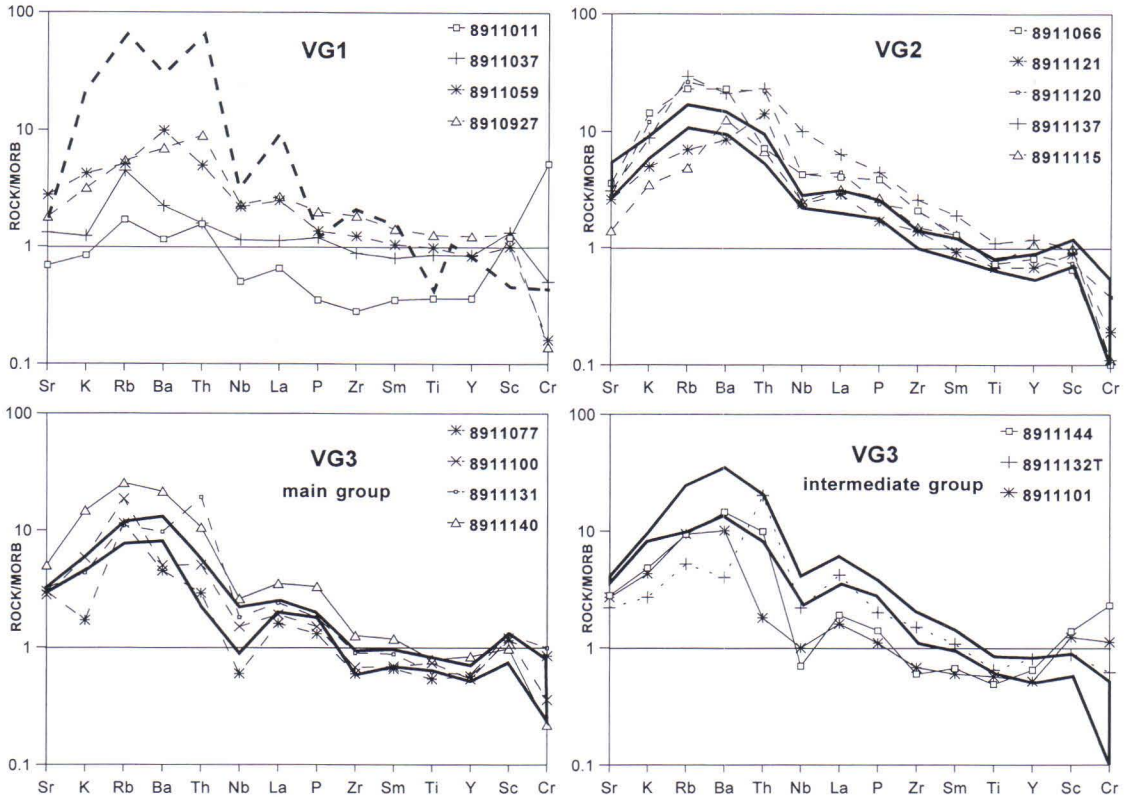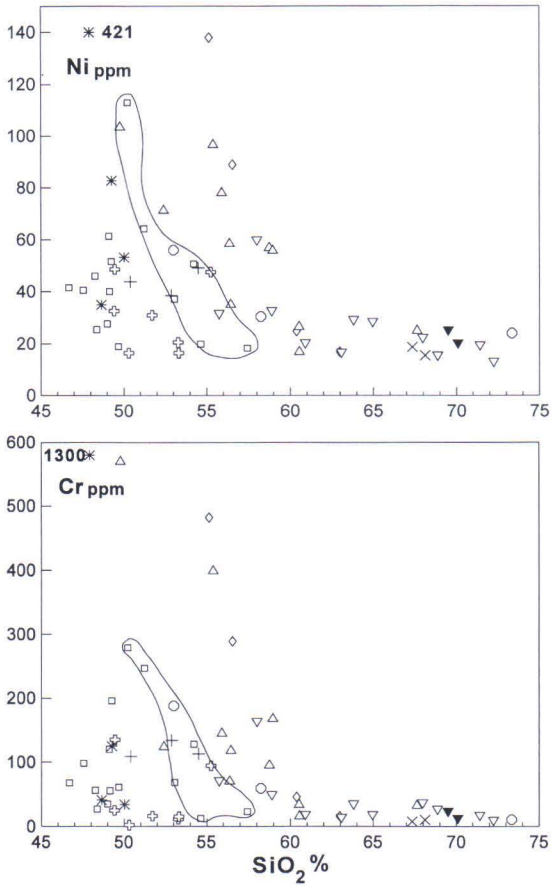
Fig. 19. Trace element patterns for selected VG1–VG3 volcanics normalized to mid-ocean ridge basalt. Normalizing values from Pearce (1982), except La (3.8 ppm) which has been interpolated from his Ce value. Cr values less than 25 ppm have been set to 25 ppm. Sample numbers are referred to in the text. Solid thick lines show the normal variation of the characteristic samples within individual groups and the dashed thick line is the average chemical composition of basement-related sedimentary rock (SG3–SG7).

samples are considered as a subgroup. Basaltic andesites and andesites dominate, and in their clear negative Nb anomaly and pattern (Fig. 22) are comparable to the mature continental island arc or ACM affinity (eg. Pearce 1983). The small negative Nb anomaly together with the rather steep spidergram, point to an EM-type mantle component. The nearly identical TiO_2 values for most samples (Fig. 17) could indicate precipitation of the Ti-bearing phase, depressing Ti in Fig. 22. Three intermediate HSB samples show abundant magnetite, indicating that, at least in part, the precipitation of magnetite is responsible for the Ti depletion.

The two VG5 samples from the HSBc deviate to higher Sr values (Fig. 18) and the pattern of the more mafic sample (8911124T) shows a less pronounced negative Nb-anomaly (Fig. 22) than other VG5 samples indicating a slightly different evolution. Three samples from the HSB are not included in Figs. 15–18 because of their altered geochemical nature. Migmatitic hornblende–mica gneiss from the HSBa shows depletion of K, Rb and Ba (data not shown), but otherwise it is geochemically comparable to the nearest VG5 sample.

Excluding the Haveri sample, the medium-K calc-alkaline basaltic andesite sample 8910884 (SiO_2 53.0%) is the most mafic sample from the TSB (Fig. 15). Characterized by
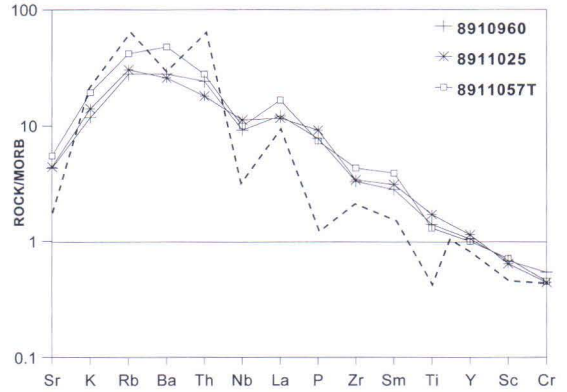
Fig. 21. Trace element patterns for VG4 hypabyssal dykes normalized to mid-ocean ridge basalt. Normalizing values from Pearce (1982), except La (3.8 ppm) which has been interpolated from his Ce value. Sample numbers are referred to in the text. Dashed thick line is the average chemical composition of basement-related sedimentary rock (SG3–SG7).

Fig. 20. Harker-type Cr and Ni (ppm) variation diagrams for the best preserved volcanics in the Tampere–Hämeenlinna area. Data from this study. Oxide totals were recalculated to 100%. See Figure 15 for symbols. Solid line encloses the VG3 intermediate group samples.

higher P_2O_5, Sr and La (Table 3, Figs. 17–18) than the HSB calc-alkaline rocks, it more closely resembles the TSB VG6 rocks. This is also seen in Fig. 22 where the negative Zr anomaly and positive La, P and Sm anomalies relative to a rather mafic nature distinguish it from the HSB rocks. Relative to sample 8910884, the low-K calc-alkaline andesite sample 8910866 (SiO_2 58.3%) has lower La, Sr, P_2O_5 (Figs. 15–18 and 22) and lower Rb and Ba (data not shown), deviating in this way from the main trend of the TSB andesites. Both these samples show abundant magnetite (Lahtinen & Korhonen 1996).

The low-K rhyolite sample 8910811 (Figs. 16 and 22) is from hypabyssal porphyry and, apart from the low K, Rb and Ba, resembles

other high silica rocks of the TSB. One slightly mineralized and altered (loss of K_2O, F and Rb) volcanic rock and one volcanic greywacke from the TSB have been tentatively classified in VG5 but should be considered as unique samples within this group.

VG6

Of the 18 VG6 samples, only two felsic samples (MBc and HSBb) lie outside the TSB and NTSB. Five altered samples, all from the TSB, are not included in Figs. 15–18. VG6 samples are mainly high-K rocks with intermediate calc-alkaline to alkaline affinities plotting in the trachy-fields (Figs. 15–16). VG6 samples show higher Sr, La and

P_2O_5 (Fig. 18) and F (Table 3) abundances than VG5 samples at similar silica levels. The particularly characteristic feature in the TSB and NTSB samples is the Ba enrichment (Table 3 and Fig. 22), seen especially in the Ba–K_2O relation (Fig. 23).

The three most mafic samples in VG6 are from the NTSB. The most mafic sample 8910860 is also differentiated (Table 3, Fig. 20), which probably has changed the element levels. The high Ba, Sr and P_2O_5 cannot be attributed solely to differentiation, however, and abundances of these elements must also have been high in the parent melt. Although differentiation has affected the trace element pattern of the sample (e.g. Ti in Fig. 22), the Nb–Zr–Y relation and strongly positive La, P

and Sm anomalies point to EM-derived melts with a subduction component. Trachyte from the NTSB plots in the tholeiitic field (Fig. 16), but this is not considered diagnostic and the geochemical similarity with felsic rocks in the TSB indicates a broadly similar origin. All four NTSB samples show abundant magnetite (Lahtinen & Korhonen 1996), suggesting that magnetite was a crystallizing phase.

Sample 8910855 (SiO_2 60.9 % in Figs. 15–18) from the TSB is more differentiated, as seen in the lower level of P and Ti in Fig. 22, but in general it is geochemically similar to the above-considered intermediate samples (Table 4, Figs. 15–18). The more felsic samples 8910903 (SiO_2 63.1%) and 8910908 (SiO_2 63.8%) are still more differentiated, as
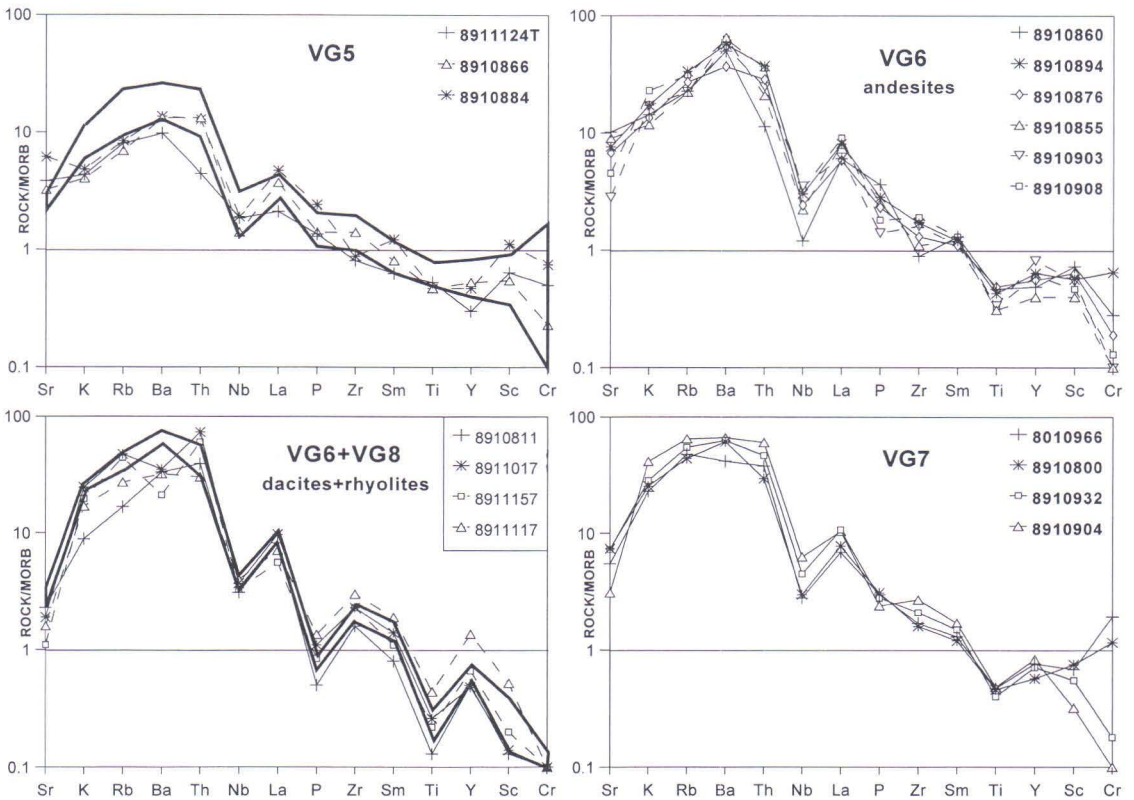

Fig. 22. Trace element patterns for selected VG5–VG8 volcanics normalized to mid-ocean ridge basalt. Normalizing values from Pearce (1982), except La (3.8 ppm) which has been interpolated from his Ce value. Cr values less than 25 ppm have been set to 25 ppm. Sample numbers are referred to in the text. Solid thick lines show the normal variation of the characteristic samples within individual groups and, in lower left figure, for VG6 dacites and rhyolites.

seen in the pronounced P and Ti anomalies in Fig. 22. Owing to their differentiated nature, the felsic trachydacites and rhyolites from the TSB (Figs. 15–18) show strong negative P and Ti anomalies in Fig. 22. The two less silicic rocks contain abundant magnetite.

Three of the VG6 samples from the western part of the TSB are strongly sheared and mineralized rocks. Sample 8910873, for example, is strongly altered, as seen in the very low Na_2O (<0.5%) and high B (0.5%); otherwise, however, it seems to have common geochemical characteristics with VG6 rhyolites of the TSB. Strongly sheared volcanic rock 8910935 has high K, Rb and Ba (data not shown), plotting this sample to very high-K field, but the primary composition probably has been more comparable to that of VG6 felsic rocks.

Sample 8911017 is the only VG6 sample from the MB. Whether it is a hypabyssal rock related to the surrounding granitoids or a true volcanic rock is unclear. It is a high-K calc-alkaline rhyolite (SiO_2 70.1% in Figs. 15–18) and geochemically similar to other VG6 rhyolites of this study. The main differences are the negative Ba-anomaly and slightly higher level of Th (Fig. 22). Agglomerate 8911157 (SiO_2 69.5%) from the HSBb, dated at 1888±11 Ma (Vaasjoki 1994), is a high-K dacite (Figs. 15–16) exhibiting similar Ba depletion (Fig. 22). It has lower La, Sr and slightly higher MgO (Figs. 17–18) than do felsic VG6 rocks of the TSB and is thus more comparable to the HSB VG5 rocks.

VG7

The four VG7 samples are very high-K alkaline rocks that plot in the trachy-fields (Figs. 15–16), and the basaltic trachyandesite is a shoshonite, which is used here as the group name. In their TiO_2, P_2O_5 and Sr abundances they resemble VG6 rocks, but La and Zr values are slightly higher (Figs. 17–18). Values of Rb, Nb, Th and sometimes F also are higher than in VG6 rocks at similar SiO_2 values (data not shown).

The two mafic samples show high Cr and Ni abundances, especially relative to the SiO_2 level. This indicates a rather primitive nature, as seen in sample 8910966 (Table 3), which has very high LILE abundances relative to the high MgO, Ni and Cr. This and the other mafic sample 8910800 show a similar trace element pattern, with deep negative Ti anomaly (Fig. 22) indicating early crystallization of Ti-bearing phase, Ti-poor source or retention of Ti in the source. Sample 8910800 is from the shoshonitic unit at Orivesi (Kähkönen 1989) and 8910904 probably from about the same strata 6 km west. While sample 8910932 closely resembles sample 8910904 (Fig. 22), it also differs in the abundant magnetite (Lahtinen & Korhonen 1996). The patterns from K to Th are at about the same level and differ from the VG6 patterns (see Fig. 22). The mafic samples are slightly differentiated, but the high Sr, La, Zr, and also high Nb despite the possible crystallization of the Ti-bearing phase, indicate the occurrence of EM-type mantle associated with subduction component. The high SiO_2 level in such primitive rocks (primitive on the basis of high Ni and Cr values) may indicate high SiO_2 in the parent magma or crustal contamination.
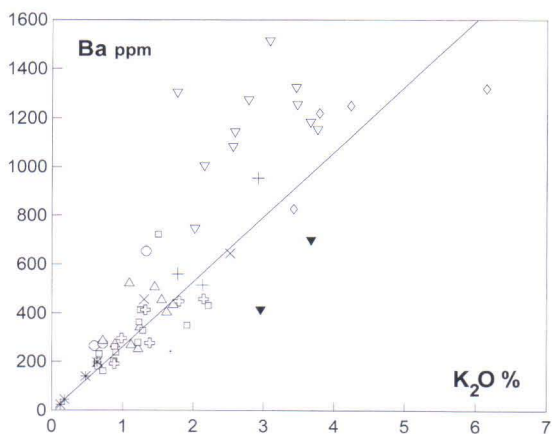

Fig. 23. Ba–K_2O diagram for the best preserved volcanics in the Tampere-Hämeenlinna area. Data from this study. Solid line shows the approximate trend for the HSB volcanics. See Figure 15 for symbols.

VG8

Two dacites of tholeiitic affinity are included to this group (Fig. 16). The volcanic gneiss 8910993 (SiO_2 67.4%) from the MBd is a medium-K to low-K rock that may be slightly mineralized. Except for lower Sr, Th, MgO and higher FeO (data not shown) and slightly higher Zr and Y (Figs. 17–18),

it is comparable in chemical composition to the HSBb VG5 sample having similar SiO_2. Sample 8911117 (SiO_2 68.1%) from near the Kiipu Zn occurrence in the HSBc is a medium-K dacite of tholeiitic affinity with high Cl, F and elevated Zn (Table 3), possibly related to mineralization effects. It is characterized by higher Zr, Sm, Ti, Y and Sc than in other felsic rocks (Figs. 18 and 22).

Source characteristics and tectonic setting

Source characteristics and possible tectonic settings were discussed above in terms of the different rock groups. The discussion is now generalized to some overall characteristics, and origins are considered in more detail. VG1 rocks have been divided into two subgroups: MORB affinity and EMORB–WPB affinity. The two MORB-affinity samples differ from the EMORB–WPB volcanics in the Ba–Nb diagram, and the sediment assimilated sample shows higher Th (Fig. 24). The MORB-affinity rocks are interpreted to be of pure DM origin, formed in a rift or marginal basin environment. High Th also characterizes the WPB-affinity Haveri sample from the TSB and points to crustal contamination. Crustal contamination seems to characterize some of the more evolved Haveri basalts (Kähkönen & Nironen 1994). The most primitive Haveri samples (Table 1 in Kähkönen & Nironen 1994) have Th/Nb (0.08–0.11), Zr/Nb (14–17) and Ba/Nb (14–27) values that also point to an EM component, and the proposed absence of a subduction component favours the extensional setting proposed by Kähkönen & Nironen (1994). A similar setting is tentatively proposed for the EMORB–WPB-affinity MBc sample, even though the similarity to the VG2 samples and higher Sr and Al_2O_3 point to a different evolution.

All VG2 samples are differentiated samples, where variable Y abundances (Fig. 18) indicate differences in the degree of mantle melting;

the approximately constant TiO_2 values at increasing Zr abundances possibly indicate precipitation of the Ti-bearing phase, which would also cause Nb depletion and shift the Th and Ba to higher values (Fig. 24). The Th–Nb, Zr–Nb and Ba–Nb relations are indicative of a large EM component, while the elevated Ba may be due to a large proportion of pelagic sediment-derived enriched component (EMI).

The occurrence of uralite (cpx/aug) and plagioclase phenocrysts in the VG3 rocks indicates that they have been the crystallizing phases. The VG3 main subgroup basalts are differentiated HAB, as seen in the low Cr and Ni, indicating extensive olivine+spinel precipitation during ascent. This, plus the occurrence of clinopyroxene before plagioclase in the crystallization sequence, indicates elevated H_2O values in the magma and would explain the high Al_2O_3 and Sr in the VG3 main group. The occurrence of a high-Al parent cannot nevertheless be totally excluded and the high Sr must also partly be due to its enrichment in the source.

Judging from the Cr and Ni values the intermediate VG3 mafic samples are more primitive than the main subgroup rocks; at the same time they are more SiO_2-rich, which could be attributed to greater amounts of H_2O during mantle melting. Note, also, that the Al_2O_3 abundances are lower than in the main subgroup, suggesting a different crystallization history. The relationship between these mafic and intermediate samples is unclear. The Ti–Zr relation (Fig.

24) suggests a Ti-bearing crystallizing phase and deviation to higher Th and Ba values.

All the VG3 rocks show a trend from almost DM-like Zr/Nb and Th/Nb ratios to EM-dominated values comparable to those of VG2. The higher Ba/Nb in the VG3 than in VG2 is interpreted as a contribution from a subduction component, and the high Th characterizing especially the intermediate rocks is due either to scavenging in the mantle wedge or to crustal contamination.

Relative to the VG3 main subgroup, the VG3 trachybasalts have higher Sr, Y, Zr and La (Fig. 18) and similar Cr and Ni (Fig. 20). The more enriched nature is due to both lower

degree of melting and higher proportion of EM component in the parent magma. The occurrence of magnetite in these trachybasalts suggests that magnetite can be a precipitating phase even in basaltic magmas. Its presence can be attributed to crustal contamination (high Rb and K) and/or to increase of water content during ascent.

The VG4 alkalic dykes and one VG2 dyke are the most enriched volcanics in this study. All are strongly differentiated and show assimilation effects, and the precipitation of Ti–Nb-bearing phases is possible, as seen in the occurrence of hornblende and sphene in some samples. In general, the Zr/Nb and Ba/Nb
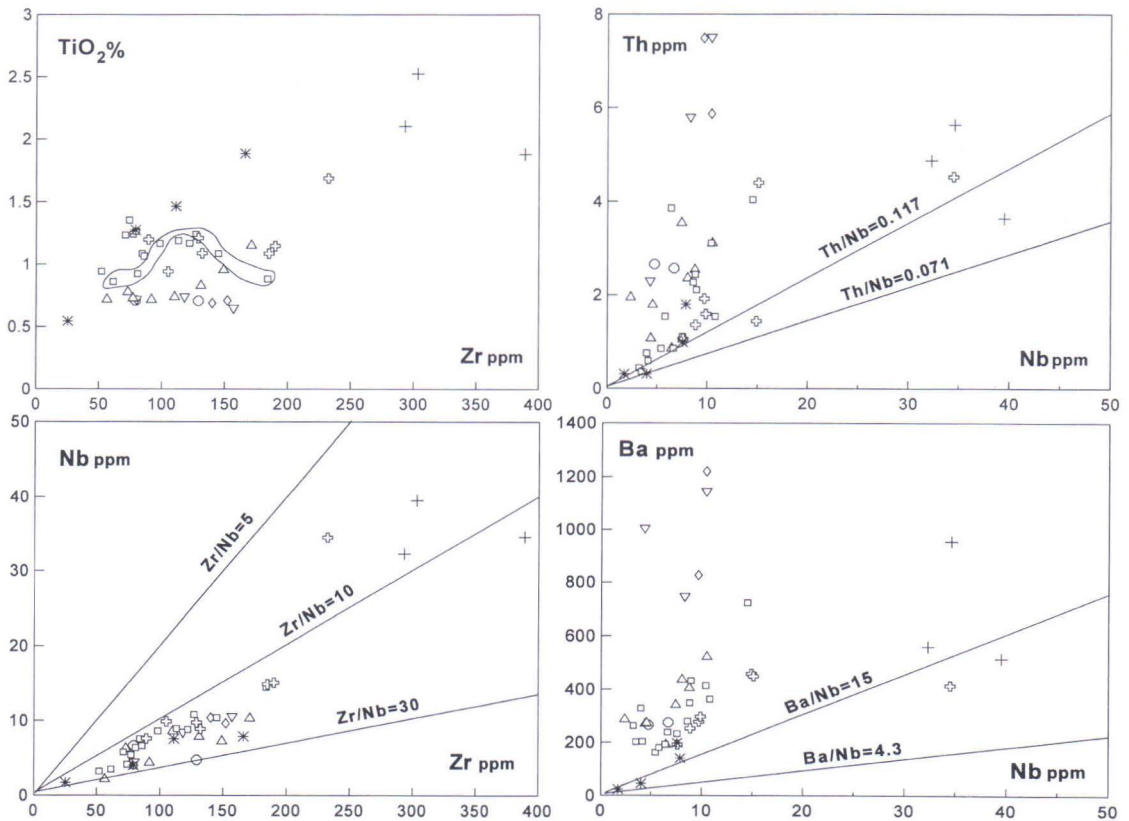

Fig. 24. TiO$_2$–Zr, Th–Nb, Nb–Zr and Ba–Nb diagrams for the best preserved mafic-intermediate (<60% SiO$_2$) volcanics in the Tampere–Hämeenlinna area. Data from this study. See Figure 15 for symbols. Solid line in the TiO$_2$–Zr diagram encloses the VG3 intermediate group samples. Th/Nb=0.117 – primordial mantle ratio; Th/Nb=0.071, Zr/Nb=30 and Ba/Nb=4.3 NMORB ratios. Data from Weaver (1991).

ratios are indicative of HIMU–EMI affinity in the EM source (see also Lahtinen 1994b), and the high Y relative to the enriched nature could indicate a low degree of melting from mainly EM parts of the mantle.

Compared with the tholeiitic VG1–VG4 rocks, the calc-alkaline to shoshonite groups VG5–VG7 show lower TiO_2, Zr and Y (Figs. 17–18) and higher Cr and Ni values (Fig. 20). More H_2O in the mantle leads to a higher degree of melting and possibly to more SiO_2 in the parent magma with consequent changes in the crystallization trend (p. 47). Crustal contamination, directly or due to mixing with crustally derived melts, may also contribute to SiO_2 enrichment. The Ti–Zr relation (Fig. 24) indicates precipitation of Ti-bearing phase and this is seen in the not uncommon occurrence of magnetite (Lahtinen & Korhonen 1996) in the calc-alkaline volcanics and in the finding not only of pyroxene+plagioclase but of hornblende pseudomorphs in the intermediate rocks in the TSB (Kähkönen 1989).

As discussed in the previous section, the mafic samples among the VG5–VG7 rocks have Zr/Nb ratios suggestive of an EM component. The HSB VG5 samples have higher Ba/Nb and Th/Nb ratios than the tholeiitic groups in the HSB and this could be interpreted as a higher proportion of H_2O-containing subduction component, which would mean a greater degree of mantle melting and lead to lower Y, La, Zr, Sr, Ti and P values (Figs. 17–18) than in other HSB rocks.

The TSB mafic rocks (VG6–VG7) differ from the HSB VG6 volcanics in having, besides higher K, also high Ba, Th, Sr, La, and P values, while Y and Zr levels are similar (Figs. 16–18). Ba enrichment is also seen in the Ba–K_2O diagram (Fig. 23), indicating higher Ba level in the TSB source. High Ba/Nb ratios are considered to be more pronounced in low Ce/Yb arc rocks due to a greater contribution of Ba from the subduction-related component (Hawkesworth et al. 1991), but our TSB rocks show high La val-

ues, in combination with an overall enriched nature. High Ba in the mantle source is thus indicated.

The sometimes high Th/U ratios of pelagic sediments (Ben Othman et al. 1989, Cousens et al. 1994) might explain the higher Th/U ratios in the TSB+NTSB, but only a small amount of Th (and also Sr), is considered to derive from subducted material (Hawkesworth et al. 1991). By contrast, low Th/U ratios are best developed in island arc basalts with low contents of incompatible elements, consistent with an approximately constant U flux from the subducted slab (McDermott & Hawkesworth 1991). If this interpretation of the behaviour of Th is correct, it is the mantle or crustal source that determines the behaviour of Th and is responsible for higher Th/U ratios in the TSB and NTSB than in the HSB, where most Th/U ratios are lower (<2.5, Fig. 13) than the MORB variation (e.g. Fig. 6 in Hawkesworth et al. 1994).

The TSB source is thus particularly characterized by high Ba, Sr, La, and possibly elevated Th, and an EMI-dominated source is indicated. The rocks with high Ba/Th ratios are probably the best examples of this EMI source. The rocks with elevated Rb and Th, depressing the Ba/Th ratio, possibly are affected by crustal contamination. At least some of the intermediate rocks in the VG5–VG7 groups may have resulted from the crystal fractionation of more mafic magmas. The real problem lies with the felsic rocks: are they differentiates from intermediate rocks or partial crustal melts? Brophy (1990) describes a situation from the Aleutian island arc where sidewall crystallization accompanied by crustal melting has produced silicic liquids (>63% SiO_2), but a maximum SiO_2 content of 63% is imposed on the fraction-generated magmas due to the rheological barrier. Although the data of this study show a slight gap between 65% and 67% (e.g. Fig. 15) for the TSB samples, the data reported by Kähkönen (1989) show no gap, but interestingly enough a

strong maximum between 62% and 65%. Kähkönen (1989) also concluded that many other processes than fractional crystallization have affected the variation trend of the TSB volcanics, and he interpreted the variation in the Shoshonitic Unit at Orivesi to be due to mixing of intermediate and felsic melts. This could account for the lower Ba/Th and Ba/Rb ratios that characterize the more evolved VG7 samples of this study (Fig. 22).

The HSB samples show more pronounced bimodality (e.g. Fig. 15) pointing to a crustal melting origin for the more felsic samples.

Medium-K tholeiitic dacite near the Kiipu Zn occurrence in the HSBc has high Zr, Ti, Y, Sc, elevated FeO and low La/Y ratio, pointing to an origin in a low degree of melting of tholeiitic basalts during extensional stage. A similar origin has been proposed for volcanogenic rocks associated with the Pukkiharju Zn–Cu prospect in the Rautalampi area (Lahtinen 1994a), but a more LILE-enriched source is proposed for the Kiipu area. The situation in the TSB is more complex, probably because crustal melting, crustal contamination and magma mixing have been operating in the genesis of siliceous rocks.

Regional considerations

The NTSB volcanics are of unknown age, but a geochemical nature comparable to that of the TSB volcanics indicates similar age and origin in general, while the association with SG1 sediments points to a high position in the regional stratigraphy, above the main Myllyniemi formation. Except for the rift/marginal basin affinity Haveri formation, the geochemistry of the TSB samples suggests a mature continental island arc or ACM origin in agreement with the interpretation of Kähkönen (1987, 1989, 1994) and Kähkönen & Nironen (1994). The mafic volcanics at Takamaa (upper volcanic unit at Ylöjärvi in Kähkönen 1989) were not sampled in this study. According to Kähkönen (1989), however, Takamaa is characterized by medium-K basalts, basaltic andesites and andesites of tholeiitic affinity, and the Ti–Zr diagram (Fig. 8 in Kähkönen 1989) shows evidence of intermediate ARC–WPB affinity, possibly indicating extensional characteristics.

The VG4 hypabyssal dyke rocks in the MB are associated with granitoids, and their late-metamorphic and late-collisional nature indicates a relatively young age. The MORB-affinity volcanics occur in the southern part of the MB and are related to rift/marginal

basin environment. The other VG1 rocks are either related to this initiating stage of rifting or related to the younger Häme group stage in the HSB.

Hakkarainen (1994) divided the HSB volcanics into earlier calc-alkaline Forssa group and later Häme group, with tholeiitic affinities erupting in an E–W trending fissure system. The results of the present study, which point to mature continental island arc or ACM affinity, are in accordance with the mature arc affinity that he indicated for the volcanics in the HSB. As discussed above, there are differences between the TSB+NTSB and HSB indicating a more mature origin for the TSB+NTSB volcanics. The distribution of the VG2–VG3 rocks (Fig. 14) coincides fairly well with the Häme group distribution (Fig. 1 in Hakkarainen 1994). The easternmost VG5 sample in the HSBa occurs in an area classified as Häme group, but according to Jokela (1991) a banded intermediate fragment in tuff breccia between two volcanic layers shows the occurrence of two volcanic phases separated by at least one deformation stage. Thus, it is unclear whether this clearly calc-alkaline andesite sample belongs to the Häme group or the Forssa group (favoured).

VG2–VG3 samples also occur in the south-

ern part of the HSBb in areas defined by Hakkarainen (1994) as Forssa group. One of these samples is strongly altered and a misclassification is possible, but otherwise it seems that the Häme group may be more widespread in this area than previously thought. Two VG2 samples in the Forssa domain (HSBc in Fig. 14) are dyke rocks and the third sample is altered

rock and is only tentatively classified as VG2. Outside of some minor differences, then, the distribution of VG2–VG3 rocks coincide well with Hakkarainen's (1994) Häme group and the distribution of VG5 rocks with his Forssa group. Some of the VG5 rocks in the HSBa and the VG1 volcanics in the MB lie in his areas of undefined volcanics.

GEOCHEMISTRY OF PLUTONIC ROCKS

Plutonic rocks predominate in the NTSB and MC and occur as a major component in the TSB, MB and HSB. Indeed, in some parts of these supracrustal belts, as in the middle of the MB, plutonic rocks are the predominant rock type. The plutonic rocks are divided into two groups: mafic plutonics, which are discussed on an areal basis, and granitoids, which are classified into eight groups with addition-

al subgroups. Factors affecting the composition of plutonic rocks are considered first, with attention to the effects of mixing and element exchange in mafic–felsic magma systems and to the variation in melt-composition during melting of various crustal source rocks. Note that the total of oxides was calculated to 100% in Figs. 26–28, while the values used in Tables 4–5 were values obtained in analysis.

Factors controlling the composition of plutonic rocks

Mafic–felsic magma systems

The general source characteristics and different evolutions of mantle-derived magmas discussed above (p. 45–48) also hold for mafic plutonics. The major problem in interpreting the data for mafic plutonics is the frequent admixture of cumulus minerals and evolved melt, which makes it difficult to deduce the composition of the parental magma. Furthermore, the close association with granitoids, and the comingling with them, mean that there could have been an exchange of alkali metals, alkali earths and transition metals between mafic and silicic melts and a mechanical mixing of crystalline components (e.g. Bloomfield & Arculus 1989, Eberz & Nichols 1990, Holden et al. 1991, Zorpi et al. 1991). The degree of mixing and hybridization depends on the composition and mixing ratio of the coexisting melts and on how well the magma

chamber was stirred by convective cells (Sparks & Marshall 1986, Rutter & Wyllie 1989). Without effective stirring and fragmentation, the element transfer is concentrated near the margins of mafic magma blobs. On the other hand, Van der Laan & Wyllie (1993) argue that the exchange processes between enclaves and host rock can lead to degrees of homogenization approaching complete equilibrium, so that in many cases enclaves will not represent the original mafic magma composition.

Geochemical studies of element transfer in mafic–felsic magma systems have mainly been made for mafic enclaves and it is not clear how well the results apply to larger systems. According to Zorpi et al. (1990), mafic magmas are enriched in K, Si, Rb, Ba, Zr, REE, Nb, P and Li and depleted in Ca and Sr. Eberz & Nicholls (1990) found that mafic enclave margins were enriched in K, Rb, Ba, Nb, Y and REE, and depleted in Si and Zr

relative to centres. Holden et al. (1991) compared mafic enclaves and their immediately adjacent hosts and divided elements into those that are more mobile (K, Rb, Ca, Mg, Mn, Ni, Cr, Zn, V, Cu, Sr, Pb, and Ba) and those that are less mobile (Zr, Hf, Nb, Th, REE, Si, Al, Ti, P and Y). All these studies run against the problem of determining the exact geochemical composition of 'primary' magmas and of deciding how much other factors, such as mechanical mixing, crystallization and possible crustal contamination from country rocks, have affected the geochemical composition. Moreover, endmember compositions, especially the fluid phase composition, affect the diffusion rates of elements. It seems clear that elements like K, Rb, Ba, and possibly to a lesser extent transition elements that easily incorporate to biotite, are enriched in mafic magmas in contact with felsic magmas. This has also been shown in experimental studies, where the stabilization of biotite in the interaction of basic and granitic magmas produced basic material with more K than coexisting felsic melt (Johnston & Wyllie 1988). The experimental results of Van Der Laan & Wyllie (1993) imply that chemical equilibration between mafic enclaves and host magma advance far during the solidification of a large silicic pluton at 920°C and 10 kbar. Their results show that mafic–felsic magma interaction, especially in stirred pluton, may change the composition of silicic granite to a more intermediate granodiorite-like composition, enriched in mafic components.

Origin of granitoids; experimental results

There are several models of granitoid genesis and only a few points are noted here, with emphasis on experimental data. The differentiation from basalt to produce granite has been proposed in some cases, as for the derivation of some A-type magmas (Turner et al. 1992). This may well work for small bodies, but it clearly does not explain large batholiths. Normal crystal settling is also considered an inadequate mechanism in high viscosity felsic magmas, but buoyant and residual liquid removal from the crystallizing phases (Rice 1981) seems probable. It is generally believed that some intermediate granitoids in particular have a close genetic link with mantle-derived rocks, either through differentiation or through melting. The restite unmixing model of White & Chappel (1977) could explain the mafic enclaves in granitoids, but often these can better be interpreted as microgranitoid enclaves produced by mingling of mafic and silicic magmas (e.g. Reid et al. 1983, Furman & Spera 1985). Basic magmas of mantle origin may interact with crustally derived anatectic silicic melts to form hybrid calc-alkaline granitoids (Castro et al. 1991). Such processes can be considered as AFC (assimilation and fractional crystallization, De Paolo 1981) or in the ultimate case MASH (melting, assimilation, storage and homogenization, Hildreth & Moorbath 1988). Although not conclusively so, felsic granitoids are generally considered as crustally derived melts, of igneous or sedimentary material or a mixture of these. Granitoid suites dominated by more intermediate rocks are commonly the product of partial melting of dominantly basaltic material or the differentiation of basalt.

Water-saturated ($P_f=P_{total}$) partial melting of tholeiite at 5 kbar (Helz 1976) produced liquids that, with increasing temperature displayed a trend from initially granitic liquid compositions, through granodiorite, to tonalite. The partial melt compositions ($P_f<P_{total}$) reported by Holloway & Burnham (1972) for this same tholeiite were tonalitic at both 5 and 8 kbar. The data of Spulber & Rutherford (1983) indicate that low-K and low-Al_2O_3 tonalitic melts are produced by a small degree (about 10–15%) of melting of tholeiite, with a major enrichment in the Al_2O_3 in hydrothermal conditions.

Rapp et al. (1991) conducted vapour-absent melting experiments at 8, 16, 22 and 32 kbar on four natural olivine-normative amphibolite rock powders, three of them low-potassium

olivine tholeiites (K_2O 0.08–0.21%), and the fourth an alkali-rich basalt (K_2O 0.82%). Amphibolitic residue at 8 kbar changed to garnet–amphibolite at 16 kbar and further to eclogite at 22–32 kbar. The authors described a general trend as partial melting proceeded, in which initially granitic melts at very low degrees of melting were rapidly diluted in K_2O to levels typical of trondhjemite. The melt compositions produced by 10–40% melting were thus tonalitic-trondhjemitic at all pressures. High-Al_2O_3 partial melts were produced at pressures above 16 kbar at 10–40% melting and low-Al_2O_3 partial melts at pressures of 16 kbar or less at low degree of melting. Indicating the importance of the protolith composition, CaO and K_2O contents of the partial melts varied, with the least calcic melts produced from the most calcium-poor starting material and potassium-rich trondhjemite melts from the alkali-rich basalt.

According to Rushmer (1991), fluid-absent partial melting of mafic amphibolites occurs over a broad temperature range, between 850 and 1000°C, and the temperature of melting is a function of the mineral composition, which reflects the bulk composition, with high silica and/or alkali contents promoting melting at lower temperatures. The melts vary from granitic in composition at lower temperatures to tonalitic at higher temperatures, and the amount of hydrate present in the rock affects the water content of the melt and consequently determines the volume-% of melt produced.

Experimental data on more evolved and intermediate compositions are sparse. Beard et al. (1993) report experiments on the melting of crustal xenoliths at 6.9 kbar and 900–1000°C. A dioritic granulite (SiO_2 57.5%) that was included began to melt, with the consumption of all modal K-feldspar, at 900 °C. Strongly metaluminous melts were produced, with a granitic composition at 900°C and more granodioritic composition at 1000°C (26% melt). Two granodioritic more felsic gneisses (SiO_2 67.9% and 71.5%) underwent extensive (30–50%)

melting between 950°C and 1000°C, producing metaluminous to mildly peraluminous very high-K (K_2O 5–6%) granitic melts (SiO_2 72–74%). Refractory pelitic granulite did not yield significant melt even at 1000°C. A notable feature was the relative stability of K-feldspar during partial melting of granodioritic gneisses, producing melts depleted in Ba as seen in high K/Ba and low Ba/Rb ratios.

The results obtained by Beard et al. (1994) for a diorite and intermediate to felsic granulites (SiO_2 62–66% and about 73% respectively) at 6.9 kbar and 850–950°C were similar to the results just described. A graphite-bearing silicic granulite (SiO_2 71.5%) did not melt, however. Melt compositions ranged from metaluminous, silicic granodiorite for the dioritic starting material to peraluminous or weakly metaluminous granites for all other materials. Although liquids became more feldspathic, less silicic, and enriched in FeO, MgO, and TiO_2 with increasing temperature, the melts derived from every starting material contained over 71% SiO_2.

According to Beard et al. (1994), the concentration of mafic components, including Fe/Mg, is largely controlled by the composition of the starting material. The elements (Ca, Na, K) enriched in feldspars show complex behaviour during partial melting. Diorite with low K_2O (0.65%) had low-K feldspar as stable phase in the residue and showed decrease in K and increase in Ca and Na/K with increased degree of source melting. Where both low- and high-K feldspars were stable phases in the residue, K and Na/K remained nearly constant and melt Ca increased with increased degree of melting. Where only high-K feldspar was stable, melt K increased and melt Ca and Na/K decreased with increased melting. These melts also had low Ba until the amount of K-feldspar in the residue diminished.

Melting experiments on peraluminous quartzo-feldspathic gneiss at lower pressures (3 and 5 kbar, 700–800°C) (Holtz & Johannes 1991) showed the occurrence of K-feldspar, plagioclase, quartz, biotite and cordierite in

the source residue at lower amounts of H_2O. K-feldspar was absent in the source residue at higher amounts of added H_2O, which produced higher degree of melting. The melt K content was highest under conditions of higher temperature and low H_2O.

In fluid-absent melting experiments carried out on a biotite- and hornblende-bearing F-rich tonalitic gneiss (SiO_2 68% and K_2O 2.1%) at 6, 10 and 14 kbar, Skjerlie & Johnston (1993) were unable to produce alkali feldspar in biotite-dehydration melting, but they suggested that combined oxidation and dehydration melting at elevated f_{O2} would have stabilized K-feldspar even under these conditions. At 6 and 10 kbar, temperatures up to 975–1000°C were needed to produce widespread biotite dehydration melting with production of 20–25% fluorine-rich granitic melt. Skjerlie & Johnston (1993) proposed that the starting material had undergone dehydroxylation, producing relatively high F-content in biotite and in that way increasing its thermal stability. The process described is considered an appropriate model for the origin of A-type granites. Garnet was found in experiments at 10 kbar, verifying that it occurs at lower pressures in the residue of more silicic protoliths than in the residue of mafic rocks (about 16 kbar).

Both water-rich, volatile-phase-present melting and volatile-phase-absent dehydration melting of sedimentary rocks may occur in the middle and lower crust, with production of anatectic 'S-type' granites. Large amounts of H_2O enable granitic melts to form at low temperatures (600–700°C, Thompson & Algor 1977), but probably only at high crustal levels because water is highly soluble in granitic melts at deeper crustal pressures (Burnham 1967, 1979). The H_2O-saturated melt has a negative dP/dT slope, which prevents the ascent of such melts without freezing (Patiño-Douce & Johnston 1991). Water-rich volatile-phase-present melting is thus probably confined to some in situ migmatites and high level granitoids, especially those characterized by abundant occurrence of res-

tites. Large amounts of H_2O during melting produce partial silicic melts rich in An and Ab and poor in Or (trondhjemitic-tonalitic) not only from metaluminous compositions but also from peraluminous greywackes (Conrad et al. 1988). Modelling of the behaviour of Rb, Sr and Ba in the incongruent melting of muscovite in the presence of vapour phase shows a depletion of feldspar in the restite and an increase in the Sr abundance relative to vapour-absent conditions (Harris & Inger 1992).

The very low porosity of metamorphic rocks at deep to mid-crustal pressures is considered to prevent large amounts of H_2O from being present during partial melting (Vielzeuf & Holloway 1988, Clemens 1990, Patiño Douce & Johnston 1991), and thus anatexis is generally considered to take place under vapour-phase-absent conditions where the hydrous phases in the rock break down during dehydration-melting reactions. Vielzeuf & Holloway's (1988) experimental melting of metapelite at 7–12 kbar under vapour-absent conditions produced a small amount of water-rich melt (<10%) due to muscovite dehydration melting at 750–850°C, and then a large amount of peraluminous granitic melt due to biotite dehydration melting in the narrow temperature range 850–875°C. In studies on the melting of more refractory pelite with low CaO (0.4%) and Na_2O (0.5%) at similar pressures, Patiño-Douce & Johnston (1991) produced smaller amounts (15–30%) of strongly peraluminous granitic melts in the temperature range 825–875°C. In both sets of experiments the liquids obtained at these temperatures were silicic and granitic, and the combined $MgO+FeO+TiO_2$ was less than 3%.

Greywackes are more fertile rocks than metapelitic rocks rich in mica and aluminosilicate and poor in plagioclase and probably are better candidates for large volumes of granitoid magmas (e.g. Miller 1985, Patiño-Douce & Johnston 1991). Ca-poor Al-metagreywackes are fertile rocks below 7 kbar, producing 30–60% melt in the temperature range

800–900°C at 10 kbar. Extensive melting takes place at significantly lower temperature in pelites (850°C C±20) than in Al-metagreywackes (950°C±30) (Vielzeuf & Montel 1994). Skjerlie et al. (1993) studied the fluid-absent melting of a layered (tonalite-pelite) crustal protolith at 10 kbar at 900, 925 and 950°C where the presence of the infertile tonalite increased the melt fraction of the more fertile pelite from 40–50% to 70–76% by changing its Na/K ratio. At the same time the melt productivity of the tonalite increased from 4–7% to 52–55%, both because of change in the relative proportions of the alkalies and because the terminal biotite reaction was displaced to lower temperature by an increase in the activity of Al_2O_3 in the melt. An interesting feature of these layered experiments was the lack of orthopyroxene and the predominant occurrence of garnet along with granitic melt compared with the more or less similar abundances of both orthopyroxene and garnet in tonalite-alone experiments.

In both vapour-phase-present and vapour-phase-absent melting experiments on amphibolites, intermediate diorites and tonalitic-to-granodioritic rocks, the first melts had higher mol. A/CNK than the starting material due to the more felsic nature of the melts, and they were often slightly peraluminous even though derived from a metaluminous source (see references in preceding paragraphs). Some scatter occurred, possibly due to the difficulty of determining Na_2O in glass. The FeO/MgO ratios were often higher in the melts than in the starting material, thus placing the melts in the tholeiitic field in the FeO/MgO–SiO_2 diagram. In the experiments of Beard et al. (1994), the highly tholeiitic (FeO/MgO 5–14) nature of the starting materials was largely retained in the partial melts. The abundant occurrence of magnetite in residues in the dioritic gneiss experiment even produced slightly lower FeO/MgO in the partial melts. The partial melts from pelitic starting material always had lower mol. A/CNK values than the

starting material, and there was normally an increase in these values to higher temperatures and to higher amounts of derived melts (see data in Patiño Douce & Johnston 1991, Vielzeuf & Holloway 1988). Ca-rich greywackes showed a different behaviour with decreasing mol. A/CNK due to temperature increase (see data in Conrad et al. 1988); evidently the presence and amount of plagioclase are critical. The FeO/MgO ratios varied in the pelitic experiments, but in general they were more or less similar to the ratios in the starting material (see data in Patiño Douce & Johnston 1991, Vielzeuf & Holloway 1988).

Accessory minerals (e.g. zircon, monazite, apatite) are enriched in Th, U and REE in variable proportions and their response during anatexis can play an important role in determining the geochemical and isotopic characteristics of crustal-derived granites (Rapp & Watson 1986, Hogan & Sinha 1991). Disequilibrium melting at high melt-segregation rates, preventing chemical equilibrium between melt and residual solid, can produce leucosomes depleted in trace elements (Sawyer 1991). Because of the low zircon solubilities (about 100 ppm) in peraluminous granite melts at low temperatures (750°C), residual zircons occur in the restite under these conditions (Watson & Harrison 1983). Small monazite grains will probably dissolve under reasonable conditions during crustal anatexis, and larger grains will probably be residual (Rapp & Watson 1986), but both zircon and monazite can act as residual phases if they occur as inclusions in restitic minerals (e.g. Watson & Harrison 1983). Watt & Harley (1993) have concluded that the dry, peraluminous nature of vapour-undersaturated melts derived from partial melting of pelite inhibits monazite and zircon solubility and results in concentration of these phases in the residue. Evidently there are many factors controlling the behaviour of accessory phases during crustal anatexis, with water-activity and melting temperature being the most important.

The critical steps in the genesis of isolated and large granitoid plutons are the segregation, ascent and emplacement of granitoid magmas. Increase in the amount of melt above the critical melt fraction (about 30–50 vol% melt) is an important factor because, under static conditions, partially melted rocks change from granular framework (crystal dominated, high viscosity) to dense suspension (melt dominated, lower viscosity) (Arzi 1978, Wickham 1987, van der Molen & Paterson 1979). This would suggest that large amounts of melt above critical melt fraction, and in many cases high temperatures (see above), are required for the formation of plutonic granites. On the other hand, our growing knowledge of granitoids originating from low degree melting suggests that physical segregation may be of great importance in genesis of granite plutons (see Brown 1994 and references therein). Brown (1994) emphasizes the importance of the deformation-enhanced melt segregation mechanism, and the ascent and emplacement of crustal-derived magmas often related to major fault systems, which may be either strike-slip in transpressional belts or extensional in strongly overthickened orogens undergoing collapse. Stoping and ballooning effects are not uncommon near the granite contacts, but often they are the effects of final granite emplacement and not conclusive evidence for the ascent mechanism.

Classification of the plutonic rocks
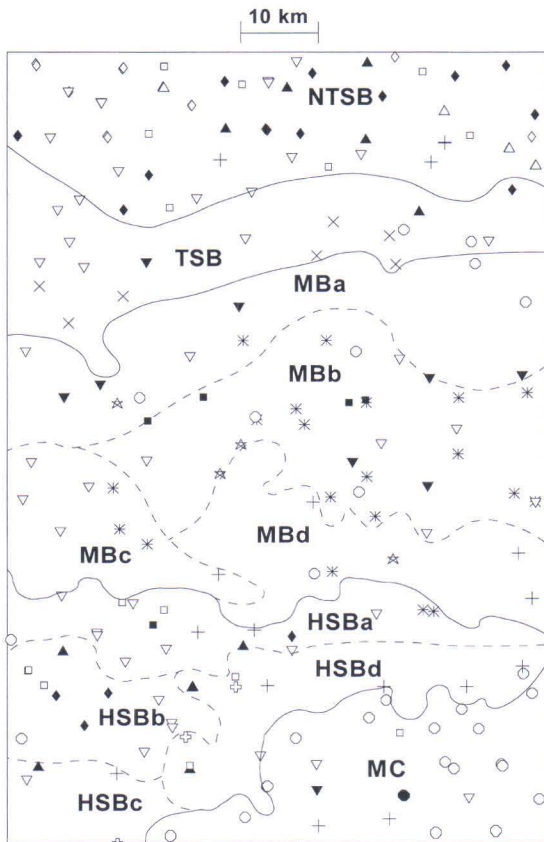
The mafic plutonics (gabbros and diorites) are considered here on an areal basis, but within areas a division is made into arc related, WPB-affinity and DM-affinity mafic rocks. Only non-cumulus and least altered samples are included in Figs. 26–28, and some representative analyses are given in Table 4. The sample locations with division into different geochemical groups are shown in Fig. 25.

The granitoids, in turn, are classified into groups and subgroups on the basis of geochemical characteristics, areal distributions and lithological characteristics. The means

Fig. 25. Sample locations of the plutonic rocks. See Figure 2 for complete lithology. Filled upright triangles – arc-related mafic rocks, open squares – WPB-affinity mafic plutonics, filled squares – WPB-affinity mafic plutonics with indication of sediment assimilation, stars – DM-affinity mafic plutonics, open crosses – mafic plutonics comparable to VG3, open upright triangles – GG1, open inverted triangles – GG2, filled inverted triangles – GG3 main group, diagonal crosses – GG3 Nokia-type, crosses – GG4, filled circles – GG4 subgroup medium-K granites of tholeiitic affinity, open diamonds – GG5, filled diamonds – GG6, open circles – GG7, asterisks – GG8.

of some subgroups are given in Table 5. Granitoid group 1 (GG1) comprises the high-K calc-alkaline granitoids from the NTSB possibly originating in conjunction with arc volcanism. The normal high-K calc-alkaline granitoids are classified as GG2 rocks, and assimilated variants as GG3 rocks, subdivided into a larger main high-K calc-alkaline group and a Nokia-type group with rocks from the Nokia and Siitama plutons (Fig. 2). The GG4

rocks are medium-K calc-alkaline granitoids, and the GG5 group comprises high-K granitoids often showing tholeiitic affinity. GG6 consists of very high-K alkaline granites of tholeiitic affinity, and GG7, with areal subgroups, consists of S-type granites. Granitoids, mainly from the MB, showing elevated TiO_2 and Zr with tholeiitic affinity are classified separately as GG8 rocks.
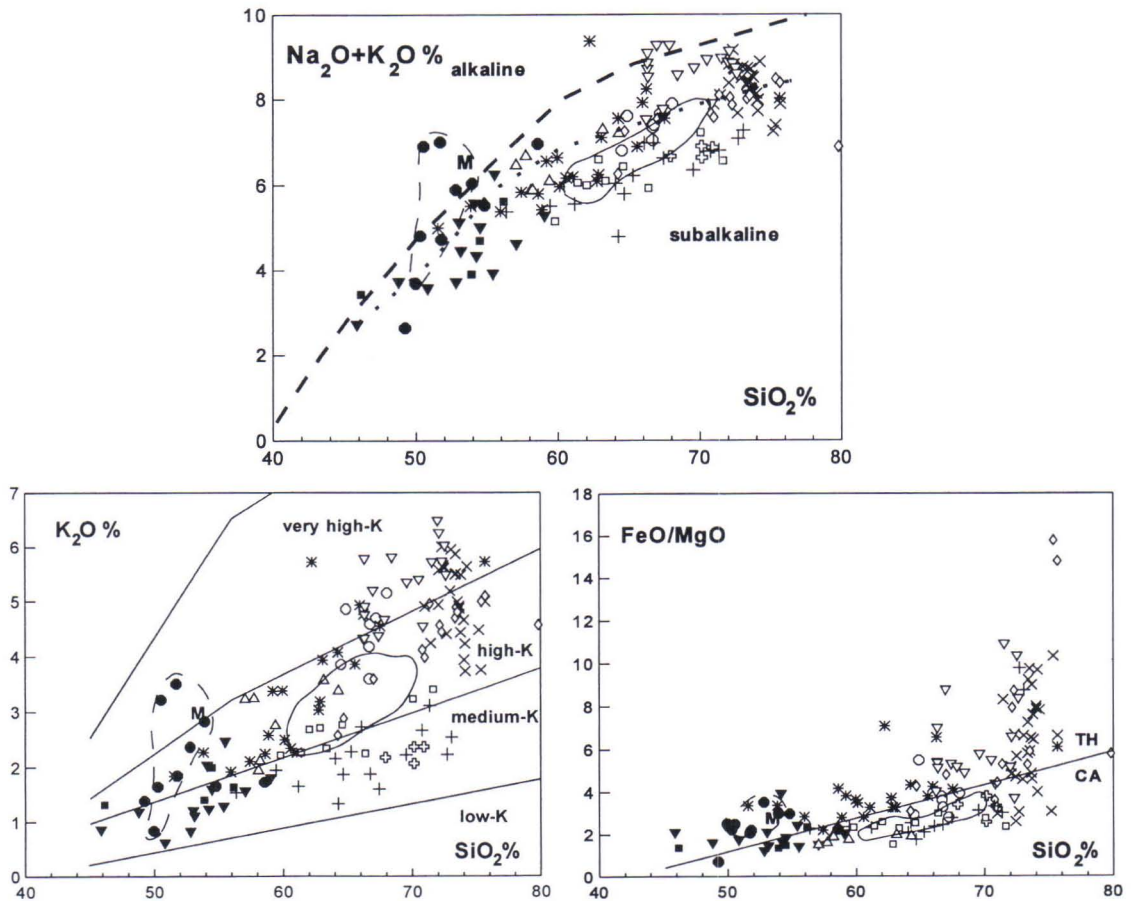

Fig. 26. Harker-type Na_2O+K_2O, K_2O and FeO/MgO variation diagrams for plutonic rocks in the Tampere–Hämeenlinna area. Data from this study. Samples with large amount of cumulus minerals are excluded. Oxide totals were recalculated to 100%. Dashed heavy line – boundary line by Irvine and Baragar (1971) and dotted heavy line – boundary line by Kuno (1966) for Na_2O+K_2O–SiO_2 diagram. Boundary lines for K_2O–SiO_2 diagram are from Kähkönen (1989). The division between tholeiitic and calc-alkaline fields on the FeO/MgO–SiO_2 diagram is from Miyashiro (1974). Filled circles – NTSB+TSB mafic plutonics, filled squares – MB mafic plutonics, filled inverted triangles – MB+MC mafic plutonics, open upright triangles – GG1, open squares – GG3 main group, open circles – GG3 Nokia-type, crosses – GG4 excluding TSB, open crosses – GG4 samples from the TSB, open diamonds – GG5, open upside triangles – GG6, diagonal crosses – GG7, asterisks – GG8. Dashed space encloses high-Ti mafic plutonics from the NTSB and solid space encloses main part of GG2.

Description of mafic plutonic rocks

NTSB+TSB

Ten diorites and gabbros were sampled in the NTSB, most of them occurring in proximity to granitoids. In addition, one mafic quartz diorite and one quartz monzodiorite with high TiO_2 were sampled. Seven of the samples form a coherent group in the TiO_2–SiO_2 diagram (Fig. 27, Table 4) and are designated as

the high-Ti group. These are tholeiitic, partly alkaline rocks with variable K_2O and characterized by high P_2O_5, Rb, Sr, Zr and La values relative to other samples with similar SiO_2 values (Fig. 28, Table 4). The low Ni, Cr and MgO values indicate differentiation (Table 4 and Fig. 27). The spidergram pattern of the most primitive gabbro (8910900; SiO_2 50.0%) is compatible with WPB affinity (Fig. 29), but

Table 4. Arithmetic mean of NTSB high-Ti mafic plutonics (6 samples) and the chemical composition of selected mafic plutonics from different areas.

Subarea Sample/S89[1]	NTSB high-Ti	TSB 10844	MBb 10848	MBd 11010	HSBa 11044	HSBb 11087	HSBc 11125	HSBd 11138	MC 11122
SiO_2	50.34	57.90	52.48	50.07	53.67	48.00	50.11	52.16	52.51
TiO_2	1.76	0.74	1.32	0.60	1.35	1.43	0.82	1.44	1.96
Al_2O_3	18.00	18.40	18.16	8.83	17.75	18.51	20.49	17.32	16.63
FeO	10.42	6.95	8.35	11.03	8.28	11.00	8.68	9.55	9.57
MnO	0.15	0.15	0.13	0.19	0.14	0.18	0.16	0.15	0.12
MgO	4.26	3.11	5.68	14.22	4.65	7.03	5.12	4.66	3.56
CaO	7.29	4.49	6.68	9.13	7.26	8.37	9.59	7.67	5.80
Na_2O	3.22	5.18	2.70	0.95	3.36	2.50	2.92	3.85	3.52
K_2O	2.20	1.71	2.00	0.59	1.56	1.15	0.59	1.17	2.91
P_2O_5	0.72	0.25	0.51	0.07	0.48	0.21	0.12	0.41	1.72
CO_2	0.09	0.10	0.03	0.13	0.06	0.02	0.10	0.15	0.10
F	0.17	0.09	0.12	0.02	0.12	0.01	0.02	0.11	0.37
S	0.06	0.01	0.05	0.57	0.08	0.10	0.01	0.08	0.14
Ba	1102	1060	448	113	336	168	175	294	1490
Cl	354	115	308	152	406	90	40	317	415
Cr	53	38	217	946	55	114	45	35	38
Nb	18.1	13.2	22.0	3.0	18.6	4.0	3.2	13.6	34.7
Ni	36	17	44	260	40	29	40	26	32
Rb	60	42	76	22	44	63	26	25	64
Sr	1102	484	429	103	565	348	370	638	1640
V	250	196	213	389	248	209	250	238	219
Y	25	18	23	14	24	23	15	24	22
Zn	139	120	134	109	124	123	88	143	170
Zr	206	114	273	51	141	129	52	167	363
Co	26	17	23	67	27	38	31	25	19
La	40.7	19.3	36.4	6.5	-	10.6	6.1	24.5	97.7
Sc	28.1	26.5	23.9	54.4	24.6	35.6	36.4	27.2	16.9
Th	2.9	2.5	5.4	1.9	4.2	1.8	1.6	2.1	5.9
U	1.1	0.9	1.6	0.6	1.9	0.6	0.4	0.9	2.1

Major elements (wt%), S (wt%) and Ba–Zr (ppm) analysed by XRF and F by ion selective electrode at the GSF laboratory; Co–U by neutron activation at the Technical Research Centre of Finland; CO_2 by wet method at XRAL in Canada.
[1] Sample numbers are referred to in the text.

the slightly negative Nb and Zr anomalies could indicate the occurrence of a subduction component or, more likely, fractionation-induced depletion.

Diorites 8910879 (SiO_2 50.5%) and 8910882T (SiO_2 51.7%) are very high-K tholeiitic alkaline rocks (Fig. 26) characterized by high enrichment of many elements (Figs. 27–29) including Cl (~500 ppm) and F (0.21–0.38%). Other characteristic features are strong positive Ba anomaly and negative Nb anomaly. One explanation for this composi-

tion could be interaction of mafic magmas with felsic magmas, as suggested by the small amount of quartz and K-feldspar; however, the low SiO_2, high Sr and high Zr and La relative to the rather low Nb do not support this idea (see p. 65). A small amount of mechanically mixed crystals is possible. The enrichment of P, Zr, Sr and La in sample 8910882T, which also exhibits extensive crystal fractionation (Ni <30 ppm and Cr <40 ppm), suggests an alkaline affinity, although the negative Nb anomaly argues against this.
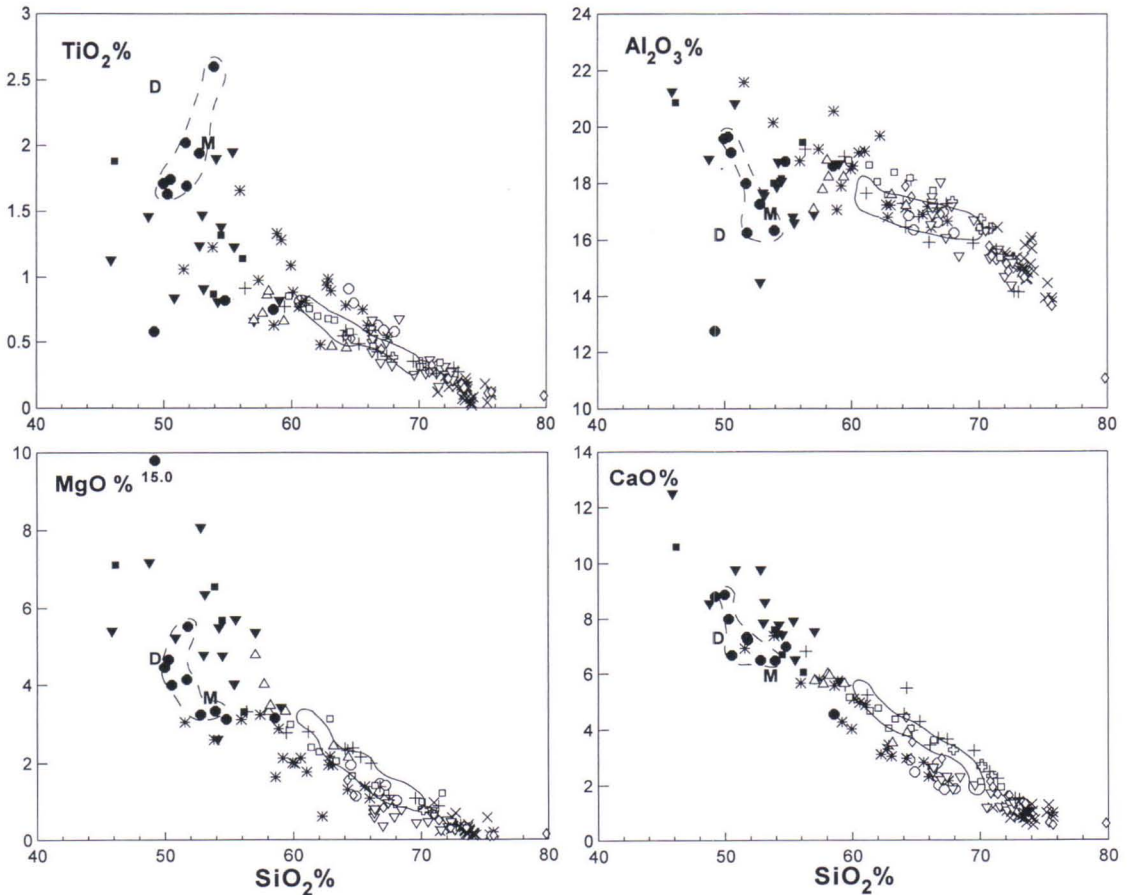

Fig. 27. Harker-type selected major element (%) variation diagrams for plutonic rocks in the Tampere–Hämeenlinna area. Data from this study. Oxide totals were recalculated to 100%. See Figure 26 for symbols and explanations. D – hypabyssal VG4 dyke 8911025 (Table 3), M – quartz monzodiorite 8911122 (Table 4) from the MC.

Samples 8910879 and 8910882T, and also sample 8910882 (see Fig. 29), contain abundant sphene, and the first sample also has abundant magnetite (Lahtinen & Korhonen 1996). Sample 8910879, with deepest negative Nb anomaly, has very coarse sphene grains (>1 mm), perhaps indicating that sphene has been a crystallizing phase in small amount, so lowering Nb in the magma. On this basis, an evolved alkaline WPB origin combined with a small amount of fractional crystallization of magnetite and sphene is proposed. The occurrence of a subduction component is unclear, but Ba, K and Rb abundanc-

es may have been increased through exchange with felsic magmas. All high-Ti samples in the NTSB have indications of WPB affinity.

Hornblende gabbro 8910892 (SiO_2 49.2%) is characterized by high MgO (15.0%), Cr (1600 ppm), Ni (342 ppm) and Co (54 ppm), and a possible enrichment of K and Rb is seen in Fig. 29. There is a clear negative Nb-anomaly, and no evidence for precipitation of Ti-bearing phase (low Ti and no magnetite), indicating a primary origin for this anomaly. The occurrence of a subduction component is suggested and a greater degree of mantle melting than for the high-Ti rocks. The fine-
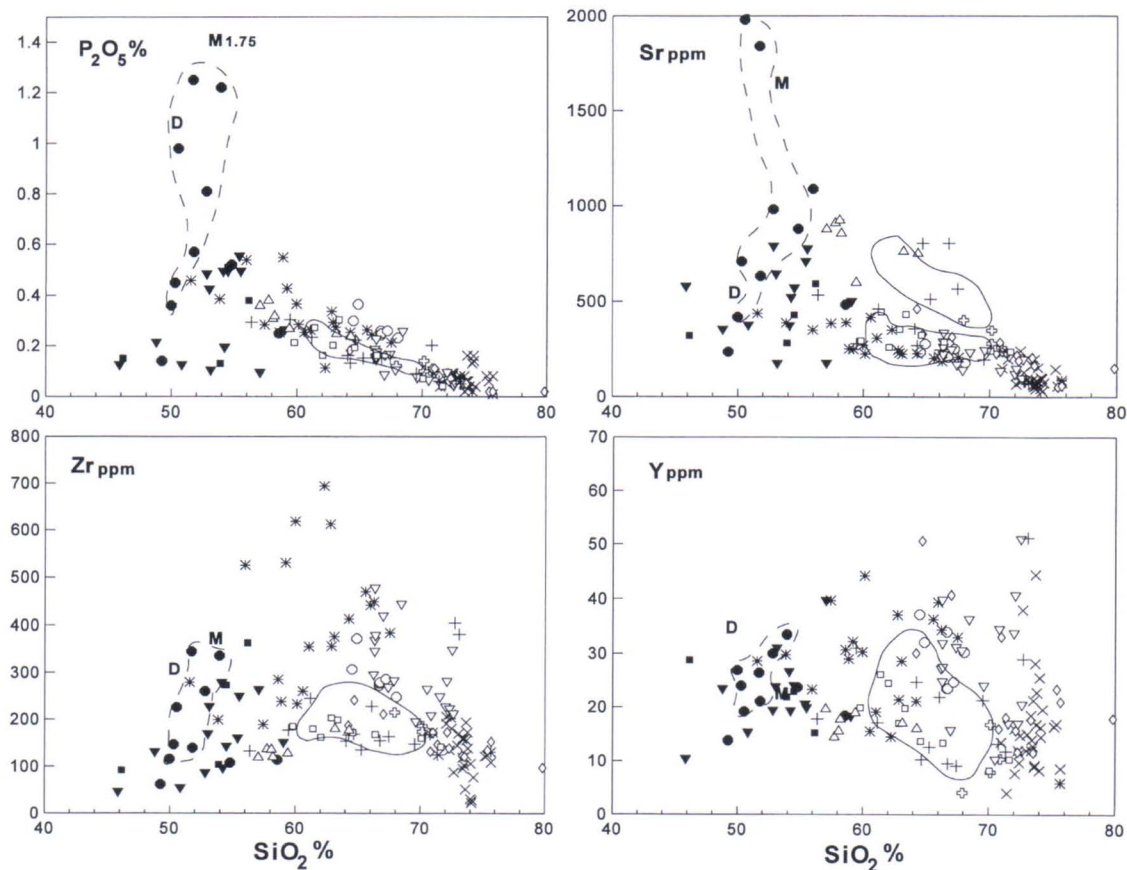

Fig. 28. Harker-type selected major element (%) and trace element (ppm) variation diagrams for plutonic rocks in the Tampere–Hämeenlinna area. Data from this study. Oxide totals were recalculated to 100%. See Figure 26 for symbols and explanations.

grained hornblende gabbro 8910805 (SiO_2 54.8%) and gabbro 8910844 (Table 3) are characterized by lower TiO_2 and Zr than the high-Ti samples (Figs. 27–28). The humped patterns with negative Nb, Zr and Ti anomalies are similar to the patterns for the VG6 basaltic andesites and andesites (compare Figs. 22 and 29), and an arc-type origin is proposed for these samples.

Hornblende gabbro 8910893 contains plagioclase cumulus, which is seen in the high CaO (13.7%), Sr (1000 ppm) and Al_2O_3 (26.9%) and low FeO, MnO, V, Y and Sc (data not shown). This sample is also altered as evident in the higher K and Rb (Fig. 29). It occurs in the HiSB and is comparable in composition to sample 8910892 (Fig. 29), and an arc-related origin is proposed. A similar arc-related origin is proposed for the hornblende gabbro 8910909 which contains abundant pyroxene. The high Sc (103 ppm) is indicative of clinopyroxene cumulus. The low Ni (31 ppm) and high Cr (670 ppm) are noteworthy.

MB

The mafic plutonics in the MB are divided into DM- and EM-dominated groups (WPB). Gabbro 8910952 (SiO_2 46.2%) is an evolved (Cr 21 ppm and Ni 23 ppm) high-K tholeiitic rock with high TiO_2 and Y (Figs. 26–28), whose granitized nature is seen in the enrichment of K, Rb and possibly Ba (Fig. 30). The geochemical characteristics are most compatible with a DM-dominated source. Owing to its strongly assimilated nature, gabbro 8911010 (Table 4) from the MBd is not included in Figs. 26–28. The nearby volcanic sample 8911011, with a near komatiite composition, has assimilated primitive MORB affinity (p. 50). Gabbro 8911010 also has high MgO, Cr and Ni (Table 4) and it contains sulphide patches seen as high S. The spidergram pattern (Fig. 30) from P to Cr is similar to that of sample 8911011 but on higher level (Fig. 19). There are clear differences, however,

er, in the higher K, Rb, Ba and La of the gabbro sample. A primitive DM affinity comparable to that for volcanic sample 8911011 is proposed, but with more sediment assimilation in the gabbro. This interpretation is favoured by the relatively high SiO_2 and negative Ba anomaly. Gabbro 8910849 contain plagioclase cumulus and idiomorphic garnets. It is a medium-K tholeiitic rock with the cumulus nature seen in the high Al_2O_3 and low MgO, V, Cr and Ni (Table 4). A particularly interesting feature is the low S, together with low Ni and very low Cu (8 ppm), possibly indicating an earlier precipitation of a sulphide phase. The spidergram pattern in Fig. 30 is scattered and difficult to interpret as there is also a positive P-anomaly,
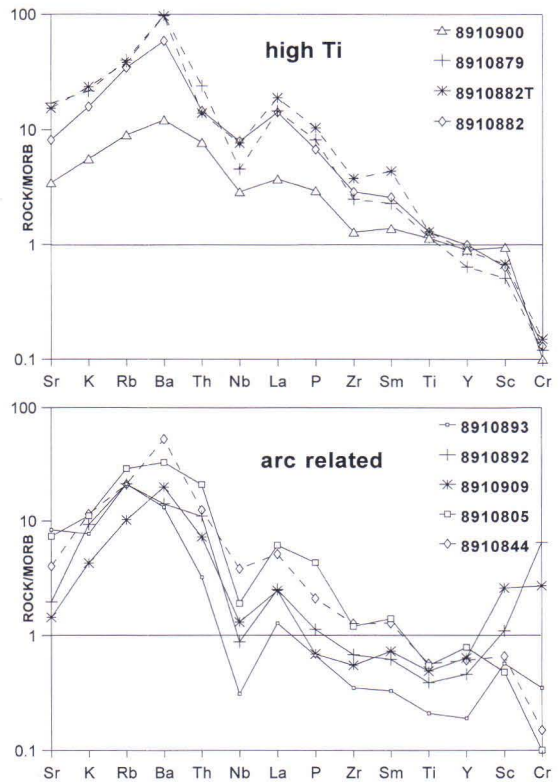

Fig. 29. Trace element patterns for selected mafic plutonics from the NTSB and TSB normalized to mid-ocean ridge basalt. Normalizing values from Pearce (1982), except La (3.8 ppm) which has been interpolated from his Ce value. Sample numbers are referred to in the text.

but a DM affinity is proposed with a small assimilated schist component (increasing SiO_2, for example).

The WPB-affinity rocks include two samples from the approximately northeast-directed lineament dividing the subareas MBa and MBb. Diorite 8910848 (SiO_2 54.5%) is a high-K calc-alkaline rock characterized by high Zr (Figs. 26–28). Norite 8910958 is characterized by plagioclase and orthopyroxene cumulus. Diorites 8910825 (SiO_2 53.9%) and 8910826T (SiO_2 56.2%) come from a large granodiorite complex and are medium-K rocks at the tholeiitic-calc-alkaline boundary (Figs. 26–28). The negative Ba and Nb anom-

alies and slightly negative P anomalies in these two samples (Fig. 30) could indicate schist assimilation or interaction with granitoid melt.

HSB+MC

The mafic plutonics in the HSB are mostly medium-K subalkaline rocks with both tholeiitic and calc-alkaline affinities (Fig. 26). The TiO_2 abundances vary from low (<1%) to about 2%. There are four samples from the HSBa. Diorite 8911044 (SiO_2 54.5%) and gabbro 8911049 (at SiO_2 55.4%) are both brecciated by granodiorite, as seen in the variable K, Rb and especially Ba and Th values (Fig. 31). A similar WPB-affinity origin is proposed for these rocks. The cumulus nature of peridotite 8911048, which is from the same massif as sample 8911049, is seen in low Al_2O_3 (6.3%) and high MgO (15.75), V (647 ppm), Cr (647), Co (76) and Sc (70). The Rb–Ba–Th relation (Fig. 31) and the occurrence of graphite (0.07%) show the effects of sediment assimilation, which at least in part is considered responsible for the negative Nb anomaly. The pattern has been affected by both pyroxene cumulus and assimilation, and the original pattern probably was steeper and more similar to that of sample 8911049. Hornblende gabbro 8911064 (SiO_2 52.8%) of medium-K calc-alkaline affinity differs from the other HSBa samples in having higher Sr (Fig. 28), Ni (159 ppm) and lower Zr (Fig. 28). These features and the spidergram pattern compatible with evolved island arc calc-alkaline basalts (e.g. Pearce 1982) favour an arc-related origin.

Hornblende gabbro 8911087 (SiO_2 48.8%) from the HSBb is a medium-K tholeiitic rock with rather high TiO_2 and Zr (Figs. 27–28 and Table 4). The high Rb (Fig. 31) indicates alteration effects and the Ba–Th relation could indicate interaction with felsic magma. The spidergram pattern is in agreement with WPB affinity. The fine- to medium-grained diorite 8911084 (SiO_2 59.0%) may also be a subvolcanic rock. It is a medium-K calc-alkaline an-
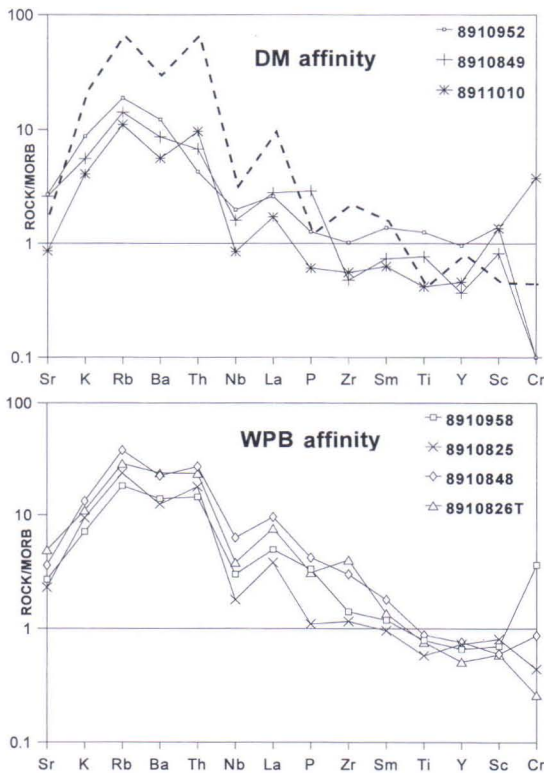

Fig. 30. Trace element patterns for selected mafic plutonics from the MB normalized to mid-ocean ridge basalt. Normalizing values from Pearce (1982), except La (3.8 ppm) which has been interpolated from his Ce value. Sample numbers are referred to in the text. Thick dashed line is the average chemical composition of basement-related sedimentary rocks (SG3–SG7).

desite in composition (Fig. 26) and, considering the evolved nature and Ti and Y relation and negative Nb anomaly, the spidergram pattern in Fig. 31 is compatible with a mature calc-alkaline ACM origin. The Rb and Th peaks may indicate of assimilation or interaction with felsic melts. Diorites 8911083 and 8911083T are cumulus rocks occurring 150 m apart. The first contains plagioclase and hornblende cumulus with an almost adcumulus texture, which lowers the level of most elements in Fig. 32. Diorite 8911083T is characterized by high P_2O_5, Sm and La (Fig. 31), possibly related to the occurrence of apatite as cumulus phase. A general WPB affinity is favoured for these two diorites.

Strongly foliated diorite 8911125 (SiO_2 50.8%) from the HSBc is a medium-K (near to the low-K boundary) tholeiitic basalt (Fig. 26, Table 4). The spidergram pattern (Fig. 31) suggests a subduction-related origin with DM-dominated mantle. Diorite 8911097 (SiO_2 54.2%) is a medium-K calc-alkaline rock (Fig. 26) with geochemical characteristics similar to diorite 8911084 (Fig. 31), and a similar arc-related origin is proposed.

There are seven samples from the HSBd, all from the large diorite/gabbro massif. Two samples (8911145 and 8911147) appear to be similar in origin to the VG3 main group, while
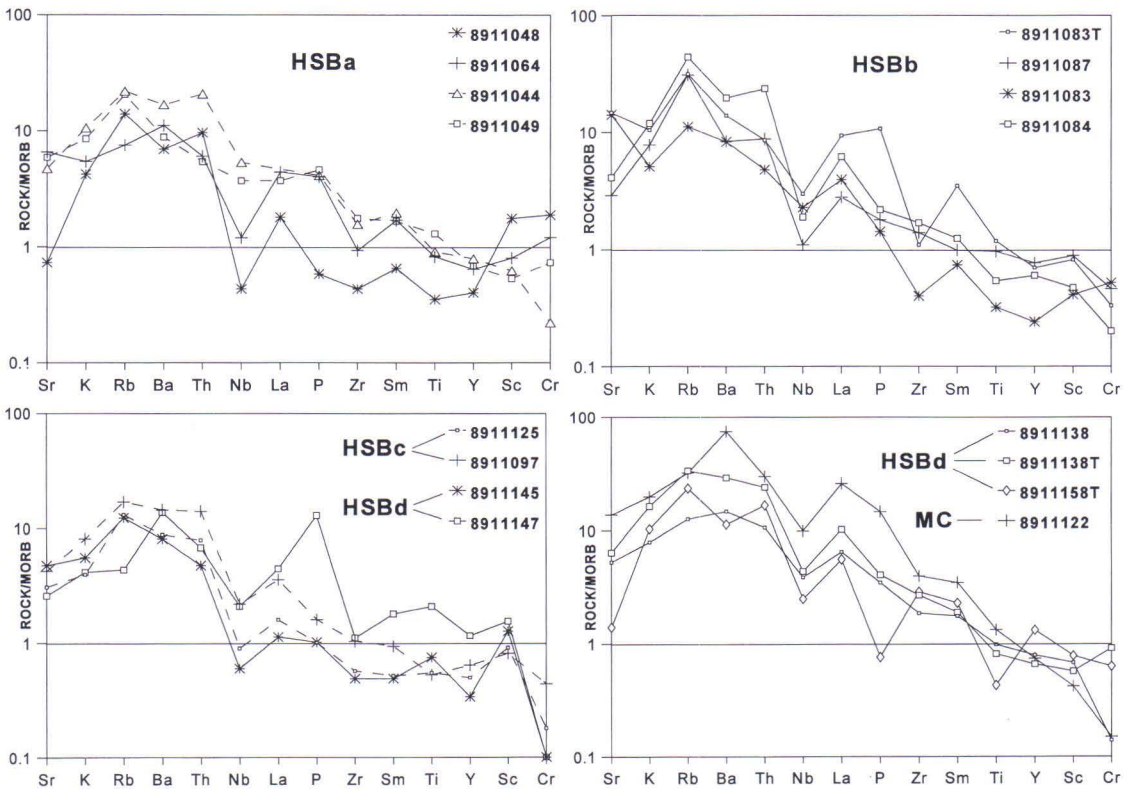

Fig. 31. Trace element patterns for selected mafic plutonics from the HSB and MC normalized to mid-ocean ridge basalt. Normalizing values from Pearce (1982), except La (3.8 ppm) which has been interpolated from his Ce value. Sample numbers are referred to in the text

the other five have a more EM-dominated source. Hornblende gabbro 8911145 (SiO_2 45.9%) is a medium-K tholeiitic rock (Fig. 26) with low Cr (11 ppm) and Ni (28 ppm) showing an evolved nature. Hornblende gabbro 8911147 contains plagioclase cumulus and idiomorphic apatite crystals. The cumulate nature of the apatite, and probably also of titanomagnetite, is seen as positive peaks of P and Ti in Fig. 31. Although the evolved (Cr 12 ppm, Ni 10 ppm) and cumulus nature of this gabbro hampers the interpretation, a similar origin to the VG3 main group is proposed. The WPB-affinity samples (Fig. 31) show a disturbed chemical composition due to frequent interaction with felsic melts and crustal contamination. All show negative Nb anomalies, suggesting the occurrence of a subduc-

tion component, but the presence at the same time of deep negative Ba, P and Ti anomalies could indicate the crystallization of apatite and biotite near the contacts to felsic magmas since the stabilization of biotite would lower the Ba level relative to Rb and Th.

Quartz monzodiorite 8911122 (M in Figs. 26–28, Table 4) from the MC is very high-K alkaline rock with high TiO_2, P_2O_5, Sr, Ba, Zr. The spidergram pattern (Fig. 31) shows enriched WPB affinity with a negative Nb anomaly, but this is not considered diagnostic for the occurrence of a subduction component. The sample includes coarse sphene, apatite and zircon as well as abundant magnetite, suggesting that the lower Nb is probably due to crystallization of sphene and/or titanomagnetite earlier in the crystallization history.

Description of granitoid rocks

GG1

Samples in this group are from the NTSB and include two gneissic granodiorites, one orthogneiss and two quartz monzodiorites, occurring within or near the HiSB. In addition, two quartz diorites (8910883 and 8910883T, about 58% SiO_2 in Figs. 27–28) were classified as GG1 rocks even though in many respects they resemble high-Sr GG2 rocks. GG1 rocks are high-K calc-alkaline mainly meta-aluminous rocks (Figs. 26 and 32) and some samples show the Ba-enriched nature that characterizes VG6 rocks from the TSB and NTSB (Fig. 33). The average of GG1 shows a similar chemical composition to VG6 andesitic volcanics (Fig. 34). The generally more mafic nature of the GG1 rocks causes Cr, Ti and P peaks, but the higher Th and Rb are the major differences relative to the VG6 group.

GG2

The GG2 rocks are the most voluminous granitoid group, comprising 45 samples. Some of the mafic and hybrid samples are not included in Figs. 26–28. Outcrops hosting the samples are characterized by abundant occurrence of mafic enclaves. Both hornblende and biotite occur in more mafic granodiorites, and only biotite in felsic samples. GG2 samples are high-K calc-alkaline meta-aluminous to peraluminous 'I-type' rocks, with some of the granodiorites from the MB showing a more peraluminous character and thus approaching the GG3 main subgroup (Fig. 32). There is a general increase in the peraluminous character with increasing silica, which is a common feature for most granitoid groups of this study. The major element character of the GG2 rocks is similar, but Zr, Sr and Y values

vary and samples have been divided into two subgroups on the basis of their Sr abundances (Fig. 28).

Table 5 shows the mean composition of the high- and low-Sr GG2 samples from the TSB and NTSB. The low-Sr group is characterized by higher Zr, Y and Th and lower Nb and Ba, which is also seen in the Ba–K_2O diagram (Fig. 33). Comparison of the averages of high-Sr GG2 (SiO_2 62.4%) and low-Sr GG2 (SiO_2 63.5%) granitoids in the NTSB and TSB with the average of least altered VG6 volcanics (SiO_2 61.7%) at similar silica levels from the same areas reveals some distinct differences (Fig. 34). In addition to clearly lower Ba, both granitoid subgroups have higher TiO_2, K_2O and Rb (av. K/Rb 250–270 compared with av. in volcanics 375). The low-Sr subgroup also has higher FeO/MgO, Zr, Th and U. Furthermore, whereas the volcanics contain abundant magnetite, there is only a small amount of magnetite in the GG2 granitoids, and that is confined to hybrid samples (Lahtinen & Korhonen 1996). From the data produced in this study, it would seem, therefore, that the GG2 granitoids, especially the low-Sr subgroups, are not cogenetic with volcanics in the NTSB and TSB. The hybrid samples show an elevated Nb, Zr and Y pattern combined with locally low Th. A strongly negative Ba anomaly characterizes some hybrid granitoids. The increase in Nb and Zr in hybrid rocks and the common association between granodiorites and WPB-affinity diorites and gabbros reveals a close association between mafic (WPB) and more felsic magmas in the genesis of the GG2 rocks in the TSB and NTSB.

The GG2 rocks in the MB are divided into low-SiO_2 (60–62%) and high-SiO_2 (66–69%) subgroups. In addition, one high silica granite is considered separately. The low-SiO_2 subgroup is characterized by mafic enclaves, which are rare in the high-SiO_2 subgroup. The low-SiO_2 rocks in the MB are similar in character to the low-Sr granodiorites in the TSB and NTSB (Table 5 and Fig. 34), with most of

the differences attributable to the slightly more mafic nature of the low-SiO_2 samples. The Th level is also significantly lower in the low-SiO_2 samples. The deviation to higher A/CNK and lower Na_2O values (Fig. 32) is probably due to the small amount of sediment assimilation or interaction with sediment-derived melt. The high-SiO_2 subgroup is characterized by porphyritic granodiorites and it shows devia-
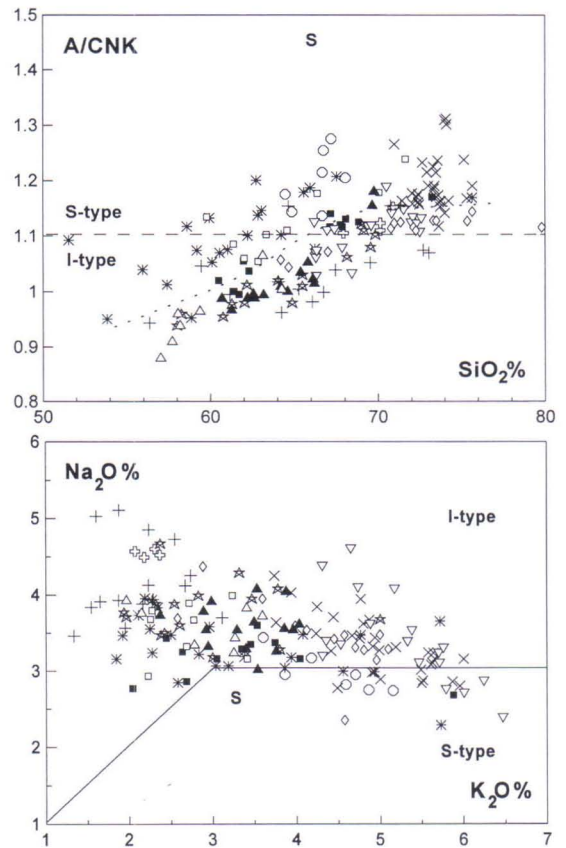

Fig. 32. A/CNK–SiO_2 and Na_2O–K_2O variation diagrams for granitoids in the Tampere–Hämeenlinna area. Data from this study. Oxide totals were recalculated to 100%. S- and I-type fields after Chappel and White (1984). Open upright triangles – GG1, filled upright triangles – GG2 granitoids from the NTSB and TSB, filled squares – GG2 granitoids from the MB, stars – GG2 granitoids from the HSB and MC, open squares – GG3 main group, open circles – GG3 Nokia-type, crosses – GG4 excluding TSB, open crosses – GG4 samples from the TSB, open diamonds – GG5, open inverted triangles – GG6, diagonal crosses – GG7, asterisks – GG8. S – average chemical composition of basement-related sedimentary rocks (SG3–SG7).
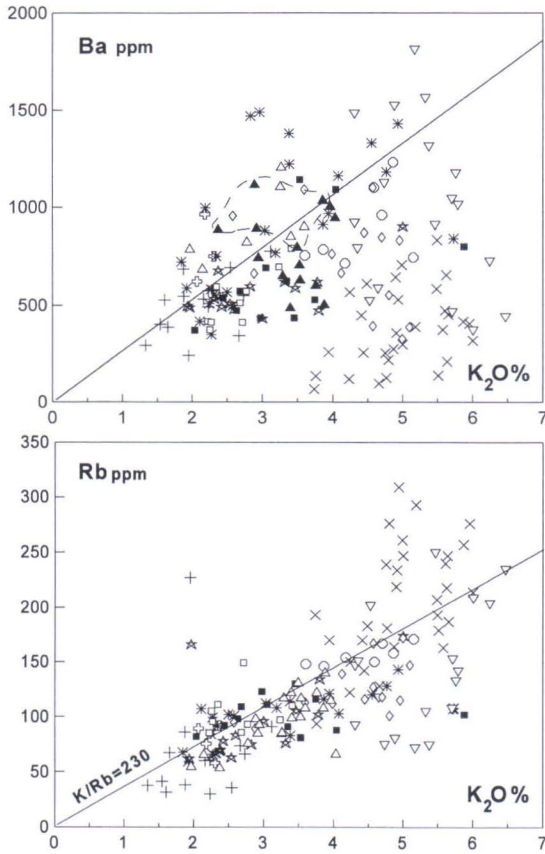
Fig. 33. Ba–K_2O and Rb–K_2O variation diagrams for granitoids in the Tampere–Hämeenlinna area. Data from this study. See Figure 32 for symbols. Solid line in the Ba–K_2O diagram is taken from Figure 23 and solid line in the Rb–K_2O diagram shows the crustal average (McLennan et al. 1990). Dashed line encloses high-Sr GG2.
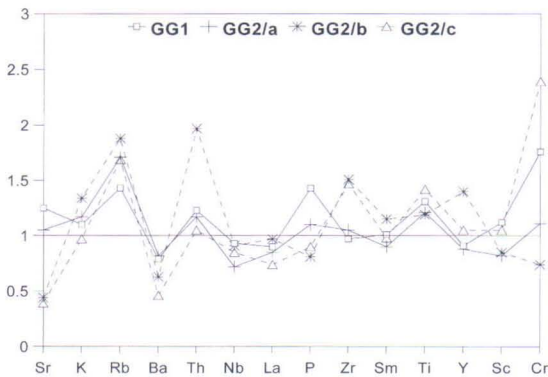

Fig. 34. Average major and trace element distributions in GG1 and selected GG2 subgroups. Results are normalized to average of intermediate (<66% SiO_2) VG6 volcanics. a-c refer to Table 5.

tions to higher A/CNK and lower Na_2O values similar to the low-SiO_2 subgroup (Fig. 32). Most of the differences between subgroup means are due to the more felsic nature of the high-SiO_2 subgroup.

Likewise, the HSB GG2 rocks consist of low-SiO_2 (60–66%) and high-SiO_2 (68–70%) subgroups. Two quartz diorites are considered separately. Comparison of values shows the mean values of the HSB low-SiO_2 subgroup to fall in between the values of the low- and high-Sr subgroups of GG2 rocks in the TSB and NTSB (Table 5). The main differences are the lower K_2O, Rb, La, Th and U in the HSB samples. The low-SiO_2 HSB samples also show a 'differentiation trend' in many Harker diagrams, e.g. decreasing Sr, Y with approximately similar Zr and Ba.

The high-SiO_2 subgroup in the HSB has lower TiO_2, Nb and La and higher Na_2O than the high-SiO_2 granodiorites in the MB (Table 5). There is a 'differentiation trend' with increasing La, Y, Zr and Th in Harker diagrams. The high-SiO_2 subgroup differs from the low-SiO_2 subgroup, indicating a different origin, but there is a trend from the mafic samples in the low-SiO_2 subgroup to the high-SiO_2 subgroup rocks that could be interpreted as a mixing line. There are very few high-K volcanic rocks or volcanic rocks within the silica range 61–67% in the HSB, and this indicates a separate origin for GG2 granitoids and the main part of the volcanism in this area. Two quartz diorites, one of them comingling with diorite (hybrid), are geochemically intermediate between high-Ti mafic plutonics in the HSB and the low-SiO_2 subgroup rocks (data not shown).

The two GG2 samples in the MC were not included in constructing the GG2 fields in Figs. 26–28. The slightly granitized strongly foliated granodiorite 8911114 (SiO_2 65.5%) is a high-K calc-alkaline nearly metaluminous rock (Fig. 32) with higher Y, Nb and F values (data not shown) than in most HSB samples. Porphyritic granite 8911129, an undeformed

granite possibly similar in age to 1.84–1.81 Ga microcline granites, should be considered as a separate sample in GG2. It differs from the microcline granites in lower silica (SiO_2 69.0%) and in calc-alkaline and only slightly peraluminous affinities (Fig. 32). Sample 8911129 also contains abundant magnetite and thus differs from the normally magnetite-free microcline granites. The high P_2O_5 (0.32%), Sr (529 ppm), elevated Zr (250 ppm), TiO_2 (0.46%) and higher F (0.09%) could indicate a genetic link with rocks of WP affinity.

GG3

The GG3 rocks have been divided into main and Nokia-type subgroups. Both subgroups are characterized by enrichment in S, As, Bi, Te and Li (Lahtinen & Lestinen 1996) compared with GG2 rocks. These same elements are enriched in sediments and indicate a close link between sedimentary rocks and GG3 granitoids.

The GG3 main subgroup granodiorites mostly occur in the MB and contain both mafic–intermediate enclaves and schist inclusions. Often they are strongly foliated and sheared. These are high-K calc-alkaline rocks, gradational to the GG2 granitoids in the MB (Figs. 26–28 and 32, Table 5) with slightly higher Al_2O_3, as also seen in the more peraluminous nature. These features are consistent with a similar origin to the GG2 granitoids in the MB with a greater contribution of assimilated sediment component.

Granodiorite 8911123 (SiO_2 62.9%) from the MC is a high-K calc-alkaline rock with elevated mol. A/CNK value (Fig. 32). The abundant microcline granite dykes may have increased K, and particularly increased Rb values, as seen in the low K/Rb ratio (149). A notable feature is the high F (0.22%), but whether this is a primary feature or due to metamorphic fluids is unclear.

The Nokia-type samples from the Nokia and Siitama plutons are porphyritic granodiorites, with mafic and intermediate enclaves occurring in three samples. The samples have a restricted SiO_2 range of 64–68% (Figs. 26–28). Most are calc-alkaline rocks, but they deviate to higher FeO/MgO ratios relative to GG2 rocks and the GG3 main subgroup. Varying from high-K to very high-K, they are strongly peraluminous rocks that approach the sediment average (Fig. 32). TiO_2, P_2O_5, Zr, La, F, Nb, Y, Rb and S levels are higher and the CaO level lower relative to the GG2 and the GG3 main group rocks (Figs. 26–28, Table 5). The lower Na_2O in the more felsic rocks plots them in the S-type field in Fig. 32. The higher levels of Li, As, Te, Zn and Bi (Lahtinen & Lestinen 1996) could be partly due to mineralizing effects, but the decreasing trend of S and As and increasing trend of Bi and Li (this not definitive) relative to silica content (data not shown) show that the elevated contents are related to the magma genesis. The proposed model for the rocks is a strong assimilated sedimentary component associated with mantle and possibly also crustal derived melts. The higher levels of Ti, P, La, Zr and F indicate that the mantle component has been of WPB affinity.

GG4

The GG4 rocks are medium-K, mainly calc-alkaline rocks, which are here considered on areal basis. The four samples from the NTSB are felsic peraluminous granodiorites characterized by elevated CaO and high Na_2O (Figs. 26–28 and 32, Table 5). Compared with the MB and HSB samples, Ba shows higher abundances at similar K_2O values and Th/U ratios are higher (Figs. 33 and 35 and Table 5). Like the NTSB samples, the three felsic GG4 granodiorites (including one gneissic variant) from the MB show elevated CaO and high Na_2O with low Y, but Sr is lower and Ba, Nb, Rb and Th$_u$ values are higher indicating a slightly different origin (Figs. 26–28, Table

Table 5. Average chemical composition of granitoids in the Tampere–Hämeenlinna area divided into groups and subgroups.

Group Subgroup[1] N	GG1 7	GG2 NT/a 5	GG2 NT/b 7	GG2 MB/c 5	GG2 HSB/d 8	GG2 MB/e 6	GG2 HSB/e 4	GG3 Nokia 7	GG3 MB/f 5	GG4 NT 4	GG4 MB/g 3
SiO_2	58.91	62.35	63.47	60.80	62.23	67.19	68.57	65.60	62.99	69.19	67.73
TiO_2	0.68	0.63	0.62	0.74	0.64	0.43	0.29	0.67	0.66	0.33	0.37
Al_2O_3	17.66	17.10	16.62	16.86	16.94	16.70	16.30	16.45	18.15	16.57	16.78
FeO	6.04	4.98	5.21	6.35	5.53	3.55	2.97	4.80	5.09	2.62	2.95
MnO	0.13	0.11	0.11	0.11	0.11	0.08	0.08	0.09	0.10	0.08	0.07
MgO	3.34	2.37	1.90	3.28	2.48	1.13	0.90	1.34	2.08	0.80	1.07
CaO	5.17	4.36	3.87	4.80	4.45	3.06	2.51	2.28	4.32	2.72	3.24
Na_2O	3.58	3.62	3.35	3.06	3.63	3.35	4.21	2.94	3.53	4.51	4.71
K_2O	2.88	3.07	3.52	2.54	2.54	3.48	3.21	4.37	2.35	2.21	2.03
P_2O_5	0.30	0.23	0.17	0.19	0.21	0.13	0.09	0.27	0.23	0.11	0.17
CO_2	0.05	0.04	0.08	0.11	0.15	0.12	0.13	0.05	0.10	0.04	0.05
F	0.9	0.07	0.08	0.09	0.08	0.05	0.03	0.13	0.08	0.07	0.03
S	0.01	0.01	0.01	0.04	0.02	0.02	<0.01	0.04	0.05	<0.01	<0.01
A/CNK[2]	0.96	0.99	1.02	1.02	1.01	1.12	1.09	1.20	1.12	1.12	1.06
Ba	915	951	730	530	519	709	628	900	474	724	473
Cl	253	268	471	276	408	168	240	167	212	111	139
Cr	81	51	34	110	46	29	22	38	39	24	27
Nb	10.1	7.8	9.9	9.3	8.7	9.1	4.7	18.0	10.7	9.7	5.6
Ni	36	33	24	42	32	23	21	30	25	20	22
Rb	83	99	109	98	75	105	85	156	98	79	48
Sr	818	685	286	258	400	242	376	237	356	322	536
V	156	121	109	136	128	61	51	87	100	47	63
Y	17.3	16.9	26.7	20.1	18.4	14.1	12.0	29.3	18.6	9.8	10.6
Zn	87	82	73	100	86	60	45	103	102	69	72
Zr	145	157	226	221	178	191	140	292	181	187	163
Co	17	13	12	16	14	7	6	9	11	5	7
La	28.3	26.5	30.4	23.2	23.6	30.6	13.3	48.6	23.4	29.5	20.9
Sc	21.9	16.0	16.5	20.5	16.5	9.1	6.0	14.8	13.9	6.3	5.6
Th	8.1	7.7	13.0	6.9	5.9	9.9	8.7	14.3	5.4	8.4	5.6
U	2.0	3.0	3.4	2.1	2.1	2.2	2.7	3.3	1.4	1.9	1.9

Major elements (wt%), S (wt%) and Ba–Zr (ppm) analysed by XRF, F by ion selective electrode at the GSF laboratory; Co–U by neutron activation at the Technical Research Centre of Finland; CO_2 by wet method at XRAL in Canada.
[1] NT – NTSB+TSB, a – high-Sr subgroup, b – low-Sr subgroup, c – <66% SiO_2, d – 66-70% SiO_2, e – 66-70% SiO_2, f – <68% SiO_2, g – 67-71% SiO_2, h – 63-66% SiO_2, k – S8911106, l – >70% SiO_2, m – <70% SiO_2, n – restite-poor, o – high-K_2O restite-poor (U data excl. 20.8 ppm), p – very high-K_2O restite-poor (U data excl. 21.9 ppm), r – Zr > 500 ppm (Ba data excl. 5210 ppm), s – Zr <500 ppm and 56-69% SiO_2.
[2] A/CNK = molecular ratio of $Al_2O_3/(CaO+Na_2O+K_2O)$.

5). The lower Rb also produces higher K/Rb ratios (Fig. 33).

The intermediate GG4 rocks in the HSB are quartz diorites to granodiorites containing abundant hornblende, and mafic enclaves characterize the sample outcrops. These intermediate rocks are comparable to the high-K GG2 rocks in the HSB (Figs. 26–28, Table 5) and show only slightly lower K_2O and slightly higher Na_2O and CaO, giving them a metaluminous nature (Fig. 32). Quartz diorite 8911079 (SiO_2 59.4%) is from a diorite body that has intruded the HSBd schists and has a high mol. A/CNK-value indicating sediment assimilation (Fig. 32). Quartz diorite 8911127 (SiO_2 56.4%) is a metaluminous rock (Fig. 32) with elevated Sr and it follows the 'differentiation' trend of mafic plutonics in the HSB

Table 5 (continued).

Group Subgroup[1] N	GG4 HSB/h 4	GG4 MC/k 1	GG5 NT/l 9	GG6 NT/m 7	GG6 NT/l 7	GG6 HSB/m 3	GG7 MB/n 5	GG7 MC/o 6	GG7 MC/p 7	GG8 MB/r 5	GG8 MB/s 13
SiO_2	64.18	72.35	72.21	66.50	71.43	67.45	72.54	73.90	72.35	59.03	61.61
TiO_2	0.55	0.27	0.21	0.47	0.23	0.47	0.16	0.12	0.20	1.07	0.80
Al_2O_3	16.43	14.00	14.71	16.79	15.09	15.77	15.10	14.51	15.04	18.12	17.60
FeO	4.95	3.24	2.18	3.36	2.15	4.31	1.81	1.57	1.65	7.04	5.99
MnO	0.11	0.08	0.07	0.09	0.06	0.08	0.06	0.05	0.04	0.11	0.10
MgO	2.18	0.37	0.36	0.59	0.33	0.96	0.35	0.28	0.28	1.93	1.77
CaO	4.38	1.46	1.41	2.33	1.16	2.16	1.20	0.95	0.89	4.01	3.88
Na_2O	3.84	4.68	3.36	3.62	2.96	3.27	3.47	3.30	3.06	3.27	3.31
K_2O	2.11	2.52	4.60	5.09	5.81	4.35	4.63	4.58	5.72	3.43	3.29
P_2O_5	0.15	0.05	0.06	0.15	0.06	0.15	0.05	0.07	0.08	0.35	0.27
CO_2	0.05	0.04	0.02	0.05	0.04	0.04	0.03	0.05	0.07	0.08	0.06
F	0.04	0.04	0.03	0.05	0.08	0.07	0.05	0.03	0.03	0.07	0.10
S	<0.01	<0.01	<0.01	0.01	<0.01	0.02	<0.01	<0.01	<0.01	0.08	0.05
A/CNK[2]	0.99	1.07	1.12	1.07	1.14	1.12	1.17	1.20	1.17	1.11	1.10
Ba	488	695	706	1381	750	743	450	317	379	1018	852
Cl	247	193	104	189	105	121	82	88	156	153	270
Cr	42	33	18	17	14	36	27	24	16	44	42
Nb	7.8	8.7	8.1	14.4	13.3	11.6	10.7	15.9	14.2	20.1	15.4
Ni	29	22	20	16	18	25	22	22	19	29	29
Rb	63	36	127	99	175	166	197	206	226	95	110
Sr	345	71	181	256	165	162	129	84	80	292	265
V	112	25	28	50	29	59	25	20	22.5	116	103
Y	18.3	51	18.7	28.4	27	30.7	27.2	13.9	13.2	27.5	30.2
Zn	72	45	53	75	47	93	66	55	48	142	116
Zr	171	381	144	373	256	255	130	129	156	596	342
Co	13	-	3	4	2	2	3	2	2	12	11
La	21.4	19.9	38.0	37.0	82	37.1	29.4	28.4	44.4	44.4	47.6
Sc	14.4	7.9	6.9	14.7	6.7	15.1	5.1	3.7	2.9	24.0	18.6
Th	8.9	2.0	10.8	5.5	23.1	14.4	14.8	19.5	30.0	9.6	11.8
U	2.9	0.4	1.8	1.6	4.5	3.8	4.0	3.5	5.9	1.8	1.8

(Figs. 26–28).

The GG4 granodiorites in the MC are strongly foliated mafic enclave-bearing rocks with widely ranging characteristics. In its highly peraluminous nature (Fig. 32) and low K/Rb ratio (178), strongly foliated granodiorite 8911105 (SiO_2 64.7%) appears to be assimilated, though these features could partially be due to shearing and the alteration associated with this. At least in part, granodiorite 8911103 (SiO_2 69.5%) is a hybrid rock and geochemically comparable to GG4 rocks in the HSB, but the Th value of 2.7 ppm is clearly lower than in the HSB GG4 rocks (8–10 ppm). Granodiorites 8911106T (SiO_2 72.7%) and 8911106 (SiO_2 73.1%) differ from the other GG4 rocks and should be considered as a subgroup. They are medium-K tholeiitic rocks with the lowest mol. A/CNK values for comparable very felsic rocks (Fig. 32). The K/Rb ratio and Zr level are very high, and FeO, Na_2O and Y are high and Th low relative to the high silica (Table 5). One interesting feature is the occurrence of magnetite in these granitoids, since HSB calc-alkaline granitoids normally are magnetite-free (Lahtinen & Korhonen 1996).

GG5

The GG5 rocks are from the NTSB and most are porphyritic granites. Two additional intermediate granodiorites and one felsic porphyry are considered separately. Mafic enclaves are found in only some sample outcrops and appear to be less common than in outcrops hosting GG2 samples. GG5 granites vary from calc-alkaline to tholeiitic affinity, but geochemically they form a more or less coherent group (Figs. 26–28, Table 5). The variation in affinity may be due to the abundant occurrence of magnetite (Lahtinen & Korhonen 1996), which may cause sampling heterogeneity especially in coarse-grained rocks of high silica nature with low MgO. The K/Rb ratio is variable (Fig. 32), but is normally higher than the crustal average of 230 (e.g. McLennan et al. 1990). Ba exhibits a decreasing trend in the Ba–K_2O diagram (Fig. 32) and some samples show strong Ba depletion indicating either K-feldspar precipitation or presence in the source residue.

Granodiorite 8910921 (SiO_2 64.7%) is a mixed rock with a very large number of mafic enclaves. Geochemically it is a high-K rock of tholeiitic affinity according to Fig. 26 and is characterized by elevated Zr and high Y (Fig. 28). Porphyritic granodiorite 8910919 (SiO_2 64.2%) is similarly characterized by the occurrence of mafic enclaves. Both these samples are of mixed nature and are only tentatively classified in the GG5 group; they could also have been included in GG2. Feldspar porphyry 8910856 differs from the other GG5 samples in having very high SiO_2 (80.3%) and it is difficult to ascertain its genetic relation to other samples

GG6

The GG6 rocks are divided into two areal subgroups: NTSB and HSB. The NTSB samples are porphyritic to coarse-grained granites with local rapakivi-like textures. Both horn-blende and biotite occur in the intermediate (SiO_2 <70%) granites, while biotite dominates in more felsic rocks. Mafic enclaves are rare, but some sample outcrops include a small number of them, and at least in one case comingling has occurred. Small amounts of magnetite are another characteristic feature (Lahtinen & Korhonen 1996). The NTSB GG6 granites are very high-K rocks with alkaline and tholeiitic affinities (Fig. 26), and they show a peraluminous character even in the proposed igneous field (Fig. 32). The intermediate samples show low MgO, CaO and high Zr, Y, Ba and Nb (Figs. 26–28 and Table 5), with decreasing though somewhat scattered trends to more felsic granites in Harker diagrams. Another characteristic feature of the intermediate samples is the high Nb/Th and K/Rb ratios (Figs. 33 and 35). The decrease from Ba-enriched nature to Ba-depleted nature in more felsic samples indicates either precipitation of K-feldspar/biotite or the occurrence of Ba-poor felsic melt. The behaviour of Na_2O (Fig. 32) and CaO (Fig. 27) is also consistent with plagioclase precipitation. The change in the K/Rb ratio (Fig. 33) might also be explained by K-feldspar/biotite fractionation since Rb has a much lower distribution coefficient than Ba for these minerals. On the other hand, the felsic granites have higher F and there is variation in Zr and Y (Fig. 28) indicating slightly different sources.

The GG6 samples in the HSB comprise porphyritic granodiorites from the HSBb and one granite from the HSBa. Porphyritic granodiorites 8911088 (SiO_2 66.2%), 8911091 (SiO_2 67.4%) and 8911134 (SiO_2 70.8%) have less K_2O and are more peraluminous than the NTSB samples (Fig. 32, Table 5). They also differ from the intermediate NTSB GG6 samples in their lower Ba and clearly higher Rb, Th and U (Figs. 26–28 and Table 5). Granite 8911002 (SiO_2 67.9%) is a very high-K rock of tholeiitic and alkaline affinity (Fig. 26).

GG7

Granites from the TSB, MB, HSB and MC that have clearly peraluminous character and plot above the proposed 'igneous' line in Fig. 32 make up the 'S-type' group GG7. The samples from the TSB, MB and HSB represent small granite or pegmatite dykes crosscutting mica gneisses and migmatites. The microcline granites from the MC form a GG7 subgroup that is further divided into high- and very high-K_2O samples.

Many GG7 granites have higher Na_2O than normally observed in S-type granites (Fig. 32), but many of them are two-mica granites, with garnet and tourmaline found locally. The GG7 granites are high silica rocks with highly scattered trace element abundances as seen, for example, in variable Th/U ratios (Fig. 35). They have low Ba level relative to K_2O and normally have low K/Rb ratios (Fig. 33).

The characteristic feature of the MC GG7 granites is the lower levels of Au, As, Bi, Sb and Cs than in GG7 rocks from other areas. This indicates a loss of these elements, probably in a fluid phase, in the MC source (Lahtinen & Lestinen 1996). The MB GG7 granites show similar major element composition to high-K_2O granites in the MC (Table 5), but higher Nb, La, Th, U, and lower Y, Sr and Ba characterize MC granites. Both high- and very high-K_2O subgroups from the MC have lower CaO and Sc, and higher P_2O_5 and CO_2 levels than the MB GG7 rocks. Granites 8910803 (SiO_2 73.3%) and 8910843 (SiO_2 72.8%) from the TSB show peraluminous character, but it is not clear whether they are associated with the GG3 Nokia-type or are S-type granites. Their classification in GG7 is thus only tentative. One granite (8910959) bearing small amounts of muscovite, garnet, and tourmaline and one pegmatite (8910832) intruding mica gneisses and migmatites in the MB deviate to higher mol. A/CNK values (1.30–1.31) and are characterized by low Zr (<30 ppm), La (<6 ppm), and Ba (<120 ppm).

Microcline granite 8911094 (SiO_2 73.4%) and aplite granite 8911014 (SiO_2 72.1%) from the HSB are geochemically similar to GG7 rocks in the MC and a cogenetic origin is proposed.

Uranium values for the MC GG7 granites are scattered: there are five samples with high U (15–22 ppm), while the normal variation is 1–7 ppm. The high values are probably due to late-stage hydrothermal fluids. The main differences between the high- and very high-K_2O GG7 subgroups are the higher TiO_2, Cl, CO_2, Zr, La, Th and U in the very high-K_2O subgroup. Some samples from the MC are distinctive and require separate discussion. Granite 8911099T (SiO_2 71.0%), occurring
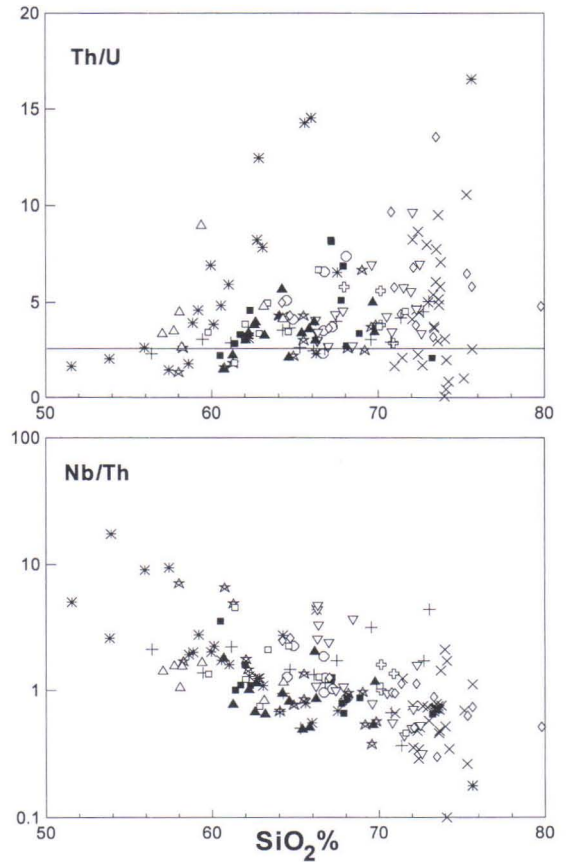

Fig. 35. Th/U–SiO_2 and Nb/Th–SiO_2 variation diagrams for granitoids in the Tampere–Hämeenlinna area. Data from this study. See Figure 32 for symbols.

near the western contact of the MC, contains both UR porphyrite and mica gneiss inclusions. Except for the lower silica and slightly higher Sr and F values, this sample is comparable to normal S-type microcline granites, and the small differences possibly are due to the occurrence of UR-porphyrite inclusions. Granite 8911128 (SiO_2 72.4%) differs from normal microcline granites in having higher Sr (240 ppm) and a small magnetite content. The garnet-, sillimanite- and muscovite-bearing granite 8911110 (SiO_2 74.0%) has high P_2O_5 (0.13%) and U (16 ppm) and low Th (1 ppm) and Nb (2 ppm). Garnet-bearing granite 8911112 (SiO_2 73.6%) also has an elevated P_2O_5 value (0.16%). Samples 8911110 and 8911112 both have low Zr (<50 ppm), Sr (<50 ppm), La (<11 ppm) and Ba (<130 ppm) and high mol. A/CNK (1.24–1.31) suggesting the occurrence of a small amount of restite (garnet±sillimanite) and a more pelitic source. Sample 8911111 (SiO_2 73.6%) is heterogeneous granite with normal S-type characteristics, but the high graphite content (0.6% C) sets it apart from the normal graphite-free MC granites. Three samples deviate to higher SiO_2 (75–76%), but otherwise they are comparable to other samples in relevant subgroup (two belong to the high-K_2O and one to the very high-K_2O subgroup).

GG8

The GG8 group comprises quartz diorites and porphyritic granodiorites and one quartz monzonite of probable feldspar cumulus origin. Mafic and intermediate enclaves are abundant and at least one sample shows comingling and hybrid origin. In addition to enclaves, small amphibole-rich patches are found locally, and a small amount of graphite ($C_{Graf.}$ 0.06–0.10%) characterizes some samples. The GG8 rocks are a heterogeneous group with variable chemical composition (Figs. 26–28) and characterized by high S, Te, As and Bi (Lahtinen & Lestinen 1996) comparable to GG3 rocks, indicating sediment assimilation.

Most of the GG8 rocks are high-K granitoids of tholeiitic affinity and even the more mafic samples exhibit strongly peraluminous character (Figs. 26 and 32). There is a trend to lower FeO/MgO ratios and to higher mol. A/CNK values approaching the sediment average. The TiO_2 and Zr and to some extent Al_2O_3, P_2O_5 and Y values are higher and the CaO and MgO values lower relative to the GG2 rocks (Figs. 26–28). At similar silica levels, the Zn, Nb and La values are higher and the Co and V values lower than in GG2 rocks (Table 5). The 'differentiation trend' of TiO_2, MgO, CaO, P_2O_5, Zr and Y (Figs. 27–28), and also Zn, V, Co and Nb (data not shown), in the GG8 group is somewhat similar to the trends of the GG3 Nokia-type and GG6 intermediate granite. A notable feature is the similar geochemical values and trends for alkaline hypabyssal dykes and the high-Zr GG8 samples, and the similar trends, although scattered, for the low-Zr mafic plutonics and low-Zr GG8 (Figs. 26–28). Ba abundances are normally high, and quartz monzonite 8910826, probably of cumulus origin, exhibits such exceptionally high Ba (5210 ppm) that it is not
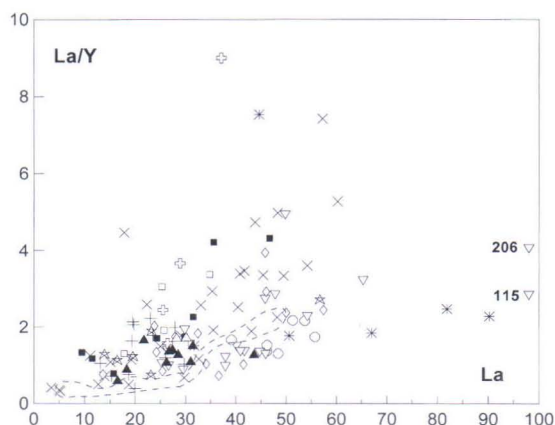

Fig. 36. La/Y–La variation diagram for felsic (>65% SiO_2) granitoids in this study. See Figure 32 for symbols. Dashed line encloses GG7 granites from the MB.

included in Fig. 33. An interesting feature is
the continuous increase in the Th/U ratio from
low (<2.5) to high (15) values, which indi-
cates zircon precipitation and/or the presence
of zircon in the source residue (Fig. 35).

The orthopyroxene-bearing quartz diorite
8910981, of hybrid origin (SiO_2 56.0%), is
from an outcrop where fine-grained diorite
comingles with quartz diorite (sample) and
mixed diorite contains feldspar crystals from

quartz diorite; such a complex situation typ-
ifies several of the more mafic GG8 rocks.
The sample falls in the high-Zr group and,
despite a high Rb value, has a pattern indic-
ative of WPB-affinity origin (data not shown).
Although there are differences, the GG8 gran-
itoids are considered to have a general origin
in the mixing of mantle melts and sediments
or sediment-derived melts.

Origin of the plutonic rocks

The sediment-assimilated nature of many of
the plutonic rocks and their comingled char-
acter and mixed origin, and the cumulated na-
ture of many mafic rocks, produce scatter in
the geochemical fingerprints. The hybrid na-
ture of many granitoids is seen in the common
occurrence of mafic enclaves and in the mixed
geochemical character. Castro et al. (1991)
have proposed a H-type (hybrid) general clas-
sification for granitoid rocks like these. In a
broad sense, the H-type classification covers
all GG1–GG4 rocks, but some interpretation
of endmembers is nevertheless attempted.
While individual plutons will, of course, have
different evolution histories, the discussion
here is focused on the general characteristics
of groups and subgroups. As regards the ex-
tent to which granitoids are subduction relat-
ed and comagmatic with volcanics, age and
geochemical differences suggest that most of
the granitoids have no direct relation with
volcanics. One problem is the lack of REE
analyses and the use instead of La and Y
abundances (Fig. 36) to deduce the behaviour
of REE.

The mafic plutonics in the NTSB and TSB
can be divided into predominant WPB affinity
and calc-alkaline arc-type plutonics where the
latter rocks are geochemically similar to high-
K calc-alkaline mafic volcanics (VG6). There
are no volcanic counterparts in the NTSB and
TSB for the high-Ti WPB-affinity mafic plu-

tonics, but the mafic volcanics at Takamaa,
the youngest volcanics in the TSB, have char-
acteristics intermediate between those of vol-
canics in the main volcanic association and
high-Ti mafic plutonics. TiO_2 is elevated, for
example (Table 1 in Kähkönen 1989). The
high-Ti mafic plutonics are highly differenti-
ated, and the precipitation of both sphene and
magnetite is considered to be responsible for
the pronounced negative Nb-anomaly in some
samples. To some degree they have interacted
with more felsic melts and, thus, the chemical
composition has changed somewhat. An ori-
gin from EM (EMI–HIMU, Lahtinen 1994b),
with differences in the degree of mantle melt-
ing, crystal fractionation and interaction with
felsic melts is proposed to account for the
observed geochemical features of these rocks.
A notable feature is the enrichment of Ba, Sr
and La in the mafic plutonics of the NTSB and
TSB compared with those of the HSB (Table
5); this is in accord with the differences found
between volcanics (p. 63), and points to a
difference in mantle composition. On the oth-
er hand, the average Th/U ratio (2.6) in high-
Ti mafic plutonics in the NTSB is lower than
Th/U ratios in the NTSB+TSB volcanics (Fig.
13). The mafic plutonics in the MB can be
divided into DM and EM types. Both types
show interaction/assimilation with sedimenta-
ry rocks or silicic melts, which increases the
levels of Rb and Th and in some cases produc-

es negative Ba anomalies.

In many cases, the HSB mafic plutonics have interacted with more silicic melts, and sediment- assimilated features are not uncommon. An interesting feature is the occurrence of mafic plutonics geochemically comparable to the VG3 volcanics showing, as noted above, the close relationship between volcanism and plutonism in the Häme group. To some extent medium-K calc-alkaline gabbros and diorites resemble the HSB calc-alkaline basaltic to andesitic volcanics, but the age of these plutonic and volcanic rocks is unknown. EM-derived mafic plutonics are the most abundant type in the HSB. Some of the samples exhibit clearly negative Nb anomalies, possibly indicating the occurrence of a subduction component. The occurrence of volcanic dykes (p. 51) with WPB affinity could indicate a similar age for the WPB-affinity mafic plutonics. The quartz monzodiorite from the MC shows enriched alkaline WPB affinity from an EM source. Geochemically it is comparable to the NTSB alkaline high-Ti mafic plutonics and shows negative Nb anomaly interpreted to be due to the precipitation of sphene and titanomagnetite.

The GG1 granitoids and arc-related mafic plutonics in the NTSB are to some extent comparable to the volcanics, and the gneissic variants may be the oldest plutonics in the NTSB. The geochemistry of the GG1 granitoids and arc-related mafic plutonics suggests EM-derived melts which have been affected by a subduction component and calc-alkaline crystallization history. The GG2 granitoids in the NTSB often are associated with WPB-affinity mafic plutonics and are hybrid rocks through the interaction with mafic WPB melts and inclusions. The restitic origin of some enclaves cannot be excluded, but abundant comingling features and the enrichment of Nb, Sr, Zr, Ti, Sm and F in hybrid rocks suggest a mixing of mafic WPB-affinity and felsic melts, at least in these cases. On the other hand, the general calc-alkaline nature of GG2

rocks, and the geochemical similarity between arc-related mafic plutonics and mafic GG2 granodiorites in the NTSB and TSB, suggest at least partial genetic link to calc-alkaline magmatism. The differences between GG2 granitoids and volcanic rocks in the NTSB and TSB (see Fig. 34) point nevertheless to separate origins.

The calc-alkaline nature of the GG2 granitoids suggests a low FeO/MgO source for the partial melt endmember; for experimental partial melts normally had higher FeO/MgO ratios than the source (p. 67). The occurrence of magnetite in the source residue would also lower the FeO/MgO ratio. It appears that Mg homogenizes faster than Fe (Watson 1982) in the interaction of basaltic and silicic magmas (Van Der Laan & Wyllie 1993), and this might lower the FeO/MgO ratio of silicic melt during effective stirring. The difficulty in extrapolating to a possible silicic endmember or endmembers is that interaction, mixing and assimilation have probably occurred in the deeper parts of the crust and been followed by differentiation. The high Th and elevated Zr, especially in the low-Sr subgroup (Table 5), indicate that the melting temperature has been high enough to dissolve accessory minerals (e.g. zircon and monazite) in high degree. Hydrothermal zircon saturation experiments (Watson & Harrison 1983) suggest that temperatures of at least 800–850°C stabilize about 200 ppm Zr in the melt. In more anhydrous conditions, temperatures must be higher. The SiO_2 abundances in the NTSB and TSB GG2 granodiorites are mostly less than 68% and this indicates a rather mafic source and possibly vapour-phase-present melting of mafic rocks and/or total mixing and homogenization in the lower crust with a more silicic endmember.

At least three endmembers are needed in the genesis of the GG2 granitoids in the NTSB and TSB: 1) WPB-affinity mantle-derived magma, 2) calc-alkaline intermediate melt, 3) silicic crustal melt. The WPB-affinity mantle-

derived magmas have been discussed above. The calc-alkaline intermediate endmember is a subduction-related mantle melt, a partial melt from calc-alkaline mafic rocks in the lower parts of the crust, or a combination of the two. Arc-related mafic plutons confirm that calc-alkaline mantle-derived magmas were present. The relatively low La/Y ratios and often low Sr (Fig. 36, Table 5) in felsic granodiorites indicate that garnet has not been present in large amounts and that plagioclase has been stable in the source residue implying <40–50 km depth (<16 kbar) if the partial melting model is preferred. These source rocks would be quartz-saturated, have low FeO/MgO, and possibly contain magnetite. They would be able to produce a low FeO/MgO ratio in the partial melt and would melt in the temperature range 850–900°C.

The higher K_2O, Th, U and lower K/Rb relative to volcanics, especially in the low-Sr subgroup GG2 granitoids, imply that a more evolved crustal endmember was present as well. The deviation to lower Ba abundances (Fig. 33) might be due to the presence of K-feldspar/biotite in the source residue, or due to a source with a different Ba–K relation than in volcanics. The stabilization of biotite in mafic magma during interaction with felsic magma could produce Ba enrichment in the mafic magma and depletion in the felsic counterpart, but whether this would be sufficient to change the Ba level in large plutons is unclear. An igneous tonalitic to granodioritic or immature sedimentary source is possible for the silicic endmember, but the mixing and homogenization of different components has occurred deeper in the crust and thus the exact composition of the silicic endmember is difficult to deduce.

A small amount of sediment component is indicated for the MB GG2 granitoids, due either to assimilation or to a layered source. The abundant enclaves in the intermediate granodiorites point to a mixed origin. Mafic enclaves are rare in more silicic granodiorites

(SiO_2 66–70%) and thus their composition is probably closer to the partial melt endmember composition. The vapour-phase-absent melting of mafic rocks produces granitic to typical trondhjemitic–tonalitic liquids, and vapour-phase absent-melting of silicic rocks produces granitic liquids; granodiorite compositions are thus rare in vapour-phase-absent conditions. The low Na_2O and elevated mol. A/CNK and MgO (Table 5) could indicate assimilation, a layered sedimentary–igneous source and/or a small amount of restitic material. The variable Th/U ratio (Fig. 35) means that zircon (enriched in U) has not dissolved and occurs as restite in some samples. The increasing La/Y ratio with increasing La (Fig. 36) is due either to differentiation or to a greater amount of garnet in the source residue. Thus, there are compositional differences suggestive of a variable source and variable conditions during melting.

The situation in the HSB is similar to that in the NTSB and TSB. Hybrid quartz diorites have a chemical composition intermediate between high-Ti mafic plutonics and intermediate granodiorites, suggesting interaction and mixing of mantle-derived melts and crustal-derived partial melts. The more silicic granodiorites (SiO_2 66–70%) have higher Na_2O and Sr than the MB rocks, indicating a more Na-rich source in the HSB. An origin due to vapour-phase-present melting of mafic to intermediate calc-alkaline rocks is proposed. A differentiated origin from homogenized mafic-granitic mixing product is unlikely due to the lower La than in the intermediate GG2 group (Table 5). The constant Th/U ratio (Fig. 35) and low La, Th, and U abundances argue against the precipitation of LREE-enriched accessory phase (monazite, allanite), which is one way for La to be depleted in the melt. The low TiO_2, Nb, La and possibly also Zr are consistent with abundant hornblende±magnetite in the source residue, supporting the vapour-phase-present conditions. The low La/Y ratios (Fig. 36) do not favour the presence of large

amounts of garnet in the residue.

The GG3 main subgroup is in many ways similar to the GG2 rocks in the MB, and a similar origin, with interaction and mixing of mantle- and crustal-derived melts is proposed. The higher mol. A/CNK, and the higher abundances of trace elements which are enriched in sedimentary rocks, suggest that there is more sediment assimilation in the GG3 main group. The GG3 Nokia-type granodiorites are strongly peraluminous rocks, especially relative to the silica level. They also have higher Ti, P, Zr, La, F, Nb and Y than the GG3 main group, arguing for a larger amount of WPB component and a larger amount of sediment assimilation. The Nokia-type rocks are not S-type because they have a strong magmatic component. The sediment assimilation has probably been a total engulfment of sedimentary rocks at deeper crustal levels. The higher Th/U ratios (Fig. 35) in some samples indicate restitic zircon in the source.

The GG4 are more primitive rocks and, besides lower K_2O, have higher CaO and Na_2O than do GG2 rocks. The GG4 rocks in the NTSB are interpreted as derived from partial melts from a mafic source under vapour-phase-present conditions, but the high Th and Rb (Table 5) favour an evolved source, and low Y is indicative of garnet and/or large amounts of hornblende in the residue. The MB GG4 rocks have a comparable origin, but a higher Sr and K/Rb ratio (av. 350 compared with 230 in NTSB samples) and low Y and Th (Table 5) indicate melting of a more primitive source. Higher Sr is due either to more Sr in the source or less plagioclase in the source residue. The HSB GG4 rocks are closely related to the GG2 rocks and of similar origin, but possibly more DM-dominated mantle endmember characterizes the GG4. Two of the GG4 samples in the MC may be related to GG4 rocks in the HSB, but the other two have different characteristics and are considered a separate subgroup. The high

FeO and low Al_2O_3 relative to SiO_2 and the high Y relative to La (Table 5) are similar to features observed in silicic tonalites in the Rautalampi area, which were interpreted to originate in low degree melting of tholeiitic source with gabbroic residue (Lahtinen 1994a); however, the higher K_2O and Zr indicate a more evolved source in the MC.

Although GG5 includes some hybrid rocks, the more silicic GG5 rocks form a fairly coherent geochemical group. The compositional gap between the GG2 granodiorites and GG5 granites, with differences, for example, in the Th level, shows that they are not related to each other through differentiation. The silicic GG5 are slightly peraluminous granites with normally low $FeO+MgO+TiO_2$ (<3%) and high FeO/MgO. The scatter in the K/Rb and Ba values points to a heterogeneous source, and some of the high K/Rb values are comparable to those in the very high-K GG6 rocks. Vapour-phase-absent melting of a tonalitic to granodioritic source is proposed, and the low Ba in some samples indicates either fractionation of K-feldspar or its presence in the source residue. High Th/U ratios (Fig. 35) suggest that zircon has to some extent concentrated in the source residue, while relatively low La/Y (Fig. 36) suggests that there is not a large amount of garnet in the residue.

The GG6 rocks in the CFGC are slightly peraluminous, alkaline to nearly alkaline rocks with high FeO/MgO ratio. The intermediate variants have high Zr, K/Rb (av. 430), Nb/Th (av. 2.6) and Ba (Table 5) indicating an affinity with WPB in the CFGC. Although a differentiation origin cannot be excluded, the lack of rocks in the silica range 54–66% favours a vapour-phase-absent melting origin. The more silicic granites have lower Ba, higher Rb and F, and variable Th, Y and Zr. Although two-feldspar fractionation (+ accessories) can explain some of these features, a more crustal component that has undergone dehydroxylation to increase F must be present at least in some silicic GG6 granites. Relative

to other GG6 rocks, the GG6 granites in the eastern part of the CFGC (Koppelojärvi) have slightly higher K_2O, Rb, Nb, Zr, F and lower Ba and K/Rb ratio for the same silica level, indicating a slightly larger crustal component. High melting and intrusion temperatures are needed to stabilize high Zr abundances in the GG6 melt (Watson & Harrison 1983), especially for intermediate rocks where the F abundances are not elevated.

The GG6 granites in the HSBb have lower K_2O and K/Rb ratio (av. 218) and they are more peraluminous than the GG6 granites in the CFGC. These features, and the higher Th and U, indicate a more crustal-like source relative to the CFGC GG6 at similar silica levels, but a vapour-phase-absent melting at relatively high temperatures is also proposed.

The GG7 S-type granites show wide variation in trace element concentrations within the normally fairly restricted SiO_2 range from 72 to 74%. The variation is due to the source, to melting conditions, to differences in the amount of restitic biotite and more rarely garnet and sillimanite, and to the presence of a later fluid phase, seen in some sporadic high U values. Vapour-phase-absent (a small amount of fluid possibly present) dehydration melting of sedimentary rocks is considered as a generally valid model for the origin of these granites. The elevated Sr, Na and Ca in some samples argues for vapour-phase-present melting conditions, which would exhaust plagioclase from the residue, but a more igneous-like source is possible as well. The GG7 granites have higher Na_2O, CaO, FeO and lower K_2O than the experimentally derived melts from pelites, and a more psammitic or layered source is required to provide abundant plagioclase in the source. Low Ba indicates the presence of K-feldspar in the source residue, either as a mineral or as an orthoclase component in residual plagioclase.

The GG7 granites in the MB and the high-K_2O GG7 granites in the MC are geochemically similar, but the higher CaO and Sr (Figs. 27–28) in the MB could indicate vapour-phase-present melting conditions in some cases. Two small granites within schists are depleted in Zr, La and Ba, indicating low melting temperatures, possibly related to muscovite dehydration melting. Relative to GG7 granites in the MC, the GG7 rocks in the MB generally have higher Y and lower La/Y ratios (Table 5, Fig. 36) indicating less garnet in the residue and melting at lower pressures (Vielzeuf & Montel 1994). Higher melting temperatures might also increase the amount of garnet in the residue (ibid.), but at the same time the melt K should increase, which is not what was observed (Table 5). The very high-K_2O subgroup has higher TiO_2, Zr, La, Th and U than does the high-K_2O subgroup and this suggests higher melting temperatures for the high-K_2O subgroup. The higher Cl and CO_2 could be the result of small differences in the fluid regime (often an infinitely small amount of fluid is present, even though the overall environment is anhydrous), stabilizing the source at slightly higher temperatures. The restite-bearing high-K_2O variants might represent still lower melting temperatures and possibly a more pelitic source. A notable difference between the MB and the MC is the loss of fluid phase (Au, As, Bi, Sb, Cs) in the MC source before the onset of vapour-phase-absent melting.

The GG8 granitoids are characterized by lower Ca, Na and Sr, and higher Ti, P, Ba, Zr, Y, and Nb than GG2 granitoids in the MB. They are peraluminous over a wide silica range, with high S, Te, As, Bi and local graphite derived from the assimilated sedimentary component. The most mafic GG8 samples are geochemically comparable to the alkaline WPB hypabyssal dykes and WPB-affinity mafic plutonics and must include a large WPB component. To explain the variations in the GG8 granitoids, they are interpreted to have originated through mixing of WPB melt in various proportions with assimilated sediment component, and partly also with crustal-derived

melts. Fractional crystallization and mixing and assimilation in many stages have complicated the evolution of the GG8 granitoids still more. The occurrence of GG8 rocks in close association with GG2 and GG3 granitoids in the MB, and the occurrence of hybrid rocks of intermediate nature between these rocks, point to the occurrence of a crustal melt component in some cases. The Th and U variation, and especially the high Th/U ratios (Fig. 35) in the intermediate granodiorites, show that

the assimilation/interaction with sediments occurred under disequilibrium conditions, leaving restitic zircon. Partly this is due to the freezing effect of assimilation, which promotes crystallization, lowers magma temperatures and hinders the zircon dissolution. The GG8 rocks are broadly similar to the GG3 Nokia-type, and the few differences between them may be due to the smaller proportion of assimilation component in the GG8 rocks.

Regional correlation and age relations

According to Simonen (1952), the age relations of plutonics in the NTSB are from mafic plutonic rocks through quartz diorite and granodiorite to granite; although the main part of the plutonics are syn-tectonic (synorogenic), massive granites have intruded after the main deformation and are thus late-tectonic (late-orogenic). Agreement with Simonen's observations is found in the correlation between GG2 samples and previously designated quartz diorite and granodiorite areas, and between GG5 and GG6 samples and his granite areas. According to the interpretation of this work, however, mafic magmatism (WPB) has been contemporaneous with the more felsic magmatism, indicating a similar age for the mafic plutonics and the quartz diorites and granodiorites; mafic magmatism may even have continued to the granite stage. Sjöblom (1990) sees a contact metamorphic aureole in the granodiorites surrounding the late-orogenic Koppelojärvi granite, whereas Nironen (pers. comm. 1995) interprets the pyroxene-bearing granitoids as an outer phase of the Koppelojärvi granite. The U–Pb zircon age of 1879±14 Ma (Patchett & Kouvo 1986) contains a high analytical error and, given the presence of a crustal component, could indicate a small contribution from inherited zircons and hence a younger age of about 1875–1870 Ma.

The GG2 Hämeenkyrö and Värmälä plutons in the TSB are syn-tectonic with respect to D1 in the TSB (Nironen 1989a) (classified as regional D2 in Kilpeläinen et al. 1994). Nironen's (1989a) U–Pb zircon ages for Hämeenkyrö (1885±2 Ma) and Värmälä (1878±3 Ma) indicate that regional D2 started before 1885 Ma (D1 in Nironen 1989a). The older U–Pb zircon age of 1901±28 Ma for Värmälä given by Kähkönen et al. (1989) has high analytical error, indicating the occurrence of older restitic zircon from pre-existing crust. The $\varepsilon_{Nd}(t)$ value of +0.1 recorded for Hämeenkyrö granodiorite (Patchett & Kouvo 1986) is difficult to interpret due to the combination of components from subduction-related magma, EM and pre-existing crust. The Varissaari gabbro from the TSB has $\varepsilon_{Nd}(t)$ of +1.3 at 1885±5 Ma (Patchett and Kouvo 1986). The high Sm and Nd values indicate an enriched source (EM), possibly comparable to the high-Ti mafic plutonics in this study. The assimilated nature of the Nokia pluton is seen in the restitic zircons, which have hindered the age determination of this rock (Nironen 1989a). The occurrence of the Nokia and Siitama plutons near to the south-dipping thrust (activated fault) indicates that the thrust has been the passway and controlled the emplacement of the plutons.

There is only one U–Pb zircon age from the

MB. The three-point isochron for a granodiorite in Valkeakoski gives an age of 1896±16 Ma (Hämäläinen & Vaasjoki 1992), and this could indicate a slightly older intrusion age than in the TSB. However, the high analytical variance, plus the common assimilation features observed in the MB, rather suggests the presence of a small amount of restitic zircon in this sample, so that the age cannot be considered definitive. The D2 tonalite intrusions in the Vammala area, situated in the MB west of the study area, are dated at 1885 Ma (Kilpeläinen et al. 1994), which is comparable with the ages recorded in the TSB. According to Matisto (1971, 1976a, 1976b, 1977), the plutonic rocks are younger than the surrounding schists and their age progression is from older mafic rocks via granodiorites to youngest granites and pegmatites.

In a study of the structural geology of the Valkeakoski area, Jokela (1991) divided the structural history into four major deformation phases. The intrusion of ultramafic and mafic intrusions occurred mostly before D2, but the youngest metagabbros are younger and have been folded by D3. The earliest tonalitic to quartz dioritic granitoids in the migmatite part of the area contain schist fragments devoid of migmatization and must have been intruded before D2 (middle) but later than D2 (early). The larger granodiorite massifs probably were intruded during D2 or later and possibly also during D3.

There are also undeformed granite–granodiorite stocks in the southern part of the MBd, which probably are syn-D3 intrusions. The pegmatite dykes are the youngest rocks and some of them cut across D4 structures (Jokela 1991). These features are in agreement with the few contact relations found in this study and imply an age of about 1885 Ma for some of the GG2 and GG3 main subgroup granitoids and a younger age of 1.88 Ga for the GG8 granitoids occurring in association with alkaline WPB dykes and WPB-affinity mafic plutonics in the MB. Some of the more mafic

foliated GG8 granitoids with deviation to a more DM-affinity mantle component may be of slightly older age.

The association of gabbro and primitive volcanics in the proposed suture (p. 95) can be compared with the situation in the Vammala area where, according to Peltonen (1995), older MORB-affinity metapicrites occur in association with syn-tectonic cumulate-textured intrusions. In contrast to the assimilated DM origin proposed here for MBd gabbro, which is comparable in geochemistry to cumulate bodies, Peltonen argues that the parental magma for ultramafic intrusions was broadly similar to that of arc tholeiites (cf. Fig. 19 in this study with Fig. 7 in Peltonen). The LILE enrichment with pronounced Ba depletion in his view represented "subduction zone component" closely resembling local turbidites. The subduction related rocks in the TSB are strongly enriched in Ba (p. 63) and are derived from EM, which is opposite (Ba-depletion, DM) to the enrichment and origin of the ultramafic intrusions. This supports an assimilated DM origin also for the Vammala area. U–Pb zircon and monazite ages of mafic pegmatoid from the Vammala cumulate are 1890 Ma (Häkli et al. 1979), and a similar age is proposed for the DM-affinity mafic intrusions in this study.

The granodiorites are considered to be younger than the surrounding schists and the microcline granites are the youngest rocks in the HSB (Simonen 1949, Matisto 1976). The only U–Pb zircon age from the HSB is 1886±14 Ma from Aulanko (Hämeenlinna) granodiorite (GG4) with $\varepsilon_{Nd}(t)$ of +1.9 (Patchett & Kouvo 1986). The large error in the age determination could indicate a small contribution of inherited zircons and a younger real age (≤1.88 Ga). On the basis of the observations of Simonen (1949), Neuvonen (1956) and Matisto (1976), a syn-tectonic origin is proposed for the quartz diorites, granodiorites and mafic plutonics in the HSB. Some of the mafic plutonics may in fact be older than

granodiorites (GG2 and GG4), but the con-temporaneous occurrence of mafic plutonics and granodiorites, comingling features be-tween them and the abundant occurrence of mafic enclaves in granodiorites suggest a sim-ilar age for most of the plutonics. Probably some of the mafic plutonic rocks are contem-poraneous with the Häme group. Structural interpretations suggest that the GG6 rocks, at least in the HSBa, are of slightly younger age (Jokela 1991, Hakkarainen 1994), and the GG7 rocks in the HSB are comparable to GG7 granites in the MC. A notable feature is the areal correlation between the Häme group (VG3) and GG4 granitoids, possibly related to a larger DM component in these rocks and/or to more primitive source rocks.

The foliated and gneissic granodiorites in the MC display general geochemical similar-ities with the HSB (GG2–GG4) granitoids and similar syn-tectonic ages are inferred, but the two GG4 samples forming a subgroup may be of younger age. The GG7 granitoids in the MC are comparable to other microcline granitoids of age 1.84–1.82 Ga (see age data in Korsman et al. 1984, Huhma 1986, Suominen 1991), but the possible coeval occurrence of quartz monzodiorite (1812±2 Ma, Vaasjoki 1995) and granite could indicate 1.84–1.81 Ga age for the GG7 granites. Although some elements

are slightly less enriched, the general geo-chemistry of quartz monzodiorite is compara-ble to the 'post-orogenic' Luonteri and Park-kila granitoids (see geochemical data in Nur-mi 1984, Nurmi & Haapala 1986) dated about 1.80 Ga (Patchett & Kouvo 1986, Korsman et al. 1984). The high-K_2O GG7 samples that contain a restitic component are confined to the southernmost part of the MC characterized by the gneissic granitoids and migmatites. Other high-K_2O GG7 granites occur near the MC–HSB boundary, and the very high-K_2O GG7 granites occur in the central MC where there is a lack of supracrustal inclusions, as seen in the smooth anomaly-free image in the aeromagnetic map (data not shown).

A general syn-tectonic age (1.89–1.88) is inferred for the GG2–GG4 and some GG8 granitoids. GG5–GG6 granites and the main part of the GG8 granitoids are interpreted as late- to post-tectonic rocks with an age span of 1.88–1.86 Ga. The age of the GG3 Nokia-type is unknown, but probably they date to the late- to post-tectonic stage. The age of the GG7 granites in the MB is unknown but is inferred to be less than 1.88 Ga (and perhaps less than 1.86 Ga). The GG7 granites in the MC have an age of 1.84–1.81 Ga and are (syn-) late-tectonic in relation to the 1.86–1.84 Ga colli-sion (see below).

PLATE TECTONIC IMPLICATIONS

Hietanen (1975) was the first to apply a plate tectonic model to the Svecofennides. The sequential accretion of two (see Gaál & Gorbatschev 1987) or more (see Park et al. 1984) island arcs to the north or northeast has been the basic model, but recently Gaál (1990) has revised the two-arc model to in-clude an earlier subduction stage to the west. Still more recently, Ekdahl (1993) revised Gaál's model (1986) by proposing prolonged subduction with three successive events to-wards the continental margin. Korja (1995) has presented a model for the general growth

of the Svecofennian crust and subsequent ex-tensional collapse along highly reflective, lis-tric shear zones. Lahtinen (1994a) has pre-sented a plate tectonic model covering the crustal evolution of the Svecofennian and Karelian domains during 2.1–1.79 Ga with three collisional stages at 1.91–1.90 Ga, 1.89–1.88 Ga and 1.86–1.84 Ga, where the last is probably an intracrustal stage and perhaps a continuation of the 1.89–1.88 Ga stage. Here the evolution of the study area is considered following the general lines suggested by Lahtinen (1994a).

The Haveri Formation in the TSB is considered to be a remnant of the >1.91 Ga rifting stage lying on the CFGC basement. The mantle component in the TSB and NTSB volcanics is of enriched EM type with high Ba, favouring the occurrence of attached mature crust. The available ε_{Nd} data (Patchett & Kouvo 1986, Huhma 1986, 1987), although sparse, indicate values of about +1 – +2 for the EM mantle, compared with values of -1 to +1 for granitoids and felsic volcanics. These latter values point to the presence of 2.0–2.1 Ga crust in the CFGC (including the TSB) (see also Lahtinen 1994a, Lahtinen & Huhma in press). The age of the rifting stage is bracketed by the 1.99 Ga whole-rock Pb–Pb age of the Haveri Formation (Vaasjoki & Huhma 1987) and by the maximum deposition age of 1.91 Ga of the Myllyniemi Formation based on detrital zircon data (Huhma et al. 1991). The VG1 volcanics in the MB and some of the SG2 sediments are related to this stage, while the VG1 rocks near the HSB may be related to the younger Häme group.

The MORB-affinity volcanics and spatially associated mafic/ultramafic plutonic bodies within or near to a major ductile shear/thrust (Koistinen 1994) suggests the presence of a suture. The supracrustal rocks in this zone are characterized by low S/Se ratios indicating magmatic sulphur input related to the volcanism (Lahtinen & Lestinen 1996). Further evidence for the occurrence of a suture is provided by the available detrital zircon data (Huhma et al. 1991, Claesson et al. 1993) and the compositional differences between the TSB and HSB. The samples providing detrital zircon data from areas north of the inferred suture contain only 8–14% of zircons of 2.0–2.1 Ga age, in contrast with a sample from Orijärvi (also Bergslagen) that has 58% of zircons in the age group. The HSB greywackes also differ geochemically from the TSB greywackes, probably because of a difference in the source characteristics. Arc-related volcanics and syn-tectonic granitoids in the HSB

have different geochemical and isotopic signatures from those in the TSB, indicating differences in both mantle and crustal composition and, in general a more 'primitive' environment in the HSB. The early rifting stage may be responsible for the occurrence of blastoclastic quartzite (sub-arkose), diopside gneiss and limestone in Kangasala, for the similar rocks low in the stratigraphy in the HSB and for the Tiirismaa quartzite.

The problem with the HSB volcanics is the lack of age data, especially from the lowermost Forssa group (VG5) volcanics. The Forssa group volcanics are older than 1.89 Ga and record the subduction to the south (already >1.91 Ga ?). The subsidence in the main rift stage and/or during arc reversal about 1905 Ga ago, following the collision of the western arc with the Archaean craton (Lahtinen 1994a), caused abundant erosion of the mountain belt, with the debris now seen as the lowermost conglomerates, turbiditic greywackes and massflows in the TSB and MB (SG3–SG7). The rifting produced fault-bounded attenuated crustal blocks, and the tectonically active zone (thrust, Nironen 1989b) separating the TSB and MB is interpreted as a reactivated trenchward-dipping backstop or backthrust which in the early stage separated the attenuated crust from the basement. Subduction began about 1905–1910 Ma ago to the north under the TSB with adjacent volcanism, and the sedimentary environment changed to forearc basin of mature continental island arc or ACM.

The subduction to the north under the TSB continued for only a short time span of 10–20 Ma, and during that time the volcanics under the Veittijärvi conglomerate in the TSB were formed. Some GG1 and arc-related mafic plutonics in the TSB and NTSB may belong to this stage, but the main plutonic activity occurred later. The sedimentary rocks show the occurrence of volcanic intercalation and they vary from directly arc-related (SG1) to a mixed source with older basement component

(some SG1 and SG8); in the TSB they occur in the upper part of the Myllyniemi formation. About 1895–1890 Ma ago the TSB and HSB began to collide and deformation commenced, with the rocks in the MB the first to be affected. The oceanic ridge collided under the HSB, giving rise to the early deformation phase noted in some volcanics (Jokela 1991) and causing subduction under the TSB to cease through locking of the subduction slab. At the same time, the position of the northern plate (TSB, CFGC) changed from overriding to passive underthrusting plate, subducting and colliding to the south. A tensional environment with associated fault-bounded basins was produced within the TSB and the TSB arc-related volcanics and hypabyssal intrusions were eroded to form the Veittijärvi-type conglomerates and associated SG1 sediments mainly in fluvial to shallow water environment. This tensional environment was also responsible for the mafic volcanics at Takamaa with characteristics intermediate between WPB and subduction-related magmas. The Mauri arkose is included in this stage.

During the onset of collision in the TSB, the heat and magma produced by the subducted oceanic ridge created a tensional environment under the HSB. A linear rift basin (see also Hakkarainen 1994) was formed upon sediments of mixed basement and earlier volcanic rocks (SG6 in the HSB). Initial hydrothermal activity was followed by eruption of massive tholeiitic lavas and pyroclastics (VG3) and emplacement of mafic plutonics (VG3-type). These rocks have a complex mixed origin in DM, EM and subduction components. Mixing has occurred mainly in the mantle, and the mixed melts have fractionated at the base of the crust as evident in the highly differentiated nature of the rocks. Locally the rocks have been affected by crustal contamination. At about the same time, other tholeiitic volcanics were extruded in the HSBb and HSBc (VG2). Although these volcanics also show signs of associated subduction component, the mantle

component has mainly been of EM type. The 'upper' felsic volcanics (VG6 in the HSB) are related to this stage.

The collision of the TSB and HSB continued about 1890–1880 Ma ago, a time of major plutonic activity. The compression was in approximately south-north direction, but due to inhomogeneity of the stress fields (oblique collision ?), fault-bounded crustal blocks, especially in the attenuated crust of the MB, and the occurrence of a suture in the MB produced local tensional environments allowing the intrusion of plutonic rocks (transpression ?). It is not clear whether tensional fractures, pull-apart basins or en-echelon "P-shear" tensional bridges (e.g. Tikoff & Teyssier 1992) were responsible for the opening of space for granitoids, but some mechanism was needed to allow the final passive emplacement of the Hämeenkyrö and Värmälä plutons (Nironen 1989a) in an overall compressional environment. Perhaps the MB experienced strong deformation and crustal shortening between rigid basement blocks because of the occurrence there of a less resistant zone of small fault-bounded, attenuated crustal blocks with abundant sediment cover. Thus, the deformation history began earlier in the MB than the TSB (see Kilpeläinen et al. 1994), was more complex in nature due to the inhomogeneity of the block structure, and continued longer because of the lesser rigidity.

During the early and main collision stages, large amounts of mantle-derived magmas were intruded in the deeper parts of the crust. The first melts were the end result of subduction processes producing water-rich magmas with arc-related signatures, which ponded in the deeper parts of the crust. The crystallization of these magmas, accompanied by the release of fluids, caused vapour-phase-present melting of mafic to intermediate crustal rocks which mixed and homogenized at deep crustal levels. Subsequently, in the absence of subduction component (more anhydrous conditions), mantle-derived magmatism

changed to more WPB-type with less melting. This affected the composition of the ponded mixed magmas and is seen in the abundant comingling features (hybrid rocks) at the present crustal level. The abundant mantle magmatism during the syn- to late-tectonic stage could be the result of lithospheric thickening, followed by upwelling of the thermal boundary and leading to magmatic underplating and high heat flow (Lahtinen 1994a, see also Korja 1995). The continuous magmatic activity and heat flow from the mantle raised the temperature of the crust, now anhydrous due to the earlier vapour-phase-present melting event, and both the WPB underplate and crustal rocks underwent vapour-phase-absent melting, with production of the GG5–GG6 and some GG8 rocks, probably in neutral to extensional environment, about 1.88–1.86 Ga ago.

Convective removal of the lowermost lithosphere should cause a rapid increase in surface elevation and in potential energy leading to extension (e.g. Platt & England, 1993). The occurrence of these 1.88–1.86 Ga granitoids presumably is related to the onset of extension and orogenic collapse. On the other hand, the occurrence of thick crust in the area precludes large-scale extension leading to thinned lithosphere and indicates that overall compressive tectonics were present during the extension. This would suggest that the onset of extension within a setting of overall steady plate convergence leads to increase in compressional stress at the margins of the area of greatest increase in potential energy (thickest crust). This is one possible model for the 1.86–1.84 Ga thrusting event (see below).

The differences between areas are due to differences in crustal and mantle components, but preliminary data suggest that the EM component was of constant composition between about 1.88 and 1.80 Ga ago (Lahtinen 1994b, this study). The melting of crustal rocks in the NTSB may have begun at intracrustal levels, and GG5 granites were formed from preexist-

ing igneous rocks. The GG4 granitoids in the NTSB appear to have solidified from a melt derived from a more 'primitive' source than that of the GG5 granites, and they may be of about the same age or slightly older. Melting of the WPB underplate is proposed as the source of the intermediate GG6 rocks, though differentiation cannot be excluded. Some silicic GG6 granites, especially the granites from Koppelojärvi, also include a crustal component. The Nokia and Siitama plutons have originated in WPB magmas inputted through the main fault zone and the engulfed sedimentary rocks. The main mixing event has occurred deeper in the crust. An important feature is the lack of sediment-assimilated granitoids north of these plutons, indicating the predominance of igneous crust beneath the TSB and NTSB and favouring the proposed backstop origin for the main thrust/fault dividing the MB and TSB.

The DM-affinity mafic plutonics in the MB may be of initial collision age, or they may date to the main collisional stage. In any event, they show the occurrence of DM and have been emplaced in local tensional sites partly coinciding with the suture and block boundaries. During the main collision, large amounts of EM melts intruded the base of the MB crust. The fractionated melts then intruded, partly through block faults, to above sedimentary rocks to produce assimilated mafic plutonics and GG8 granitoids with continuous mixing of different components. At about the same time, or earlier, the GG2–GG4 granitoid melts intruded the MB derived at least in part from pre-existing igneous rocks. These melts, mixed and comingled with WPB magmas, and they often have a strong assimilated sediment component. In later stages, the WPB magmatism changed to a more alkaline affinity. At the same time, the major part of the GG8 and possibly also some GG2–GG4 granitoids intruded. Belonging to this stage are the rocks in the northeasterly directed lineament dividing the MBa and MBb (Fig. 2), the Kylmäkoski

coarse-grained granitoids in the MBc and the associated mafic rocks in southeastern direction, and possibly also the major part of the large granitoid complexes in the MBb. GG7 rocks in the MB are related either to later stages of this collision or to the 1.86–1.84 Ga collision (see below).

During the collision event 1890–1880 Ma ago, the situation in the HSB was similar to that in the TSB and NTSB, but the more 'primitive' mantle and crustal sources produced geochemical differences. The GG6 granitoids in the HSBb show more crustal source than the intermediate GG6 granites in the NTSB. The foliated and gneissic calc-alkaline granitoids of the MC are correlated with similar rocks in the HSB at about 1.88 Ga age. Some granitoids of tholeiitic affinity may be slightly younger.

The 1.86–1.84 Ga collision (Lahtinen 1994a, references therein) probably was of intracrustal origin as there is no evidence to indicate a suture between the HSB and areas to the south (but see Edelman & Jaanus-Järkkälä 1983). The MC is part of the late Svecofennian granite–migmatite (LSGM) zone of Ehlers et al. (1993), which is a distinct tectonic unit of crustal thickening showing strong deformation coupled with high-grade metamorphism and intrusion of 1.84–1.83 Ga old granite sheets during transpressional deformation. Väisänen et al (1994) suggest that older structures have been deformed by the main regional folding F3 (<1.87 Ga) and, at least in part, are associated with a new or prolonged episode of thrusting. The deformation continued, with 1.83 Ga magmatism, in late-D3 extensional shear zones which were tentatively correlated with the first generation listric shear zones recorded in seismic reflection studies. According to Korja & Heikkinen (1995), these listric shear zones use the boundary between the middle and lower crust as detachment and may record the extensional collapse of the overthickened crust.

Erosion and cooling, at least locally, to about 500°C and the declining magmatic activity to 1.86 Ga (see discussion in Lahtinen 1994a) might indicate slight cooling in the upper crust, but the situation in deeper parts of the crust could have been different, with both advective and conductive heat flow from the mantle to the mainly infertile lower crust. The important question is the timing of the 1.86–1.84 Ga (1.87–1.83 Ga) thrusting: was it a continuous collision or did it occur in a restricted time period preceded by a period of neutral to extensional regime. The GG7 granites in the MC related to this stage are derived from a mainly anhydrous (fluid loss) psammitic or layered source by vapour-phase-absent melting at middle to upper crustal levels. Typically these are restite-poor rocks, where the lower temperature variants (high-K_2O) occurring near HSB contacts probably have been the first to intrude. The restite-bearing variants occur in association with migmatites and gneissic granitoids and may be of more local derivation.

Psammitic rocks are fertile rocks, which produce large amounts of melts at 800–900°C and below 7 kbar (Vielzeuf & Montel 1994). Hölttä (1986) reports about 5 kbar pressures in migmatites from comparable areas SW of the MC and this pressure estimate is adopted for the MC. The very high-K_2O GG7 granites give indication of slightly higher melting temperatures associated with a small amount of CO_2 and saline fluid. One possible source for these fluids is the alkaline WPB magmas. The occurrence of very high-K_2O GG7 granites in the middle parts of the MC, the lack of other rock types, the undeformed nature, the possible association with 1812 Ma quartz monzodiorite and the higher predicted melting temperatures could indicate younger intrusion ages of about 1.82–1.81 Ga for these granites. The large magnetic anomaly in approximately northeast direction in the southwest part of the MC, associated with porphyritic magnetite-bearing undeformed granite enriched in P,

Sr, La and Zr, together with the high total contents of La, P and Sr in regional till data (not shown), may indicate a greater amount of enriched-type granitoids (WPB-related) in this area.

Tectonic thickening cannot alone explain the rise of metamorphic temperature in this belt; other heat sources are needed (e.g. Korsman & Kilpeläinen 1986). The prolonged high heat flow from the mantle and the highly radiogenic heat production within earlier granitoids have promoted melting (Lahtinen 1994a) with possible additional advective heat derived from mantle-derived magmas. At least some of these granites are associated with late-D3 and listric shear zones (Väisänen et al. 1994, Korja & Heikkinen 1995) and may have been formed through decompression melting in association with dilatancy pumping along crustal-scale shear zones/fault systems (Brown 1994, Pitcher 1993).

DISCUSSION AND CONCLUSIONS

The origin and evolution of the different rock types have been discussed above, leaving a need here only for some general conclusions. The sedimentary rocks in the study area were divided into basement-related and arc-related groups, with the basement-related group characterized by more weathered source, higher Th/U (recycled), enrichment in Cr and Ni and depletion of Ba. The high levels of both felsic- and mafic-source-related elements in the basement-related rocks favour a bimodal source, characterized by a komatiite component (Archaean), to account for the high Cr and Ni. Although an average source dominated by bimodal rocks can offer some explanation of the high Th, Sc and Cr, a quartz depletion in the source area is required in addition. Jatulian quartzites are one possible sink. The depletion of barium is mainly due to its loss from terrigenous sediments during weathering and diagenesis, with subsequent enrichment in pelagic sediments and inclusion in enriched mantle (EMI) component.

Arc-related sedimentary rocks in the Tampere Schist Belt (TSB) and Mica gneiss–migmatite Belt (MB) clearly differ from the basement-related sedimentary rocks and have a chemical composition approaching the TSB volcanics. The wide variation in chemical composition and low degree of weathering indicate rapid erosion of arc material and subsequent deposition in arc-related basins without any strong mixing in large river-delta systems. Although the distinction between these groups is normally clear, some greywackes exhibit mixed characteristics.

The results of this study have been evaluated through comparison with those of Kähkönen & Leveinen (1994) for the central TSB. Although the different sampling and analytical techniques do not allow a direct comparison, our sedimentary groups SG3–SG5 can in general be correlated with the rocks of the Myllyniemi formation, and the SG1 rocks resemble the uppermost volcanics-associated formations. The occurrence of SG3–SG5 and also SG1 rocks not only in the TSB but in the MB, especially in the central and northern parts, suggests a common evolution for these two areas. Greywackes in the Hämeenlinna Schist Belt (HSB) display a more mature nature with high Cr, indicating either more Archaean detritus or heavy mineral enrichment (fine-grained chromite).

The results of the present study are in general accord with the results of Kähkönen (1987, 1989, 1994) and Kähkönen & Nironen (1994) for the TSB volcanics, and those of Hakkarainen (1994) for the HSB volcanics. The mantle characteristics and crustal evolution in these areas have been considered. The rocks of the TSB and HSB exhibit different

characteristics: whereas the TSB volcanics show dominant high-K to very high-K calc-alkaline to shoshonitic nature with abundant andesitic rocks, the HSB older volcanics (Forssa group) show dominant medium-K calc-alkaline nature with fewer andesites. In both areas there is indication of EM and mature crust, but the higher K, Th, Sr, La, P, Th/U, and high Ba relative to K_2O in the TSB indicate more enriched mantle component (EMI) and probably thicker crust as well. Although partially indirect, the geochemical and isotopic data suggest an older (2.0–2.1 Ga) and more mature crust underlying the TSB and the North of TSB (NTSB) belonging to the Central Finland Granitoid Complex (GFGC)(see also Lahtinen 1994a, Lahtinen and Huhma in press). The higher Th, producing higher Th/U ratios in the TSB volcanics, remains somewhat problematic since the younger EM-derived mafic plutonics have lower Th/U ratios.

The Hirsilä Schist Belt (HiSB) in the NTSB shares geochemical features with the TSB suggesting a similar evolution history. Mid Ocean Ridge Basalt (MORB)-affinity volcanics and spatially associated Depleted Mantle (DM)-affinity assimilated plutons suggest the existence of a suture in the MB. To account for the observed geochemical characteristics, the origin of the linear rift Häme group volcanic rocks (VG3) is tentatively attributed to ridge subduction and mixing of DM, EM and a subduction component. The close association that Neuvonen (1956) suggested between the Häme group volcanics and certain mafic plutonics is supported by the comparable geochemical data of the VG2 and VG3 volcanic rocks and mafic plutonics.

Nurmi & Haapala (1986) argue that subduction-related mantle magmas acted as indirect and direct sources of syn-kinematic (syn-tectonic) I-type granitoids, with the granitoids in the CFGC representing deeper levels of the crust. Front & Nurmi (1987) in turn proposed a partial melting model of igneous material for the syn-kinematic granitoids, in which the tonalitic rocks in schist belts were derived from a basaltic source, whereas the granodiorites and granites were the result of different magma pulses and the melting of more crustal meta-igneous material and/or differentiation lower in the crust. The granitoids in the CFGC were attributed to a lower degree of melting of thicker crust. Nironen (1989a) proposed that repeated mixing and mingling of crustal magma with mantle-derived magma, or with magma derived from partial melting of a subducted oceanic slab, together with partial melting and/or assimilation of crustal rocks, were responsible for the generation of different granitoids. The interpretations of Lahtinen (1994a) are largely parallel, suggesting derivation of the syn-tectonic tonalites in the Savo Schist Belt (SSB) from primitive island arc rocks. On the other hand, the great crustal thickness in the SSB has been interpreted as collision induced and this means that the main difference between the SSB and CFGC is not the crustal thickness during the melting event but the more evolved source rocks in the CFGC (ibid.).

The syn-tectonic granitoids in the TSB and NTSB are dominated by high-K calc-alkaline metaluminous to slightly peraluminous granodiorites with abundant mafic enclaves and local comingling features producing hybrid rocks. At least three endmembers, occurring in different proportions, are needed to account for the compositional variations: 1) calc-alkaline intermediate melt, 2) silicic crustal melt and 3) WPB-affinity mantle-derived magma. Arc-related mafic plutons and more mafic granodiorites require a contribution from arc-related calc-alkaline magma, whereas the geochemical differences between granitoids and volcanics call for the occurrence of a crustal-derived silicic melt. Interaction and possibly mixing have occurred deep in the crust and the composition of this crustal endmember is thus poorly defined. A vapour-phase-present melting of a mainly intermediate igneous source is tentatively considered the most dominant

source for the crustal silicic endmember producing high-K granodiorites, while a more mafic crustal source is required for the few medium-K granodiorites in the NTSB. A change in the composition of mantle melts to Within Plate Basalt (WPB) affinity indicates lower degrees of mantle melting under more anhydrous conditions. These mantle melts have interacted with the calc-alkaline and crustal melts, possibly producing a mixed component in deeper parts of the crust. The abundant hybrid rocks are due to interaction of the mafic and more silicic melts in the studied intrusion level.

Similar situations characterize the MB, HSB and Microcline granite Complex (MC) where the more silicic granodioritic endmembers are present in addition. The differences between the mantle and crustal components in the HSB and the TSB+NTSB are seen as lower K, Rb, La, Th and U in the HSB granitoids, consistent with similar features found in volcanics. Tonalites are largely lacking in the MB, but some granodiorites are of low-K type and close to tonalitic composition. They show assimilated features and may in part be derived from greywackes or from a layered greywacke-igneous source, but the geochemistry requires an igneous component in most cases.

Late- to post-tectonic granites in the NTSB coincide with a regional magnetic high and fall into high-K and very high-K groups. The composition of these rocks indicates more anhydrous melting conditions, and a mainly vapour-phase-absent melting of an intermediate tonalitic to granodioritic source is proposed for the high-K granites. The less silicic very high-K granites are alkaline to nearly alkaline rocks with high FeO/MgO, Zr, Ba, K/Rb and Nb/Th, and they are related to WPB through differentiation or melting of the mafic underplate. The lack of rocks in the silica range 54–66% argues the latter, melting model, and the high Zr indicates high-temperature vapour-phase-absent melting as well as high intrusion temperatures. The occurrence of orthoclase-

and pyroxene in the marginal phase of one pluton points to dry conditions. The more silicic granites have lower Ba, higher Rb and F, and variable Th, Y, and Zr, requiring the occurrence of a more crustal component as well. In general, the late- to post-collisional granites in the HSB have a more crustal-like source, seen, for example, in low K/Rb and higher Th and U with more peraluminous nature.

The MB is characterized by abundant occurrence of granitoids (GG8) that have a close genetic link with alkaline WPB dyke rocks and WPB-affinity mafic plutonics. The granitoids are peraluminous over a wide silica range, with high S, Te, As, Bi and local graphite derived from an assimilated sedimentary component. They are interpreted to have originated through mixing of WPB melts in different proportions with an assimilated sediment component, and partly also with crustal derived melts. The assimilation/interaction with sediments in many cases has occurred under disequilibrium conditions, leaving restitic zircon. Similar rocks intrude the sediments in the TSB (GG3 Nokia-type) and most of them are included in the late- to post-tectonic group. An important feature is that most of the granitoids in the MB have a large mantle-derived component associated with the ubiquitous sediment assimilation component. Another important feature is that these assimilation features are not found in granitoids from the northern part of the TSB or from the NTSB, suggesting the absence of voluminous sedimentary rocks beneath these areas.

The age of the younger GG7 granites in the MB is unknown, but a general age less than 1.88 Ga (<1.86 Ga) is inferred. Some of these granites may have originated in vapour-phase-present melting of sedimentary rocks, but vapour-phase-absent melting is presumed be the more normal course.

The microcline granites in the MC belong to the 1.84–1.81 Ga belt of 'late-kinematic' granites. Partial melting (S-type) and granitization of supracrustal rocks have been pro-

posed for their origin (Nurmi & Haapala 1986 and references therein). Although a granitization origin cannot be ruled out for a few restite-bearing samples, the restite-poor nature of most samples, with clear compositional differences from sedimentary rocks, favours a partial melting origin. A sedimentary psammitic or layered pelite-igneous source is needed to account for the elevated Na_2O and CaO in the MC granites, but a more pelitic source is possible for the few restite-bearing granites occurring in association with migmatites. A characteristic feature is the loss of fluid phase (Au, As, Bi, Sb, Cs), also noticed to some extent in the migmatites, before the onset of mainly vapour-phase-absent melting. The MC granites can be divided into high-K_2O and very high-K_2O groups, where higher TiO_2, Zr, La, Th and U of the latter indicate higher melting temperatures, and the higher Cl and CO_2 suggest the presence of a small amount of fluid, possibly water-poor. The very high-K_2O rocks are confined to the central area of the MC and may be slightly younger than the high-K_2O rocks mostly located near the boundary with the HSB. Low Ba in most GG7 granites indicates the occurrence of K-feldspar in the source residue, and the lower Y and higher La/Y ratios in the MC indicate a greater amount of garnet in the source residue and melting at higher pressures than in the MB.

The problem in the syn- to post-tectonic classification of granitoids is in part related to the palaeodepth of intrusion and brittle-ductile transition, and granites of similar ages may thus exhibit both syn- and post-tectonic features (e.g. Brown 1994). Most of the granitoids considered here as syn-tectonic (syn-collision) were intruded during local D2 preceded by crustal thickening during D1 (Kilpeläinen et al. 1994) and possibly also by pre-D1 structures related to early thrusting (Koistinen et al. in press). Although these granitoids could thus also be described as late- to post-collision granitoids relative to the main crustal thickening, here they are

called syn-tectonic because they have been affected by the latest phases of collision, regardless of whether these phases were transpressional or purely extensional and related to orogenic collapse. The division between syn- and late- to post-tectonic granitoids is also gradational depending on what type of extensional domain characterized their intrusion site and whether they were further deformed in the same or a later deformation event. This classification is further complicated by the 1.84–1.81 Ga microcline granites in the southern belt, which may show syn-tectonic and late-tectonic features relative to the 1.86–1.84 Ga collision, but are either late- or post-tectonic in nature relative to the 1.89–1.88 Ga collision.

Some plate tectonic implications can also be suggested following the lines laid down in a previous paper (Lahtinen 1994a). Rifting occurring before 1.91 Ga is exemplified by the volcanics of the Haveri formation (see also Kähkönen & Nironen 1994) and possibly by the sporadic sub-arkoses associated with limestones. Subduction began in the south, and the 1.91–1.90 Ga collision further to the northeast (Lahtinen 1994a) produced abundant debris in the TSB and the northern part of the MB. This collision was followed by subduction reversal, and a short-lived subduction to the north, under the TSB, commenced at 1905 Ga. The ridge subduction was responsible for the Häme group volcanics and possibly for the earliest deformation noted by Jokela (1991). During the initial stages of collision, extensional fault bounded basins associated with high-Ti upper Takamaa volcanics and abundant SG1 sedimentation were formed within the TSB.

Thrusting of hydrous rocks and the ponding of water-rich subduction-related magmas in the lower and middle crust during the main collision stage, together with subsequent magmatic underplating (WPB), produced vapour-phase-present melting and tonalitic migmatization at 1.89–1.88 Ga. The tonalitic leu-

cosomes are due to in situ melting and/or to subsolidus leucosomes formed through the mobilization of quartz and feldspars from the host rock by pressure solution during tectonic stresses (e.g. Sawyer & Barnes 1988). High Cl in migmatites argues for the occurrence of abundant aqueous fluid during migmatization as proposed by Kilpeläinen et al. (1994). The fluid circulation, thrusting of magmatically heated island arc crust and the occurrence of abundant mantle-derived magmatism are considered the viable heat sources. Peak metamorphic temperatures at 670°C and 5–6 kbar in the MB (Kilpeläinen et al. 1994) were probably buffered by the vapour-phase-present melting of sedimentary rocks. The lower crust temperatures may have been 800–900°C if a small amount of melting of mafic to intermediate metaigneous source can be assumed. Thus, the heat distribution in the crust was irregular, and conductive heat flow dominated in the lower crust, in contrast to the advective heat flow associated with fluid circulation in the thick (Lahtinen & Korhonen 1996) sedimentary pile in the MB that then formed the middle crust. The middle and upper crust of the NTSB lacked a thickened water-rich sedimentary pile and thus the heating in this area was mainly due to conductive heat flow from the mantle and to advective heat from magmas. The lack of voluminous fluid circulation and the insulating effect of the crust may have resulted in slower temperature increase in the NTSB upper and middle crust than in the MB.

The continuous magmatic activity and high heat flow from the mantle, combined with the more anhydrous conditions in the mantle and the lower and middle crust due to the lack of fluid input (no subduction) and to the occurrence of preceding melting events, promoted vapour-phase-absent melting at higher temperatures (900–1000°C) in the lower and middle crust of the NTSB. This led to formation of the 1.88–1.86 Ga late- to post-tectonic granites. Some orthopyroxene-bearing granitoids in the MB suggest a derivation from anhydrous low-

er crust, but the middle and upper crust in the MB probably was still hydrous, at least in part, suggesting a longer episode of drying for the MB than for the NTSB.

Prolonged conductive and partly advective heat flow from the mantle and radiogenic heat production are considered responsible for the large-scale vapour-phase-absent melting of anhydrous greywacke and/or layered pelite-igneous source rocks (escaped fluid phase; loss of C, S and B in migmatites) in the middle and upper crust (about 6–7 kbar and 800–900 °C) and formation of the restite-free 1.84–1.81 Ga granites. This melting was preceded by intracrustal thickening and possibly, at least in the case of restite-free high-temperature melts, was associated with decompression during extensional collapse (Korja & Heikkinen 1995), The restite-bearing granites closely associated with migmatites and the granitic leucosomes in migmatites are of more local derivation and related to a lower degree of melting of a more pelitic source, also at lower temperatures (e.g. Korsman 1977). A notable feature is the gain in Cl, F and possibly Rb in the MC granitic migmatites suggesting the occurrence of an external fluid phase, at least locally. The intrusion of 'post-orogenic' magmatism is related to the extensional stage at 1.82–1.80 Ga.

The results of this study show that a regional rock geochemical study encompassing all rock types can provide valuable information on geological and geochemical processes. Regional differences and similarities in geochemistry, petrogenesis and areal distribution of different rock types and the groups within them can be used in the delineation of the areas. Many important rocks units are not, of course, sampled by this method, and many critical geological boundaries are either very thin or internally complex. Fortunately, many detailed thematic geochemical studies and studies on stratigraphy, metamorphism, structure, isotope composition and age had been made in the study area, providing a ready framework for our work. Incorporation of

these earlier findings made it possible to characterize schist belts and the associated plutonic rocks according to their different evolution stages. The results clearly demonstrate the usefulness of this type of approach in studying the geochemical and geological evolution of the Fennoscandian Shield.

ACKNOWLEDGEMENTS

REFERENCES

Allégre, C.J. & Turcotte, D.L. 1985. Geodynamic mixing in the mesosphere boundary layer and the origin of oceanic islands. Geophysical Research Letters 12, 207–210.

Anderson, D.L. 1994. The sublithospheric mantle as the source of continental flood basalts; the case against the continental lithosphere and plume head reservoirs. Earth and Planetary Science Letters 123, 269–280.

Aro, K. & Laitakari, I. 1987. Oriveden seudun Svekofenninen mafinen juoniparvi – Svecofennian dyke swarm in Orivesi. In: Aro, K. & Laitakari, I. (Editors), Suomen diabaasit ja muut mafiset juonikivilajit – Diabases and other mafic dyke rocks in Finland. Geological Survey of Finland, Report of Investigation 76, 85–89.

Arzi, A.A. 1978. Critical phenomena in the rheology of partially melted rocks. Tectonophysics 44, 173–184.

Baker, M.B., Grove, T.L. & Price, R. 1994. Primitive basalts and andesites from the Mt. Shasta region, N. California: products of varying melt fraction and water content. Contributions to Mineralogy and Petrology 118, 111–129.

Beard, J.S., Abitz, R.J. & Lofgren G.E. 1993. Experimental melting of crustal xenoliths from Kilbourne Hole, New Mexico and implications for the contamination and genesis of magmas. Contributions to Mineralogy and Petrology 115, 88–102.

Beard, J.S., Lofgren, G.E., Krishna Sinha, A. & Tollo, R.P. 1994. Partial melting of apatite-bearing charnockite, granulite, and diorite: Melt compositions, restite mineralogy, and petrological implications. Journal of Geophysical Research 99, 21591–21603.

Ben-Avraham, Z., Nur, A. Jones, D. & Cox, A. 1981. Continental accretion: from oceanic plateaus to allochthonous terranes. Science 213, 47–54.

Ben Othman, D., White, W.M. & Patchett, J. 1989. The geochemistry of marine sediments, island arc magma genesis, and crust–mantle recycling. Earth and Planetary Science Letters 94, 1–21.

Bhatia, M.R. 1983. Plate tectonics and geochemical composition of sandstones. The Journal of Geology 91, 611–627.

Bhatia, M.R. & Crook, K.A.W. 1986. Trace element characteristics of greywackes and tectonic setting discrimination of sedimentary basins. Contributions to Mineralogy and Petrology 92, 181–193.

Blatt, H., Middleton, G. & Murray, R. 1980. Origin of sedimentary rocks. Second edition. New-Jersey: Prentice-Hall. 782 p.

Bloomfield, A.L. & Arculus, R.J. 1989. Magma mixing in the San Francisco Volcanic Field, AZ. Contributions to Mineralogy and Petrology 102, 429–453.

Brandon, A.D., Hooper, P.R., Goles, G.G. & Lambert, R. St.J. 1993. Evaluating crustal contamination in continental basalts: the isotopic composition of the Picture Gorge Basalt of the Columbia River Basalt Group. Contributions to Mineralogy and Petrology 114, 452–464.

Breit, G.N. & Wanty, R.B. 1991. Vanadium accumulation in carbonaceous rocks: A review of geochemical controls during deposition and diagenesis. Chemical Geology 91, 83–97.

Brophy, J.G. 1990 Andesites from northeastern Kanaga Island, Aleutians. Contributions to Mineralogy and Petrology 104, 568–581.

Brown, M. 1994. The generation, segregation, ascent and emplacement of granite magma: the migmatite-to-crustally-derived granite connection in thickened orogens. Earth-Science Reviews 36, 83–130.

Burnham, C.W. 1967. Hydrothermal fluids at the magmatic stage. In: Barnes, H.L. (ed.) Geochemistry of hydrothermal ore deposits. New York: Holt, Reinhart & Winston, 38–76.

Burnham, C.W. 1979. The importance of volatile constituents. In: Yoder, H.S. (ed.) The evolution of igneous rocks (Fiftieth anniversary perspectives). Princeton: Princeton Univ. Press, 439–482.

Campbell, D.S. 1980. Structural and metamorphic development of migmatites in the Svecokarelides, near Tampere, Finland. Transactions of Royal Society Edinburgh, Earth Science 71, 185–200.

Carlson, R.W. 1991. Physical and chemical evidence on the cause and source characteristics of flood basalt volcanism. Australian Journal of Earth Sciences 38, 525–544.

Castro, A., Moreno-Ventas, J. & De la Rosa, J.D. 1991. H-type (hybrid) granitoids: a proposed revision of the granite-type classification and nomenclature. Earth-Science Reviews 31, 237–253.

Chase, C.G. 1981. Oceanic island Pb: Two-stage histories and mantle evolution. Earth and Planetary Science Letters 52, 277–284.

Chappel, B.W. & White, A.J.R. 1984. I- and S-type granites in the Lachlan Fold Belt, southeastern Australia. In: Keqin, X. & Guanchi, T. (eds.) Geology of granites and their metallogenic rela-

tions. Beijing: Science Press, 87–101.

Claesson, S., Huhma, H., Kinny, P.D. & Williams, I.S. 1993. Svecofennian detrital zircon ages - implications for the Precambrian evolution of the Baltic Shield. Precambrian Research 64, 109–130.

Clemens, J.D. 1990. The granulite–granite connexion. In: Vielzeuf, D. and Vidal, Ph. (eds.) Granulites and crustal evolution. Dordrecth: Kluwer, 25–36.

Condie, K.C. 1993. Chemical composition and evolution of the upper continental crust: Contrasting results from surface samples and shales. Chemical Geology 104, 1–37.

Condie, K.C. & Wronkiewicz, D.J. 1990. The Cr/Th ratio in Precambrian pelites from the Kaapvaal Craton as an index of craton evolution. Earth and Planetary Science Letters 97, 256–267.

Conrad, W.K., Nicholls,. I.A. & Wall, V.J. 1988. Water-saturated and -undersaturated melting of metaluminous and peraluminous crustal compositions at 10 kb: Evidence for the origin of silicic magmas in the Taupo volcanic zone, New Zealand, and other occurrences. Journal of Petrology 29, 765–803.

Cousens, B.L., Allan, J.F. & Gorton, M.P. 1994. Subduction-modified pelagic sediments as the enriched component in back-arc basalts from the Japan Sea: Ocean Drilling Program Sites 797 and 794. Contributions to Mineralogy and Petrology 117, 421–434.

De Paolo, D.J. 1981. A neodymium and strontium isotopic study of the Mesozoic calc-alkaline granitic batholiths of the Sierra Nevada and Peninsular Ranges, California. Journal of Geophysical Research 86, 10470–10488.

Dickinson, W.R. & Suczek, C.A. 1979. Plate tectonics and sandstone compositions. American Association of Petrology and Geology, Bulletin 63, 2164–2182.

Eberz, G.W. & Nicholls, I.A. 1990. Chemical modification of enclave magma by post-emplacement crystal fractionation, diffusion and metasomatism. Contributions to Mineralogy and Petrology 104, 47–55.

Edelman, N. & Jaanus-Järkkälä, M. 1983. A plate tectonic interpretation of the Precambrian of the archipelago of SW Finland. Geological Survey of Finland, Bulletin 325. 33 p.

Ehlers, C., Lindroos, A. & Selonen, O. 1993. The late Svecofennian granite–migmatite zone of southern Finland – a belt of transpressive deformation and granite emplacement. Precambrian Research 64, 295–309.

Ekdahl, E. 1993. Early Proterozoic Karelian and Svecofennian formations and the evolution of the

Raahe–Ladoga ore zone, based on the Pielavesi area, central Finland. Geological Survey of Finland, Bulletin 373. 137 p.

Front, K. 1981. Hämeenkyrön batoliitin litogeokemia, kivilajit ja suhde ympäröiviin liuskeisiin. Unpublished master's thesis, University of Helsinki, Department of Geology. 59 p.

Front, K. & Nurmi, P.A. 1987. Characteristics and geological setting of synkinematic Svecokarelian granitoids in southern Finland. Precambrian Research 35, 207–224.

Furman, T. & Spera, F.J. 1985. Co-mingling of acid and basic magma with implications for the origin of mafic I-type xenoliths: Field and petrochemical relations of an unusual dike complex at Eagle Lake, Sequoia National Park, California, USA. Journal of Volcanology and Geothermal Research 24, 151–178.

Gaál, G. 1986. 2200 million years of crustal evolution. The Baltic Shield. Bulletin of the Geological Society of Finland 58, 149–168.

Gaál, G. 1990. Tectonic styles of early Proterozoic ore deposition in the Fennoscandian shield. Precambrian Research 46, 83–114.

Gaál, G. & Gorbatschev, R. 1987. An outline of the Precambrian evolution of the Baltic Shield. Precambrian Research 35, 15–52.

Gill, J. 1981. Orogenic andesites and plate tectonics. Berlin: Springer-Verlag. 390 p.

Green, T.H. & Pearson, N.J. 1987. An experimental study of Nb and Ta partitioning between Ti-rich minerals and silicate liquids at high pressure and temperature. Geochimica Et Cosmochimica Acta 51, 55–62.

Griffiths, R.W. & Campbell, I.H. 1990. Stirring and structure in mantle plumes. Earth and Planetary Science Letters 99, 66–78.

Häkli, T.A., Vormisto, K. & Hänninen, E. 1979. Vammala, a nickel deposit in layered ultramafite, southwest Finland. Economic Geology 74, 1166–1182.

Hakkarainen, G. 1994. Geology and geochemistry of the Hämeenlinna–Somero volcanic belt, southwestern Finland: a Paleoproterozoic island arc. In: Nironen, M. & Kähkönen, Y. (eds.) Geochemistry of Proterozoic supracrustal rocks in Finland. Geological Survey of Finland, Special Paper 19, 85–100.

Hämäläinen, A. & Vaasjoki, M. 1991. Geochronological map of Southern Finland. Geological Survey of Finland.

Harris, N.B.W. & Inger, S. 1992. Trace element modelling of pelite–derived granites. Contributions to Mineralogy and Petrology 110, 46–56.

Hawkesworth, C.J. & Ellam, R.M. 1989. Chemical fluxes and wedge replenishment rates along re-

cent destructive plate margins. Geology 17, 46–49.

Hawkesworth, C.J. & Gallagher, K. 1993. Mantle hotspots, plumes and regional tectonics as causes of intraplate magmatism. Terra Nova 5, 552–559.

Hawkesworth, C.J., Hergt, J.M., McDermott, F & Ellam, R.M. 1991. Destructive margin magmatism and the contributions from the mantle wedge and subducted crust. Australian Journal of Earth Sciences 38, 577–594.

Hawkesworth, C.J., Gallagher, K., Hergt, J.M. & McDermott, F. 1994. Destructive plate margin-magmatism: Geochemistry and melt generation. Lithos 33, 169–188.

Helz, R.T. 1976. Phase relations of basalts in their melting at P_{H2O}= 5 kb. Part. II. Melt compositions. Journal of Petrology 17, 139–193.

Hietanen, A. 1975. Generation of potassium-poor magmas in the northern Sierra Nevada and the Svecofennian of Finland. Journal of Research U.S. Geological Survey 3, 631–645.

Hildreth, W. & Moorbath, S. 1988. Crustal contributions to arc magmatism in the Andes of Central Chile. Contributions to Mineralogy and Petrology 98, 455–489.

Hogan, J.P. & Sinha, A.K. 1991. The effect of accessory minerals on the redistribution of lead isotopes during crustal anatexis: A model. Geochimica Et Cosmochimica Acta 55, 335–348.

Holden, P., Halliday, A.N., Stephens, W.E. & Henney, P.J. 1991. Chemical and isotopic evidence for major mass transfer between mafic enclaves and felsic magma. Chemical Geology 92, 135–152.

Hollow, J.R. & Burnham, C.W. 1972. Melting relations of basalt with equilibrium water pressure less than total pressure. Journal of Petrology 13, 1–29.

Hölttä, P. 1986. Observations on the metamorphic reactions and PT conditions in the Turku granulite area. In: Korsman, K. (ed.) Development of deformation, metamorphism and metamorphic blocks in eastern and southern Finland. Geological Survey of Finland, Bulletin 339, 43–58.

Holtz, F. & Johannes, W. 1991. Genesis of peraluminous granites I. Experimental investigation of melt compositions at 3 and 5 kb and various H_2O activities. Journal of Petrology 32, 935–958.

Huhma, H. 1986. Sm–Nd, U–Pb and Pb–Pb isotopic evidence for the origin of the early Proterozoic Svecokarelian crust in Finland. Geological Survey of Finland, Bulletin 337. 48 p.

Huhma, H. 1987. Provenance of early Proterozoic and Archaean metasediments in Finland: a Sm–Nd isotopic study. Precambrian Research 35, 127–143.

Huhma, H., Claesson, S., Kinny, P.D. & Williams, I.S. 1991. The growth of Early Proterozoic crust: new evidence from Svecofennian zircons. Terra Nova 3, 175–179.

Ingersoll, R.V. 1988. Tectonics of sedimentary basins. Geological Society of America, Bulletin 100, 1704–1719.

Irvine, T.N. & Baragar, W.R.A. 1971. A guide to the chemical classification of the common volcanic rocks. Canadian Journal of Earth Sciences 8, 523–548.

Jokela, J. 1991. Valkeakosken alueen kallioperän integroitu rakennetulkinta. Unpublished master's thesis, University of Turku, Department of Geology. 88 p.

Johnston, A.D. & Wyllie, P.J. 1988. Interaction of granitic and basic magmas: experimental observations on contamination processes at 10 kbar with H_2O. Contributions to Mineralogy and Petrology 98, 352–362.

Kähkönen, Y. 1987. Geochemistry and tectonomagmatic affinities of the metavolcanic rocks of the early Proterozoic Tampere Schist Belt, southern Finland. Precambrian Research 35, 295–311.

Kähkönen, Y. 1989. Geochemistry and petrology of the metavolcanic rocks of the early Proterozoic Tampere Schist Belt, southern Finland. Geological Survey of Finland, Bulletin 345. 104 p.

Kähkönen, Y. 1994. Shoshonitic and high-K metavolcanic rocks in the southern parts of the Paleoproterozoic Tampere schist belt, southern Finland: evidence for an evolved arc-type setting. In: Nironen, M. & Kähkönen, Y. (eds.) Geochemistry of Proterozoic supracrustal rocks in Finland. Geological Survey of Finland, Special Paper 19, 101–115.

Kähkönen, Y. & Huhma, H. 1993. An Archaean cobble in a Svecofennian conglomerate near Tampere, southern Finland. In: Autio, S. (ed.) Current Research 1991–1992. Geological Survey of Finland, Special Paper 18, 31–36.

Kähkönen, Y. & Leveinen, J. 1994. Geochemistry of metasedimentary rocks of the Paleoproterozoic Tampere schist belt, southern Finland. In: Nironen, M. & Kähkönen, Y. (eds.) Geochemistry of Proterozoic supracrustal rocks in Finland. Geological Survey of Finland, Special Paper 19, 117–136.

Kähkönen, Y. & Nironen, M. 1994. Supracrustal rocks around the Paleoproterozoic Haveri Au–Cu deposit, southern Finland: Evolution from a spreading center to a volcanic arc environment. In: Nironen, M. & Kähkönen, Y. (eds.) Geochemistry of Proterozoic supracrustal rocks in Finland. Geological Survey of Finland, Special Paper 19, 141–159.

Kähkönen, Y. Huhma, H. & Aro, K. 1989. U–Pb zircon ages and Rb–Sr whole-rock isotope studies of early Proterozoic volcanic and plutonic rocks

near Tampere, southern Finland, Precambrian Research 45, 27–43.

Kähkönen, Y., Lahtinen, R. & Nironen, M. 1994. Paleoproterozoic supracrustal belts in southwestern Finland. In: Pajunen, M. (ed.) High temperature-low pressure metamorphism and deep crustal structures. Meeting of IGCP project 304 'Deep Crustal Processes' in Finland, September 16–20, 1994. Geological Survey of Finland, Guide 36, 43–47.

Keleman, P.B. 1990. Reaction between ultramafic rock and fractionating basaltic magma I. Phase relations, the origin of calc-alkaline magma series, and the formation of discordant dunite. Journal of Petrology 31, 51–97.

Keleman, P.B., Johnson, K.T.M., Kinzler, R.J. & Irving, A.J. 1990. High field strength element depletions in arc basalts due to mantle-magma interaction. Nature 345, 263–273.

Kilpeläinen, T.,Korikovsky, S., Korsman, K. & Nironen, M. 1994. Tectono-metamorphic evolution in the Tampere–Vammala area. In: Pajunen, M. (ed.) High temperature-low pressure metamorphism and deep crustal structures. Meeting of IGCP project 304 'Deep Crustal Processes' in Finland, September 16–20, 1994. Geological Survey of Finland, Guide 36, 27–34.

Kohonen, J. 1994. Post-depositional K-feldspar breakdown and its implications for metagraywacke provenance studies – an example from north Karelia, eastern Finland. In: Nironen, M. & Kähkönen, Y. (eds.) Geochemistry of Proterozoic supracrustal rocks in Finland. Geological Survey of Finland, Special Paper 19, 161–171.

Koistinen, T. (ed.), 1994. Precambrian basement of the Gulf of Finland and surrounding area 1: 1 000 000. Geological Survey of Finland.

Koistinen, T, Klein, V., Koppelmaa, H., Korsman, K., Lahtinen, R., Nironen, M., Puura, V., Saltykova, T., Tikhomirov, S. & Yanovskiy, A. in press. Paleoproterozoic, Svecofennian orogenic belt. In: Koistinen, T. (ed.) Explanation to the maps of Precambrian basement and magnetism of the Gulf of Finland and surrounding area. Geological Survey of Finland, Special Paper xx, xx–xx.

Korja, A. 1995. Structure of the Svecofennian crust – growth and destruction of the Svecofennian orogen. Institute of Seismology University of Helsinki, Report S–31. 36 p.

Korja, A. & Heikkinen, P.J. 1995. Proterozoic extensional tectonics of the central Fennoscandian Shield: results from the Baltic and Bothnian Echoes from the Lithosphere experiment. Tectonics 14 (2), 504–517.

Korsch, R.J., Roser, B.P. & Kamprad, J.L. 1993. Geochemical, petrographic and grain-size varia-tions within single turbidite beds. Sedimentary Geology 83, 15–35.

Korsman, K. 1977. Progressive metamorphism of the metapelites in the Rantasalmi–Sulkava area, southeastern Finland. Geological Survey of Finland, Bulletin 290. 82 p.

Korsman, K. & Kilpeläinen, T. 1986. Relationship between zonal metamorphism and deformation in the Rantasalmi–Sulkava area, southeastern Finland. In: Korsman, K. (ed.) Development of deformation, metamorphism and metamorphic blocks in eastern and southern Finland. Geological Survey of Finland, Bulletin 339, 33–42.

Korsman, K., Hölttä, P., Hautala, T. & Wasenius, P. 1984. Metamorphism as an indicator of evolution and structure of the crust in eastern Finland. Geological Survey of Finland, Bulletin 328. 40 p.

Korsman, K., Niemelä, R. & Wasenius, P. 1988. Multistage evolution of the Proterozoic crust in the Savo schist belt, eastern Finland. In: Korsman, K. (ed.) Tectono-metamorphic evolution of the Raahe–Ladoga zone. Geological Survey of Finland, Bulletin 343, 89–96.

Kouvo, O. & Tilton, G.R. 1966. Mineral ages from the Finnish Precambrian. The Journal of Geology 74, 421–442.

Koyaguchi, T. 1986. Textural and compositional evidence for magma mixing and its mechanism, Abu volcano group, southwestern Japan. Contributions to Mineralogy and Petrology 93, 33–45.

Kuno, H. 1966. Lateral variation of basalt magma types across continental margins and island arcs. Bulletin of Volcanology 29, 195–222.

Lahti, S. 1981. On the granitic pegmatites of the Eräjärvi area in Orivesi, southern Finland. Geological Survey of Finland, Bulletin 314. 82 p.

Lahtinen, R. 1994a. Crustal evolution of the Svecofennian and Karelian domains during 2.1–1.79 Ga, with special emphasis on the geochemistry and origin of 1.93–1.91 Ga gneissic tonalites and associated supracrustal rocks in the Rautalampi area, central Finland. Geological Survey of Finland, Bulletin 378. 128 p.

Lahtinen, R. 1994b. Preliminary notes on the geochemical characteristics of mantle during 1.93–1.79 Ga beneath the Svecofennian domain, Finland. Mineralogical Magazine 58 A, 507–508.

Lahtinen, R. & Korhonen, J. V. 1996. Comparison of petrophysical and rock geochemical data in the Tampere–Hämeenlinna area, southern Finland. Geological Survey of Finland, Bulletin 392. 45 p.

Lahtinen, R. & Lestinen, P. 1996. Background variation of ore-related elements and regional-scale mineralization in Palaeproterozoic bedrock in the Tampere–Hämeenlinna area, southern Finland. Geological Survey of Finland, Bulletin 390. 38 p.

Lahtinen, R. & Huhma, H. Isotopic and geohemical constraints on the evolution of the 1.93–1.79 Ga Svecofennian crust and mantle in Finland. Precambrian Research (in press.)

Laitakari, I. 1986. Orivesi. Geological Map of Finland 1:100 000, Pre-Quaternary rocks, Sheet 2142. Geological Survey of Finland.

Laitakari, I. 1987. Hämeen Subjotuninen diabaasijuoniparvi. Summary: The Subjotnian dyke swarm of Häme. In: Aro, K. & Laitakari, I. (eds.) Suomen diabaasit ja muut mafiset juonikivilajit. Summary: Diabases and other mafic dyke rocks in Finland. Geological Survey of Finland, Report of Investigation 76, 99–116.

LeBas, M.J., LeMaitre, R.W., Streckeisen, A. & Zanettin, B. 1986. A chemical classification of volcanic rocks based on total alkali-silica diagram. Journal of Petrology 27, 745–750.

Leeman, W.P. & Harry, D.L. 1993. A binary source model for extension-related magmatism in the Great Basin, Western North America, Science 262, 1550–1554.

Le Maitre, R.W. (ed.), 1989. A classification of igneous rocks and glossary of terms. Oxford: Blackwell. 193 p.

Leveinen, J. 1990. Tampereen liuskevyöhykkeen kerrostumat Pulesjärven profiilissa. Unpublished master's thesis, University of Helsinki, Department of Geology. 134 p.

Luukkonen, A. 1994. Main geological features, metallogeny and hydrothermal alteration phenomena of certain gold and gold–tin–tungsten prospects in southern Finland. Geological Survey of Finland, Bulletin 377. 153 p.

Mäkelä, K. 1980. Geochemistry and origin of Haveri and Kiipu, Proterozoic strata-bound volcanogenic gold-copper and zinc mineralizations from southwestern Finland. Geological Survey of Finland, Bulletin 310. 79 p.

Matisto, A. 1961. Tampere. Geological Map of Finland 1:100 000, Pre-Quaternary rocks, Sheet 2123. Geological Survey of Finland.

Matisto, A. 1964. Kangasala. Geological Map of Finland 1:100 000, Pre-Quaternary rocks, Sheet 2141. Geological Survey of Finland.

Matisto, A. 1968. Die Meta-Arkose von Mauri bei Tampere. Bulletin de la Commision Géologique de Finlande 235. 21 p.

Matisto, A. 1970. Valkeakoski. Geological Map of Finland 1:100 000, Pre-Quaternary rocks, Sheet 2132. Geological Survey of Finland.

Matisto, A. 1973. Toijala. Geological Map of Finland 1:100 000, Pre-Quaternary rocks, Sheet 2114. Geological Survey of Finland.

Matisto, A. 1976a. Toijalan kartta-alueen kallioperä. Summary: Pre-Quaternary rocks of the Toijala map-sheet area. Geological Map of Finland 1:100 000, Explanation to the Maps of Pre-Quaternary Rocks, Sheet 2114. Geological Survey of Finland. 26 p.

Matisto, A. 1976b. Valkeakosken kartta-alueen kallioperä. Summary: Pre-Quaternary rocks of the Valkeakoski map-sheet area. Geological Map of Finland 1:100 000, Explanation to the Maps of Pre-Quaternary Rocks, Sheet 2132. Geological Survey of Finland. 34 p.

Matisto, A. 1976c. Kangasalan kartta-alueen kallioperä. Summary: Pre-Quaternary rocks of the Kangasala map-sheet area. Geological Map of Finland 1:100 000, Explanation to the Maps of Pre-Quaternary Rocks, Sheet 2141. Geological Survey of Finland. 27 p.

Matisto, A. 1977. Tampereen kartta-alueen kallioperä. Summary: Pre-Quaternary rocks of the Tampere map-sheet area. Geological Map of Finland 1:100 000, Explanation to the Maps of Pre-Quaternary Rocks, Sheet 2123. Geological Survey of Finland. 50 p.

McDermott, F. & Hawkesworth, C.J. 1991. Th, Pb, Sr isotope variations in young arc volcanics and oceanic sediments. Earth and Planetary Science Letters 104, 1–15.

McKenzie, D.P. & O'Nions, R.K. 1991. Partial melt distributions from inversion of rare earth element concentrations. Journal of Petrology 32, 1021–1091.

McLennan, S.M., Taylor, S.R., McCulloch, M.T. & Maynard, J.B. 1990. Geochemical and Nd–Sr isotopic composition of deep-sea turbidites: crustal evolution and plate tectonic associations. Geochimica Et Cosmochimica Acta 54, 2015–2050.

Meen, J.K. 1990. Elevation of potassium content of basaltic magma by fractional crystallization: the effect of pressure. Contributions to Mineralogy and Petrology 104, 309–331.

Miller, C.F. 1985. Are strongly peraluminous magmas derived from pelitic sedimentary sources? The Journal of Geology 93, 673–689.

Miyashiro, A. 1974. Volcanic rock series in island arcs and active continental margins. American Journal of Science 274, 321–355.

Molen, van der, I. & Paterson, M.S. 1979. Experimental deformation of partially-melted granite. Contributions to Mineralogy and Petrology 70, 299–318.

Moore, G.F., Curray, J.R. & Emmel, F.J. 1982. Sedimentation in the Sunda Trench and forearc region. Geological Society of London Special Publications 10, 245–258.

Nesbitt, H.W. & Young G.M. 1982. Early Proterozoic climates and plate motions inferred from major element chemistry of lutites. Nature 299,

715–717.

Nesbitt, H.W., Markovics, G. & Price, R.C. 1980. Chemical processes affecting alkalis and alkaline earths during continental weathering. Geochimica Et Cosmochimica Acta 44, 1659–1666.

Neuvonen, K.J. 1954a. Forssa. Geological Map of Finland 1:100 000, Pre-Quaternary rocks, Sheet 2113. Geological Survey of Finland.

Neuvonen, K.J. 1954b. Stratigraphy of the schists of the Tammela–Kalvola area, southwestern Finland. Bulletin de la Commision Géologique de Finlande 166. 85 p.

Neuvonen, K.J. 1956. Forssan kartta-alueen kallioperä. Summary: Pre-Quaternary rocks of the Forssa map-sheet area. Geological Map of Finland 1:100 000, Explanation to the Maps of Pre-Quaternary Rocks, Sheet 2113. Geological Survey of Finland. 37 p.

Nironen, M. 1989a. Emplacement and structural setting of granitoids in the early Proterozoic Tampere and Savo schist belts, Finland – implications for contrasting crustal evolution. Geological Survey of Finland, Bulletin 346. 83 p.

Nironen, M. 1989b. The Tampere schist belt: structural style within an early Proterozoic volcanic arc system in southern Finland, Precambrian Research 43, 23–40.

Nurmi, P.A. 1984. Applications of lithogeochemistry in the search for Proterozoic porphyry-type molybdenum, copper and gold deposits, southern Finland. Geological Survey of Finland, Bulletin 329. 40 p.

Nurmi, P.A. & Haapala, I. 1986. The Proterozoic granitoids of Finland: granite types, metallogeny, and relation to crustal evolution. Bulletin of the Geological Society of Finland 58, 203–233.

Nurmi, P.A., Front, K., Lampio, E. & Nironen, M. 1984. Etelä-Suomen svekokarjalaiset porfyyrityyppiset molybdeeni- ja kupariesiintymät, niiden granitoidi-isäntäkivet ja litogeokemiallinen etsintä. Summary: Svecokarelian porphyry-type molybdenum and copper occurrences in southern Finland: their granitoid host rocks and lithogeochemical exploration. Geological Survey of Finland, Report of Investigation 67. 88 p.

O'Hara, M.J. 1980. Non-linear nature of the unavoidable long-lived isotopic, trace and major element contamination of a developing magma chamber. Philosophical Transactions of Royal Society 297, 215–227.

Ojakangas, R.W. 1986. An early Proterozoic greywacke-slate turbidite sequence: the Tampere schist belt, southwestern Finland. Bulletin of the Geological Society of Finland 58, 241–261.

Papunen, H. 1985. The Kylmäkoski nickel-copper deposit. In: Papunen, H. & Gorbunov, G.I. (eds.) Nickel-copper deposits of the Baltic Shield and Scandinavian Caledonides. Geological Survey of Finland, Bulletin 333, 264–273.

Park, A.F., Bowes, D.R., Halden, N.M. & Koistinen, T.J. 1984. Tectonic evolution at an early Proterozoic continental margin: the Svecokarelides of eastern Finland. Journal of Geodynamics 1, 359–386.

Patchett, J. & Kouvo, O. 1986. Origin of continental crust of 1.9–1.7 Ga age: Nd isotopes and U–Pb zircon ages in the Svecokarelian terrain of South Finland. Contributions to Mineralogy and Petrology 92, 1–12.

Patiño Douce, A.E. & Johnston, A.D. 1991. Phase equilibria and melt productivity in the pelitic system: implications for the origin of peraluminous granitoids and aluminous granulites. Contributions to Mineralogy and Petrology 107, 202–218.

Pearce, J.A. 1982. Trace element characteristics of lavas from destructive plate margins. In: R.S. Thorpe (ed.) Andesites. Orogenic andesites and related rocks. Chichester: Wiley, 525–548.

Pearce, J.A. 1983. Role of sub-continental lithosphere in magma genesis at active continental margins. In: Hawkesworth, C.J. & Norry, M.J. (eds.) Continental Basalts and Mantle Xenoliths. Cheshire: Shiva, 230–249.

Peltonen, P. 1995. Petrogenesis of ultramafic rocks in the Vammala Nickel Belt: Implications for crustal evolution of the early Proterozoic Svecofennian arc terrane. Lithos 34, 253–274.

Platt, J.P. & England, P.C. 1993. Convective removal of lithosphere beneath mountain belts: thermal and mechanical consequences. American Journal of Science 293, 307–336.

Pitcher, W.S. 1993. The Nature and Origin of Granite. Glasgow: Blackie Academic & Professional. 321 p.

Puchelt, H. 1972. Barium. In: Wedepohl, K.H. (ed.) Handbook of Geochemistry. Berlin:Springer-Verlagen.

Rapp, R.P. & Watson, E.B. 1986. Monazite solubility and dissolution kinetics: implications for the thorium and light rare earth chemistry of felsic magmas. Contributions to Mineralogy and Petrology 94, 304–316.

Rapp, R.P., Watson, E.B. & Miller, C.F. 1991. Partial melting of amphibolite/eclogite and the origin of Archean trondhjemites and tonalites. Precambrian Research 51, 1–25.

Rautio, T. 1987. Tampereen liuskejakson litostratigrafia ja paleosedimentologia Kolunkylän ja Veittijärven alueilla. Unpublished master's thesis. University of Oulu, Department of Geology. 108 p.

Reid, J.B., Evans, O.C. & Fates, D.G. 1983. Magma mixing in granitic rocks of the central Sierra

Nevada, California. Earth and Planetary Science Letters 66, 243–261.

Rice, A. 1981. Convective fractionation: a mechanism to provide cryptic zoning (macrosegregation) layering, crescumulates, banded tuffs and explosive volcanism in igneous processes. Journal of Geophysical Research 86, 405–417.

Ringwood, A.E. 1990. Slab-mantle interactions. 3. Petrogenesis of intraplate magmas and structure of the upper mantle. Chemical Geology 82, 187–207.

Rogers, J.J.W. & Adams, J.A.S. 1969. Thorium. In: Wedepohl, K.H. (ed.) Handbook of Geochemistry. Berlin: Springer-Verlagen.

Rosenberg, P. 1990. Tutkimustyöselostus Pirkkalan kunnassa Vatanen 1, Lintumäki 1, Poikkiaro 1 sekä Sorkkala 1–2 nimisillä valtausalueilla, Kaiv. Rek. No 4179/1–2 ja 4331/1–3, suoritetuista malmitutkimuksista. Geological Survey of Finland, unpublished report, M06/2123/–90/1/10.

Rosenberg, P. 1992. Kultatutkimukset Valkeakosken Kaapelinkulman alueella vuosina 1986–92. Geological Survey of Finland, unpublished report, M19/2132/–92/1/1.

Rosenberg, R.J., Kaistila, M. & Zilliacus, R. 1982. Instrumental neutron activation analysis of solid geochemical samples. Journal of Radioanalytical Chemistry 71, 419–428.

Rushmer, T. 1991. Partial melting of two amphibolites: contrasting experimental results under fluid-absent conditions. Contributions to Mineralogy and Petrology 197, 41–59.

Rutter, M.J. & Wyllie, P.J. 1989. Experimental study of interaction between hydrous granite melt and amphibolite. Geology Magazine 126, 633–646.

Ryerson, F.J. & Watson, E.B. 1987. Rutile saturation in magmas: implications for Ti–Nb–Ta depletion in island arc basalts. Earth and Planetary Science Letters 86, 225–239.

Salters, V.J.M. & Shimizu, N. 1988. World-wide occurrence of HFSE-depleted mantle. Geochimica Et Cosmochimica Acta 52, 2177–2182.

Sandström, H. 1996. The analytical methods and the precison of the element determinations used in the regional bedrock geochemistry in the Tampere–Hämeenlinna area, southern Finland. Geological Survey of Finland, Bulletin 393. 25 p.

Sawyer, E.W. 1991. Disequilibrium melting and the rate of melt-residuum separation during migmatization of mafic rocks from the Grenville Front, Quebec. Journal of Petrology 32, 701–738.

Sawyer, E.W. & Barnes, S.-J. 1988. Temporal and compositional differences between subsolidus and anatectic migmatite leucosomes from the Quetico sedimentary belt, Canada. Journal of

Metamorphic Geology 6, 437–450.

Sederholm, J.J. 1897. Über eine archäische Sedimentformation im südwestlichen Finland und ihre Bedeutung für die Erklärung der Enstehungsweise des Grundebirges. Bulletin de la Commision Géologique de Finlande 6. 254 p.

Seitsaari, J. 1951. The schist belt northeast of Tampere in Finland. Bulletin de la Commission Géologique de Finlande 153. 121 p.

Simonen, A. 1948. On the Petrology of the Aulanko Area in Southwestern Finland. Bulletin de la Commision Géologique de Finlande 143. 66 p.

Simonen, A. 1949a. Hämeenlinna. Geological Map of Finland 1:100 000, Pre-Quaternary rocks, Sheet 2131. Geological Survey of Finland.

Simonen, A. 1949b. Hämeenlinnan kartta-alueen kallioperä. Summary: Pre-Quaternary rocks of the Hämeenlinna map-sheet area. Geological Map of Finland 1:100 000. Explanation to the Maps of Pre-Quaternary Rocks, Sheet 2131. Geological Survey of Finland. 45 p.

Simonen, A. 1952. Viljakkala–Teiskon kartta-alueen kallioperä. Summary: Pre-Quaternary rocks of the Viljakkala–Teisko map-sheet area. Geological Map of Finland 1:100 000, Explanation to the Maps of Pre-Quaternary Rocks, Sheet 2124. Geological Survey of Finland. 74 p.

Simonen, A. 1953. Viljakkala–Teisko. Geological Map of Finland 1:100 000, Pre-Quaternary rocks, Sheet 2124. Geological Survey of Finland.

Simonen, A. 1980a. The Precambrian in Finland. Geological Survey of Finland, Bulletin 304. 58 p.

Simonen, A. 1980b. Prequaternary rocks of Finland. 1:1 000 000. Geological Survey of Finland.

Simonen, A. & Kouvo, O. 1951. Archean varved schists north of Tampere in Finland. Bulletin de la Commision Géologique de Finlande 154, 93–114.

Sisson, T.W. & Grove, T.L. 1993a. Experimental investigations of the role of H_2O in calc-alkaline differentiation and subduction zone magmatism. Contributions to Mineralogy and Petrology 113, 143–166.

Sisson, T.W. & Grove, T.L. 1993b. Temperatures and H_2O contents of low-MgO high-alumina basalts. Contributions to Mineralogy and Petrology 113, 167–184.

Sjöblom, B. 1990. Mäntän kartta-alueen kallioperä. Summary: Pre-Quaternary rocks of the Mänttä map-sheet area. Geological Map of Finland 1:100 000, Explanation to the Maps of Pre-Quaternary Rocks, Sheet 2231. Geological Survey of Finland. 64 p.

Skjerlie, K.P. & Johnston, A.D 1993. Fluid-absent melting behaviour of an F-rich tonalitic gneiss at mid-crustal pressures: Implications for the gener-

ation of anorogenic granites. Journal of Petrology 34, 785–815.

Skjerlie, K.P., Patiño Douce, A.E. & Johnston, A.D. 1993. Fluid absent melting of layered crustal protolith: implications for the generation of anatectic granites. Contributions to Mineralogy and Petrology 114, 365–378.

Sparks, R.S.J. & Marshall, L.A. 1986. Thermal and mechanical constraints on mixing between mafic and silicic magmas. Journal of Volcanology and Geothermal Research 29, 99–124.

Spulber, S.D. & Rutherford, M.J. 1983. The Origin of Rhyolite and Plagiogranite in Oceanic crust: An Experimental Study. Journal of Petrology 24, 1–25.

Stigzelius, H. 1944. Über die Erzgeologie des Viljakkala-gebietes im südwestlichen Finnland. Bulletin de la Commision Géologique de Finlande 134. 91 p.

Suominen, V. 1991. The chronostratigraphy of southwestern Finland with special reference to Postjotnian and Subjotnian diabases. Geological Survey of Finland, Bulletin 356. 100 p.

Tatsumi, Y., Hamilton, D.L. & Nesbitt, R.W. 1986. Chemical characteristics of fluid phase released from a subducted lithosphere and origin of arc magmas: evidence from high-pressure experiments and natural rocks. Journal of Volcanology and Geothermal Research 29, 293–309.

Taylor, S.R. & McLennan, S.M. 1985. The Continental Crust: Its Composition and Evolution. Oxford: Blackwell. 312 p.

Thompson, A.B. & Algor, J.R. 1977. Model systems for anatexis of pelitic rocks. I Theory of melting relations in the system $KAlO_2$–$NaAlO_2$–Al_2O_3–H_2O. Contributions to Mineralogy and Petrology 3, 247–269.

Tikoff, B. & Teyssier, C. 1992. Crustal-scale, en echelon "P-shear" tensional bridges: A possible solution to the batholithic room problem. Geology 20, 927–930.

Turner, S.P., Foden, J.D. & Morrison, R.S. 1992. Derivation of some A-type magmas by fractionation of basaltic magma: An example from the Pathaway Ridge, South Australia. Lithos 28, 151–179.

Uto, K. 1986. Variations of Al_2O_3 content in Late Cenozoic Japanese Basalts: A re-examination of Kuno's high-alumina basalt. Journal of Volcanology and Geothermal Research 29, 397–411.

Van Der Laan, S.R. & Wyllie, P.J. 1993. Experimental interaction of granitic and basaltic magmas and implications for mafic enclaves. Journal of Petrology 34, 491–517.

Vaasjoki, M. 1994. Valijärven hapan vulkaniitti: minimi Hämeen liuskejakson iäksi. Summary: Radiometric age of a meta-andesite at Valijärvi, Häme schist zone, southern Finland. Geologi 46 (7), 91–92.

Vaasjoki, M. 1995. Rengon Rouvinmäen kvartsi-montsodioriitti: uusi posttektoninen granitoidi. Summary: The Rouvinmäki quartzmonzodiorite at Renko: a new posttectonic granitoid. Geologi 47 (6), 79–81.

Vaasjoki, M. & Huhma, H. 1987. Lead isotopic results from metabasalts of the Haveri formation, southern Finland: an indication of early Proterozoic mantle derivation. Terra Cognita 7, 159.

Vaasjoki, M. & Sakko, M. 1988. The evolution of the Raahe–Ladoga zone in Finland: isotopic constraints. In: Korsman, K. (ed.) Tectono-metamorphic evolution of the Raahe–Ladoga zone. Geological Survey of Finland, Bulletin 343, 7–32.

Väisänen, M., Hölttä, P., Rastas, J., Korja, A. & Heikkinen, P. 1994. Deformation, metamorphism and the deep structure of the crust in the Turku area, southwestern Finland. In: Pajunen, M. (ed.) High temperature-low pressure metamorphism and deep crustal structures. Meeting of IGCP project 304 'Deep Crustal Processes' in Finland, September 16–20, 1994. Geological Survey of Finland, Guide 36, 35–41.

Valloni, R. & Maynard, J.B. 1981. Detrital modes of recent deep-sea sands and their relation to tectonic setting: a first approximation. Sedimentology 28, 75–83.

Vielzeuf, D. & Holloway, J.R. 1988. Experimental determination of the fluid-absent melting relations in the pelitic system. Consequences for crustal differentiation. Contributions to Mineralogy and Petrology 98, 257–276.

Vielzeuf, D. & Montel, J.M. 1994. Partial melting of metagreywackes. Part I. Fluid-absent experiments and phase relationships. Contributions to Mineralogy and Petrology 117, 375–393.

Watson, E.B. 1982. Basaltic contamination by continental crust: some experiments and models. Contributions to Mineralogy and Petrology 80, 73–87.

Watson, E.B. & Harrison, T.M. 1983. Zircon saturation revisited: temperature and composition effects in a variety of crustal magma types. Earth and Planetary Science Letters 64, 295–304.

Watt, G.R. & Harley, S.L. 1993. Accessory phase controls on the geochemistry of crustal melts and restites produced during water-undersaturated partial melting. Contributions to Mineralogy and Petrology 114, 550–566.

Weaver, B.L. 1991. The origin of ocean island basalt end-member compositions: trace elementand isotopic constraints. Earth and Planetary Science Letters 104, 381–397.

White A.J.R. & Chappel, B.W. 1977. Ultrametamorphism and granitoid genesis. Tectonophysics 43, 7–22.

Wickman, S. 1987. Crustal anatexis and granite petrogenesis during low pressure regional matamorphism; the Trois Seigneurs Massif, Pyreness, France. Journal of Petrology 28, 127–169.

Zindler, A. & Hart, S.R. 1986. Chemical geodynamics. Annual Rew. Earth Planet. Sci. 14, 493–571.

Zorpi, M.J., Coulon, C. & Orsini, J.B. 1991. Hybridization between felsic and mafic magmas in calc-alkaline granitoids - a case study in northern Sardinia, Italy. Chemical Geology 92, 45–86.